

Bureau of Mines Report of Investigations/1985

Fracture Zone Dewatering To Control Ground Water Inflow in Underground Coal Mines

By Robert D. Schmidt



UNITED STATES DEPARTMENT OF THE INTERIOR

REPRODUCED BY
NATIONAL TECHNICAL
INFORMATION SERVICE
U.S. DEPARTMENT OF COMMERCE
SPRINGFIELD, VA. 22161





Report of Investigations 8981

Fracture Zone Dewatering To Control Ground Water Inflow in Underground Coal Mines

By Robert D. Schmidt



UNITED STATES DEPARTMENT OF THE INTERIOR
Donald Paul Hodel, Secretary

BUREAU OF MINES
Robert C. Horton, Director

UNIT OF MEASURE ABBREVIATIONS USED IN THIS REPORT

ft	foot	h	hour
ft ²	square foot	h/d	hour per day
ft/yr	foot per year	in	inch
gpd	gallon per day	mg/L	milligram per liter
gpd/ft	gallon per day per foot	m/h	meter per hour
gpd/ft ²	gallon per day per square foot	min	minute
gpm	gallon per minute	min/d	minute per day
		pct	percent

Library of Congress Cataloging in Publication Data:

Schmidt, R. D. (Robert D.)

Fracture zone dewatering to control ground water inflow in underground coal mines.

(Bureau of Mines report of investigations ; 8981)

Bibliography: p. 33-34.

Supt. of Docs. no.: I 28.23:8981

1. Mine drainage. 2. Mine water. 3. Coal mines and mining—Appalachian Region. I. Title. II. Series: Report of investigations (United States. Bureau of Mines) ; 8981.

TN23.U43 [TN321] 622s [622'.334] 85-6000 16

CONTENTS

	<u>Page</u>
Abstract.....	1
Introduction.....	2
Appalachian hydrogeologic setting.....	3
Fracture zones.....	3
Fracture zone detection and usage.....	4
Underground coal mine water-related problems.....	5
Mine inflow survey.....	6
Point sources of inflow.....	7
Floor conditions in a wet section.....	9
Water quality in a wet section.....	10
Approaches and problems of past mine dewatering efforts.....	10
Modeling the fracture zone flow problem.....	10
Model development.....	11
Basic equations.....	11
Regional confined flow.....	12
Regional unconfined flow.....	12
Combined confined and unconfined flow.....	13
Elementary solutions.....	13
Complex potential function.....	13
Uniform flow.....	14
Flow toward a well.....	14
Flow across a permeability discontinuity.....	14
Modeling fracture zones.....	15
Matrix equations.....	16
Plotting piezometric head contours.....	18
Validation.....	18
Program DWATR.....	18
Idealized fracture zone simulation.....	19
Appropriate applications for DWATR.....	19
Sunshine Mine dewatering site.....	20
Analysis of field data.....	22
Parameterization of the aquifer setting.....	23
Static background simulations.....	24
Simulation of dewatering well operations.....	26
Simulation of alternate dewatering well settings.....	29
Sunshine Mine dewatering field test.....	30
Fracture trace analysis, well drilling and development.....	30
In-mine dewatering results.....	31
Analysis.....	31
Conclusions.....	32
References.....	33
Appendix A.--DWATR program modules.....	35
Appendix B.--Input variable description.....	36
Appendix C.--DWATR source listing.....	40

ILLUSTRATIONS

1. Fracture zone cross-sectional representation.....	4
2. Fracture zone in exposed highwall.....	4
3. Three types of mine fracture intercepts.....	8
4. Roof bolt hole inflow source.....	8
5. Development of poor floor conditions at an active face.....	9

ILLUSTRATIONS--Continued

	<u>Page</u>
6. Confined flow setting.....	12
7. Unconfined flow setting.....	12
8. Confined and unconfined flow, combined.....	13
9. Permeability discontinuity.....	14
10. Jump in potential at a line doublet.....	16
11. Idealized fracture zone setting.....	16
12. Inhomogeneity in a strip.....	18
13. Idealized fracture zone piezometric surface.....	19
14. Location of the Sunshine Mine dewatering test site in the Monongahela River basin of West Virginia.....	20
15. Sunshine Mine location within the Kingwood syncline.....	20
16. Fracture traces and well locations in the vicinity of Crab Orchard Run...	21
17. Geologic cross section at AA'.....	21
18. Geologic cross section at BB'.....	21
19. Geologic cross section at CC'.....	22
20. Permeability zone representation of fracture traces near Crab Orchard Run	24
21. Simulated piezometric surface beneath Crab Orchard Run.....	26
22. Average pumping and total drawdown, wells P and R.....	27
23. Observation well drawdown (daily total).....	27
24. Simulated piezometric surface due to dewatering well pumping.....	28
25. Simulated piezometric surface resulting from maximum sustained pumping...	29
26. Simulated piezometric surface resulting from sustained pumping of wells B and C.....	29
27. Interpreted geologic cross section along Crab Orchard Run.....	30

TABLES

1. Coal mine water inflow survey.....	7
2. Probable effects of high inflow on coal cutting time.....	9
3. Crab Orchard Run well and aquifer data.....	22
4. Summary of calculated values of transmissivity, permeability, and storativity from all pump tests.....	23
5. Static background parameter values.....	25
6. Actual and simulated static heads.....	25
7. Steady state dewatering parameter values.....	27
8. Well P and R actual and simulated pump test results.....	28

FRACTURE ZONE DEWATERING TO CONTROL GROUND WATER INFLOW IN UNDERGROUND COAL MINES

By Robert D. Schmidt¹

ABSTRACT

This Bureau of Mines investigation focuses on the identification and control of ground water inflow problems that occur in the active sections of underground Appalachian coal mines. A fracture inflow survey of eight underground mines was conducted. Three types of mine fracture intercepts were identified, which are typical of wet section mining conditions. A mine in Preston County, WV was selected as the site for a fracture zone dewatering experiment. Fracture trace analysis was used to site dewatering wells in a fracture valley setting ahead of mine development. The design, implementation, and results of this dewatering experiment are presented.

A hydrology simulator was also developed and applied to the fracture zone flow problem at the field site. The model uses a semianalytic, boundary integral technique to simulate fracture zones as discrete regions of high average permeability. Comparisons are made between simulated and actual dewatering results.

This investigation suggests that fracture zones are responsible for the sudden release of stored ground water, which often occurs as mining sections advance beneath fracture valley topography. It is concluded, therefore, that dewatering operations that are designed to intercept the component of ground water that is stored in fracture zones will be most effective in controlling infiltration to active mine sections.

¹Hydrologist, Twin Cities Research Center, Bureau of Mines, Minneapolis, MN.

INTRODUCTION

Ground water flow into underground coal mines has been a problem for miners since the inception of the industry. As underground mining operations remove coal, the void space created by the workings acts as an open drain, intercepting or otherwise disrupting normal ground water flow.

High-volume inflows at the active mining face are of special concern. They contribute directly to reduced mine productivity by creating difficult, uncomfortable, and sometimes hazardous working conditions for miners, and by reducing machine efficiency. Mine operating costs are further affected by the necessity for in-mine water handling and subsequent treatment of acidic mine discharge.

Controlling mine infiltration by using pumped wells to dewater aquifer source beds adjacent to mine development is a fairly common surface mining practice. Few published accounts exist, however, of dewatering methods applied to underground mines, particularly to underground Appalachian coal mines. The reluctance of the industry to attempt underground mine dewatering in Appalachia is due in part to discouragingly low permeabilities of many aquifer units (1).² Tightly interbedded and well cemented sandstone and shale units are commonly associated with eastern U.S. coal seams. The low intergranular permeability of these units restrict the pumping capacity of water wells, while the cost effectiveness of mine dewatering is closely tied to individual well pumping capacity. Mine dewatering quickly becomes prohibitively expensive if a large number of low yield wells are necessary to adequately dewater source beds in the vicinity of underground mine development.

The complexity of the hydrogeologic setting throughout much of Appalachia is

another factor that has deterred mine dewatering attempts. Inhomogeneities in aquifer porosity and permeability resulting from naturally occurring geologic fracture development contribute much to this complexity.

This paper will report on a Bureau of Mines investigation into the occurrence and control of underground mine water inflows in the Appalachian coal regions, where ground water flow in sandstone aquifers with low primary permeability is dominated by the relatively high secondary permeability of rock fracture zones.³

This investigation includes the following:

1. A survey of fracture related water inflow problems occurring in eight eastern U.S. underground coal mines.

2. The application of fracture trace analysis, a hydrogeologic technique for siting high yield municipal water wells, to the positioning of mine-aquifer dewatering wells in the vicinity of an active underground mine.

3. The application of a computer modeling technique for simulating the effect of dewatering wells sited on highly permeable zones of concentrated rock fracturing.

4. The design, implementation, and monitoring (at one of the eight mines surveyed) of a mine-aquifer dewatering attempt intended to exploit naturally occurring geologic fracture zones, as preferred sites for dewatering wells.

²Underlined numbers in parentheses refer to items in the list of references preceding the appendixes.

³Throughout this report, the terms primary and secondary permeability are used. Primary permeability refers to the natural intergranular permeability of a rock unit, while secondary permeability refers to that which results from a network of closely spaced rock fractures. The terms intergranular and fracture permeability will also be used.

APPALACHIAN HYDROGEOLOGIC SETTING

In early models of ground water flow in the Appalachian plateau (2-5), conglomerates, sandstones, coal seams, and some siltstones were considered to be aquifers, with shales, clay, and siltstones considered aquitards. The dissected upland areas of this plateau, are considered hydrologically isolated, with each hill having in general the following characteristics:

Infiltration zones occurring in upland areas.

Downward vertical percolation of ground water occurring slowly through aquitards.

Lateral flow above an aquitard resulting in sidehill springs and seeps.

Local ground water discharge zones occurring along the base of hills in stream valleys.

Regional ground water flow continuing in a longer, deeper path toward more deeply incised stream valleys.

Underground mines acting as underdrains that greatly alter the natural flow systems that existed prior to mining.

The hydrologic system of the Appalachian plateau is one of multiple perched water tables, overlying deeper regional aquifers.

The previously cited studies emphasized the importance of sandstones, conglomerates, and coals as layered hydrogeologic units in the northern Appalachian coal fields. Each of these early studies mentioned the presence of fractures and their possible influence on permeability, vertical flow through confining layers, and interconnections between aquifers. However, fracture flow was apparently considered of secondary importance when compared with intergranular flow. More recent studies (6-7) have indicated ground water flow in shallow aquifer units is greatly affected by zones of concentrated rock fracturing.

FRACTURE ZONES

Naturally occurring zones of concentrated rock fracturing, commonly called fracture zones, are important elements in

understanding the hydrogeologic effects of underground mining operations in Appalachian coal regions.

Fracture zones are comparatively narrow regions of intensely fractured rock. They are generally less than 1 mile in length, 20 to 50 ft across, and extend to depths of 100 to 300 ft. For the most part, fracture zones are oriented vertically (8). Typically, it is believed that the increasing overburden pressures with depth reduce the frequency and size of rock fractures.

Fracture permeability is a particularly significant if not a dominant consideration in the shallow rock strata of northern Appalachia at depths that range from 50 to 250 ft. Fracture zone permeability may be 10 to 1,000 times greater than the intergranular permeability of sandstone units. It is estimated that 5 to 10 zones of fracture concentration exist in any 100-acre area (9).

Fracture zones often coincide with stream valley topography, however they appear to be independent of regional structural trends.

Intense fracturing occurs beneath valley bottoms, supposedly because fracture zones are zones of structural weakness in the Earth's crust that are susceptible to erosion and valley formation (10). Thus the aquifer beneath a narrow, deeply incised valley can be broadly viewed as a highly permeable zone of concentrated rock fracturing (11-12). Not surprisingly, the water inflow problems of underground coal mines occur most often when mining activity is conducted beneath valley settings.

Figure 1 depicts the fracture pattern of an idealized zone of fracture concentration. Zones consist of vertical joints, faults, and cracks that are connected horizontally by bedding plane fractures (9).

In multiple aquifer settings, fracture zones may act as vertical hydraulic connections between separate aquifer units. In contrast to the low permeability shale units through which very little vertical

leakage would ordinarily occur, the potential for vertical leakage via fracture zones (including direct surface infiltration) is much greater. With mining activity, the intersection of fracture zone and coal seam is potentially an area of concentrated inflow to the mine workings.

Figure 2 is an example of a fracture zone, seen in cross section at an abandoned limestone quarry in Preston County, WV. Although this photograph does not show the land surface, left and right boundaries of the fracture zone are apparent, as is increased weathering of fractured rock due to enhanced surface infiltration.

FRACTURE ZONE DETECTION AND USAGE

Fracture traces are the surface expression of underlying zones of fracture concentration. Discerning these traces using stereopaired aerial photographs was first reported in reference 13 where they were used to locate fracture zones in limestone formations.

Reference 13 distinguishes between two types of linear features visible on aerial photographs as follows:

A photogeologic fracture trace is a natural linear feature consisting of topographic (including straight stream segments), vegetation, or soil tonal alignments, visible primarily on aerial photographs, and expressed continuously for less than one mile. Only natural linear features not obviously related to outcrop pattern of tilted beds, lineation and foliation, and stratigraphic contacts are classified as fracture traces.

A photogeologic lineament is similarly defined, except that it is expressed continuously for at least one mile, and more likely expressed continuously or discontinuously for many miles.

Fracture trace analysis refers specifically to the process of locating and assessing the hydrologic significance of linear features less than a mile in length. Stereopaired, low-level aerial photographs (1 in = 2,000 ft) are the

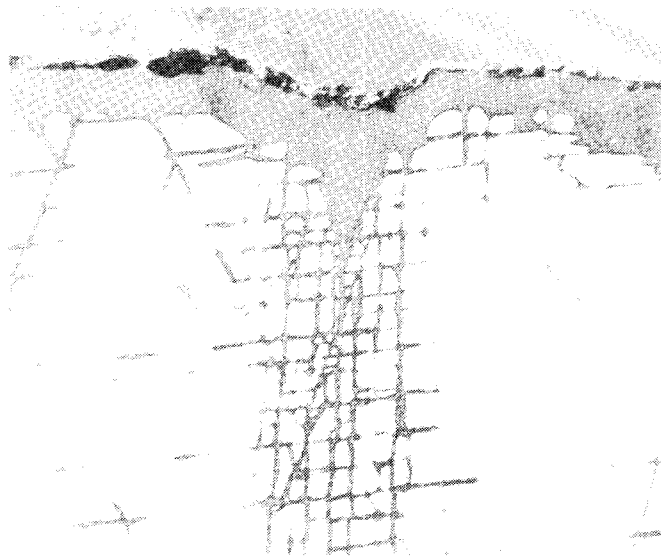


FIGURE 1. - Fracture zone cross-sectional representation (9).

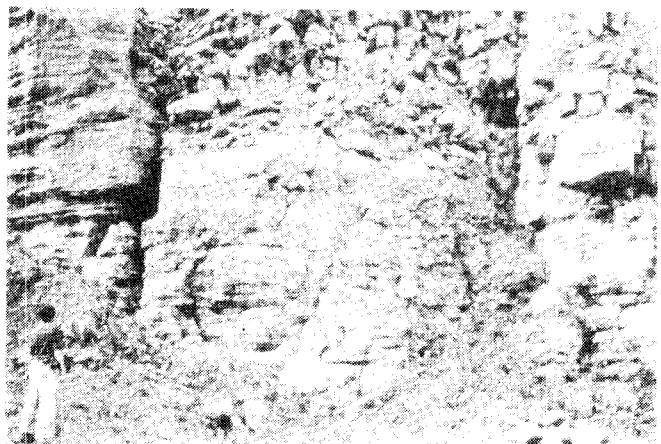


FIGURE 2. - Fracture zone in exposed highwall.

principal means of discerning these linear features.

Fracture trace analysis has been used by private concerns and various government agencies in the siting of municipal and domestic water wells and also in attempting to identify high risk roof fall areas in underground mines (14).

The intersections of fracture zones have been found to be particularly productive sites for water wells. As of 1979, at least 123 municipal water wells in Pennsylvania had been sited on fracture zone intersections. The average yield of fracture sited wells was 10 to 1,000 times greater than nonfracture sited wells (9).

A recent publication (6) details the technique of locating fracture zones and

the procedures and problems unique to fracture sited water well drilling.

UNDERGROUND COAL MINE WATER-RELATED PROBLEMS

Two water-related problems are most commonly associated with active operation of an underground coal mine in northern Appalachia (15-16).

1. Formation of acid mine drainage (AMD).

2. High-volume ground water inflows that interfere with mining activity.

The AMD problem has been thoroughly researched. AMD results from the oxidation and dissolution of sulfides commonly associated with coal and adjacent rock. Pyrite is the most common sulfur mineral, and the source of nearly all the acidity, iron, and sulfate in mine discharges (15). Most acidic mine water is generated in the inactive and abandoned portion of underground mine workings. Federal and State regulations prohibit the discharge of mine drainage pollutants into surface waters, and the costs of handling and treating acidic discharges are a substantial economic burden to coal mining companies. Control of acid mine water has been the focus of two recent dewatering experiments conducted in inactive and abandoned underground mines in Appalachia (1, 17).

The second water-related problem associated with mining is a quantity rather than a quality problem. It is far less well documented than AMD, but it is equally as important to the economics of coal mining. The present study indicates that ground water interference with mining activity is especially severe when sources of mine inflow are concentrated in active coal producing sections of a mine.

In a typical five-entry room and pillar coal mining section the continuous miner, roof bolter, and shuttle car operations are concentrated in an area that is seldom more than 300 ft² (18). Significant inflows of ground water, which impact mining conditions at the developing coal face, will have a far greater effect on coal production than ground water inflow almost anywhere else in the mine. A

section experiencing ground water inflow to the point where mining operations are significantly impeded is commonly termed a wet section.

Typical wet sections experience many of the following water-related problems (19):

1. High-volume inflow in an operating section--

Can cause temporary or permanent shutdown of the section.

Requires labor to move extra pumping and pipe equipment to flooded section.

Requires extra water handling capacity to deal with peak inflow.

2. Reduced floor stability causes--

Restricted equipment and miner maneuverability.

Soft fireclay to become viscous fluid, floor heaving, and roof falls.

Equipment and labor to be used for removal of muddy floor material along haulageways and manways.

3. Increased equipment wear, maintenance, and loss of efficiency caused by--

Dirt and clay washed into mechanical parts, increased frictional resistance and wear, increased maintenance, and shorter life expectancy.

Wet floor, lateral movement of rails and ties, and extra maintenance of rail system.

Reduced traction and increased rolling resistance of rubber-tired vehicles.

Equipment and labor used to extract machines that become bogged down in muddy sump areas.

4. Decreased safety, comfort, and productivity of miners caused by--

Water in contact with worn trailing cable splices, which trips breakers and makes reset difficult.

Muddy wet floors that cause slippery footing.

Wet, cold working conditions that increase miner fatigue, reduce efficiency and alertness, and increase absenteeism.

5. Decreased coal quality caused by--
Higher water content, which decreases BTU's.

Sediment washed into coal, which decreases BTU's and increases ash.

These particular water-related problems have long been recognized by the coal industry on a qualitative basis. However, in contrast to the AMD problem there

appears to be little if any comprehensive and quantitative analysis of their impact reported in published literature.

Significant leakage into underground workings can occur in roof strata, floor strata, or the coal seam, although significant roof inflow is apparently the most common. A survey of 10 wet mines (1) indicated that rock fractures in the mine roof and floor rock were the dominant sources of ground water inflow in all 10 mines.

MINE INFLOW SURVEY

As part of this investigation, eight underground mining operations experiencing ground water problems were visited. An initial telephone survey was made to identify mines (primarily in Appalachia) experiencing serious water problems. A distinction was made between water problems that were entirely of a quality nature (AMD) and those that were primarily caused by the quantity of water entering mine workings.

During each on-site visit, mines were qualitatively noted as exhibiting strong, moderate, or weak evidence of fracture controlled inflow. These subjective criteria were defined as follows:

Strong criteria.--Multiple examples of leakage from obvious cracks, fractures or roofbolt holes with many sources flowing in a steady stream (5 gpm or greater). Numerous reports from mining personnel of similar inflows.

Moderate criteria.--Multiple examples of leakage from cracks, fractures, and boltholes. A few flowing in steady streams but mostly drippers (1 gpm or less). Some reports from mining personnel of seasonal affects and past point source inflow.

Weak criteria.--Leakage from cracks, fractures, and boltholes evident only as drippers. Few reports of past point source inflow, no seasonal affects, no wet sections.

A summary of the results of this survey appears in table 1.

Of the eight underground mines visited, five were placed in the strong fracture inflow category, and three in the

moderate category. One surface operation was judged to be in the weak category. Fracture inflow was most evident in the roof rock of the eight underground mines.

This small sampling of mines revealed that the high volume point sources of inflow occur primarily at recently exposed workings whereas diffuse leakage is more common in older workings. In six of eight underground mines, mine and section foremen expressed their greatest concern about water problems at the active face, despite the fact that in most cases the inflow rate in these wet sections was a very small proportion of total mine inflow. Apparently most mine operators do not interpret a water problem as serious until it interferes directly with the operation of the continuous miner, shuttle car, or roof bolter, i.e., with coal production.

If major sources of inflow to the mine were diffuse or located in caved, abandoned, inactive, or other old workings in the mine, the problem was more likely to be seen entirely as an AMD problem that added to production expenses but was not considered serious enough to merit any special attention or preventive measures. Conventional methods of collection, pumping, and treatment were employed to deal with this water.

The most acidic water in a mine often was flowing from the caved or abandoned workings. Water flowing from active workings became degraded primarily as a result of mixing with more acidic water, in various mine sumps.

TABLE 1. - Coal mine water inflow survey

Location and coal seam	Depth to coal, ft	Mining method	Sections visited	Observed most inflow from--			Fracture involvement		
				Roof	Coal	Floor	Weak	Moderate	Strong
Preston County, WV, ¹ Upper Freeport.....	100- 300	RP	1	X		X			X
Clearfield County, PA, Brookville.....	200- 250	RP	2	X	X				X
Greene County, PA, Pittsburgh.....	200- 400	RP	2	X		X		X	
Indiana County, PA, Upper Freeport.....	250- 450	RP	2	X					X
Cambria County, PA, ² Lower Kittanning.....	500- 550	RP	1	X					X
Clearfield County, PA, Middle Kittanning....	100- 300	RP	1	X				X	
Tuscaloosa, AL, Pratt.	550- 650	RP	2	X					X
		LW							
Carbondale, CO, A.....	200-1,000	RP	1	X				X	
		LW							
Rockdale, TX, unknown.	100- 150	OP	3	HW	HW	HW	X		
				Serious water problems--		Floor deterioration observed	Water quality, pH		
				At face	Elsewhere		At source	Mine discharge	
Preston County, WV, ¹ Upper Freeport.....	100- 300	RP	1	X		X	6.5-7.0	3.0-3.5	
Clearfield County, PA, Brookville.....	200- 250	RP	2	X		X	³ 4.4	³ 3.0	
Greene County, PA, Pittsburgh.....	200- 400	RP	2		X	X	6.5-7.0	2.9-3.0	
Indiana County, PA, Upper Freeport.....	250- 440	RP	2	X	X	X	7.0-8.5	NT	
Cambria County, PA, ² Lower Kittanning.....	500- 550	RP	1	X		X	³ 7.4	³ 3.0-3.0	
Clearfield County, PA, Middle Kittanning....	100- 300	RP	1		X		NM	NM	
Tuscaloosa, AL, Pratt.	550- 650	RP	2	X	X	X	7.0-8.5	NT	
		LW							
Carbondale, CO, A.....	200-1,000	RP	1	X	X		8.5-9.5	NT	
		LW							
Rockdale, TX, unknown.	100- 150	OP	3	X			NM	NT	

HW Highwall. NT No treatment.

LW Longwall. OP Open pit.

NM No measurement. RP Room and pillar.

¹Bureau of Mines dewatering project.

²EPA-Wahler Associates dewatering project.

³From literature.

POINT SOURCES OF INFLOW

Point inflow sources in the active sections, especially in the roof rock, appeared to be very much fracture dependent. Inflow sources were observed most often to occur in one of three ways:

1. Contact between the mine workings and a natural geologic joint or fault.

2. Localized mining induced roof fractures that connect the mine workings with natural fracturing.

3. Roof bolt holes, which happen to be drilled into joints or bedding plane fractures.

Figure 3 is a simple schematic showing the three types of mine-fracture intercepts in cross section. Figure 4 shows an example of the roof bolt hole intercept. Note in this figure that adjacent roof bolts are producing no water whatsoever.

The roof bolt hole source is very much like a well drilled (4 to 6 ft) upside down, inside the mine. It also causes the most difficulty for miners (bolter crews especially) since they are required, in the drilling and bolting process, to work directly beneath a hole which may initially produce a 20- to 25-gpm inflow.

Fracture inflow in the mines surveyed occurs in two phases, similar to water well inflow. In the initial time-dependent phase, ground water stored in the intercepted fracture zone is released into the mine. This phase is characterized by an initially very high inflow rate which then tapers off over a period of days, weeks, or sometimes months. This time dependent interval of mine inflow is believed to depend on the following:

1. The areal extent of saturated rock fracturing (or the extent of the fracture zone) that has been tapped.
2. The recharge rate to the fracture zone (direct surface recharge could be occurring).
3. The direction and extent of mine development which may subsequently intersect the same fracture zone at a lower elevation, creating a preferred flow path for ground water inflow.

Generally, after a period of time, a steady state infiltration pattern develops at the fracture-mine intercept. In the steady-state phase, inflow is constant, though often considerably diminished from its initial rate. The steady-state inflow rate is for the most part determined by the rate at which the intercepted fracture (network) is recharged, either by ground water from the surrounding unfractured rock or by surface inflow from streams.

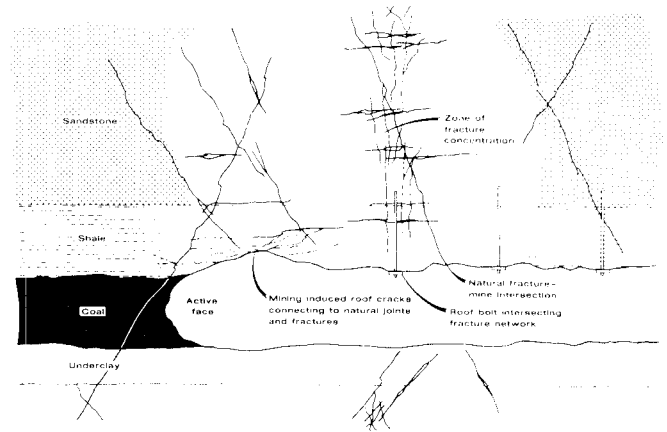


FIGURE 3. - Three types of mine fracture intercepts.

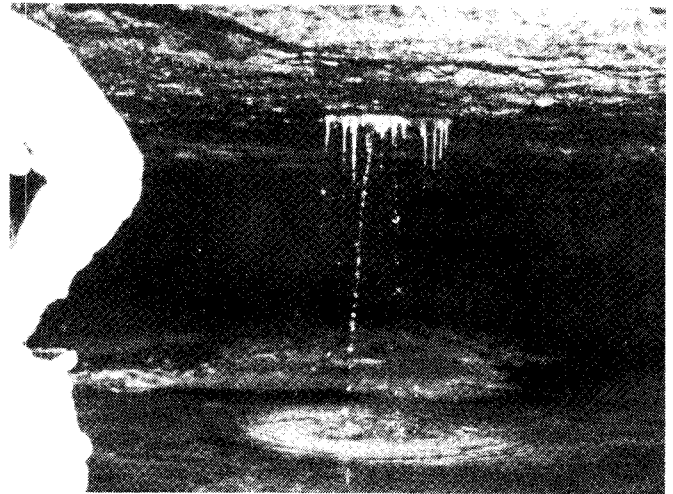


FIGURE 4. - Roof bolt hole inflow source.

In this survey, mine operators reported that it was not uncommon for a steady-state mine inflow source to intermittently revert to its initial high flow rate during periods of heavy rain or during spring snowmelt, where a good surface connection apparently existed.

The pattern of inflow in a mine influenced by fractures is therefore very often a transient one, with the highest inflow sources generally concentrated at the newly exposed workings, i.e., the active face. These sources then diminish as the face advances away from them but new sources closer to the face continually develop. Miners refer to this as water that "follows the face." This pattern of mine infiltration is characteristic of a wet section.

The occurrence of mine-fracture intercepts was observed most often in the roof, although mine-fracture intercepts in lower aquifer units are likely to occur in similar fashion. Very often, however, if the floor material is a soft fireclay, it forms an effective seal (aquitard) above the aquifer units that are below the mine. This clay seal rapidly deteriorates however, when exposed to the combined effects of roof leakage and heavy vehicle traffic.

FLOOR CONDITIONS IN A WET SECTION

As indicated previously, the severity of a mine water problem is related only partly to the quantity of water entering the mine workings. The location of inflow sources in the mine coupled with the affects of inflow on mine working conditions (mainly floor conditions) are equally important in determining the serious nature of a mine water problem.

In this survey, floor conditions near the face were the principal water-related problem reported by section foremen, especially in mines with a fireclay underlayment. Soft fireclay deteriorates when water from roof leakage causes swelling, and constant traffic churns the clay material into mud. Ruts, sumps, and low wet areas tend to develop on haulage routes. To compound the problem, as the fireclay aquitard deteriorates, piezometric pressures in the underlying aquifer cause an increase in infiltration

through the mine floor. Figure 5 shows the development of this often observed floor problem.

Fireclay material scraped from the floor was often seen piled in abandoned entries after it had been churned into mud and was impeding rubber tired haulage between face and belt head. Crushed rock and planking in troublesome areas were also observed to be common temporary fixes, as was simply loading the fireclay material out with the coal.

Very little information of a quantitative nature is available in the literature concerning the effects of ground water inflow on coal mine production. However, it has been reported (16) that production may be higher by 50 to 75 tons per shift in a dry section than in a wet section with poor floor conditions.

A question asked of two section foremen during this survey may shed some light on the reason for the mine operator's concern with water at the active face. Section foremen in two of the mines that had recently experienced wet conditions were asked to estimate the number of minutes in an 8-h day (480 min) in which the continuous miner in their section was actually cutting coal. They were then asked to estimate the effect high inflow at the face (50 to 100 gpm) and bad floor conditions would have on coal cutting time. Table 2 summarizes their responses.

TABLE 2. - Probable effects of high inflow on coal cutting time per 8-h shift

	Mine 1	Mine 2
Cutting time, min:		
Dry conditions.....	90-100	120-150
Wet conditions.....	<15- 30	<15- 45
Lost production...pct..	17- 30	13- 30

These foremen attributed the lost production time to slower response of shuttle cars traveling over muddy and deeply rutted floors, increased electrical problems, and slower, less efficient performance of equipment operators and helpers working in wet muddy conditions. One of these foremen added that persistently wet mining conditions were often accompanied by higher than average miner absentee rates as well.

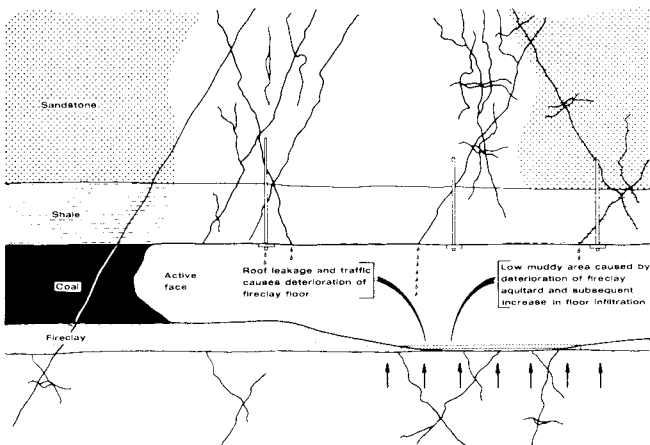


FIGURE 5. - Development of poor floor conditions at an active face.

WATER QUALITY IN A WET SECTION

The mine inflow survey revealed that in four of the five eastern U.S. underground mines surveyed, the pH of water at the point of inflow ranged from 6.5 to 8.5. Fracture inflow in one mine had a pH of 4.4 and was known to be coming from an overlying abandoned mine. Four of five mines treated their water for acidity prior to discharge, with mine effluent pH ranging from 3.0 to 4.5.

With respect to acidity and iron content, mine water at the point of infiltr-

ation was comparatively high quality if it had a more or less undisturbed ground water source. Undisturbed sources of fracture water included the surrounding unfractured aquifer material, glacial or alluvial deposits, or direct surface infiltration, i.e., streams, rainfall, snowmelt, etc. Mine inflow coming from disturbed sources such as abandoned mine workings or mine spoils was often degraded at the point of infiltration to the mine.

APPROACHES AND PROBLEMS OF PAST MINE DEWATERING EFFORTS

Several possible well dewatering schemes to control leakage into underground mines have been studied. One of the first proposed exploiting highly permeable fracture zones as possible high yield well sites for dewatering underground mines (20). A second study (21) discussed the benefits that might be achieved by reducing head levels in bedrock aquifers located immediately above and below underground coal mines. The concept of connector wells or gravity wells for mine dewatering was also introduced in these reports.

The dewatering methods proposed by these studies are intended entirely as a means of reducing acidic mine drainage from abandoned and inactive mine workings. The development and production problems that result from localized high

inflows in active mine sections are not addressed, and the dewatering methods proposed are not readily adapted to deal with the transient flow conditions that occur in active mining sections.

Of the several different coal mine dewatering schemes proposed, pumped well dewatering of sandstone aquifers to control AMD in inactive mine workings was only recently attempted (1).

Exploration and pump tests of wells revealed that ground water flows into the study area of the mine were concentrated along two fracture zones that appeared to intersect in the area of greatest inflow. These preferred and rather narrow flow paths were not revealed until after completion of observation wells and dewatering wells.

MODELING THE FRACTURE ZONE FLOW PROBLEM

The justification for including fracture zones in the siting process for dewatering wells may arise from a number of past research experiences including the following:

1. The apparent importance of mine-fracture intercepts as inflow sources in both active and inactive underground workings.

2. Past dewatering attempts that describe the prohibitively high cost of mine dewatering with wells of comparatively low yield (i.e., wells drilled without regard to preferred flow paths).

3. The more or less well established technique for locating fracture zones (fracture trace analysis) and the past use of fracture-sited wells to obtain the high-capacity pumping necessary of municipal water wells.

4. The association of high volume storage water release in wet sections with the high storage and transmissive properties of fracture zones.

5. Computer models that describe the advantageous flow pattern and higher yield of wells sited on high permeability fracture zones.

Of particular interest is the analytical justification for fracture dewatering revealed by computer modeling of fracture zone-dewatering well problems.

Depending on how the fracture flow problem is conceptualized, models of flow in fractured media generally take one of three basic approaches, termed, equivalent porous media, double porosity, or discrete fracture (22).

The equivalent porous media approach treats the fractured rock mass as statistically equivalent to a continuous and homogeneous porous medium. This is perhaps the simplest characterization of fracture flow processes.

The double porosity approach is a continuous approach also. In this approach, the fractured medium is represented by porous blocks of material surrounded by a porous network of fissures. The two systems are linked by an equation that describes flow from blocks to fissures, which involves the pressure differential between the two systems at any point (23-24).

Discrete fracture models focus attention on the geometry of individual fractures, attempting to duplicate such

features as aperture size, orientation, roughness, etc. Models that conceive of fractures as parallel planer plates (25) fall into this category.

This approach was combined with boundary element methods to model uniform flow in a porous medium incorporating multiple intersecting fracture channels (26).

For the fracture zone flow problem of this investigation, a modeling approach must be selected that is consistent with the following:

1. The geologic characterization of fracture zones.
2. The availability of field data for describing a particular fracture zone network.
3. What is considered to be the scale of the dewatering problem area, or region of hydrologic interest.

In keeping with these guidelines, the computer code developed for this investigation is a straightforward application of a semianalytical technique (27) for simulating flow regions incorporating discrete zones of differing permeability. As such, program DWATR can be classified as an equivalent porous media model of a fractured rock mass.

MODEL DEVELOPMENT

In this approach to the modeling of dewatering activity, zones of concentrated rock fracturing are treated as discrete regions of high average permeability. Flow in the aquifer is treated as two dimensional in the horizontal plane.

The modeling approach is based on superposition of elementary analytic solutions to features such as uniform flow, flow toward a well, and flow across a discontinuity in permeability. Program DWATR is also equipped with streamline tracing routines in order to track ground water particle movement.

The following section contains a summary of the basic equations for flow in a homogeneous confined or unconfined aquifer, followed by a presentation of the elementary solutions for uniform flow, flow toward a well, and flow across a discontinuity in permeability.

BASIC EQUATIONS

The components q_x , q_y , and q_z of the specific discharge vector $[L/T]$ in an isotropic porous medium are given by Darcy's law,

$$q_x = -k \frac{\partial \phi}{\partial x}, \quad q_y = -k \frac{\partial \phi}{\partial y}, \quad \text{and}$$

$$q_z = -k \frac{\partial \phi}{\partial z}, \quad (1)$$

where k is the permeability $[L/T]$ and ϕ is the piezometric head $[L]$ as measured from the bottom confining layer, which is taken to be horizontal. Continuity of flow yields

$$\frac{\partial q_x}{\partial x} + \frac{\partial q_y}{\partial y} + \frac{\partial q_z}{\partial z} = 0. \quad (2)$$

Substitution of equation 1 into equation 2 gives the Laplace equation

$$\nabla^2 \phi = 0. \quad (3)$$

Equation 3 is the differential equation for steady-state flow in an isotropic porous medium.

Regional Confined Flow

For the case of two-dimensional confined ground water flow, as illustrated in figure 6, a discharge vector with components Q_x and Q_y [L^2/T] is introduced, which represents the flow of ground water through planes of unit width, normal to the x and y axis and extending over the height, H , of the aquifer, so that

$$Q_x = \int_0^H q_x dz = H \cdot q_x \text{ and}$$

$$Q_y = \int_0^H q_y dz = H \cdot q_y. \quad (4)$$

In writing equation 4, use is made of the Dupuit-Forchheimer assumption whereby the piezometric head, ϕ , does not vary with z , so that q_x and q_y do not vary with z . Substituting Darcy's law (equation 1) into equation 4 gives

$$Q_x = \frac{-\partial kH\phi}{\partial x} \text{ and } Q_y = \frac{-\partial kH\phi}{\partial y}. \quad (5)$$

A discharge potential, Φ [L^2/T], is introduced whereby

$$\Phi = kH\phi + C_c, \quad (6)$$

so that the components of the discharge vector follow from

$$Q_x = \frac{-\partial \Phi}{\partial x} \text{ and } Q_y = \frac{-\partial \Phi}{\partial y}. \quad (7)$$

The constant C_c is arbitrary and vanishes from Q_x and Q_y .

Regional Unconfined Flow

For the case of unconfined flow, illustrated in figure 7, the components Q_x and

Q_y of the discharge vector follow from

$$Q_x = \int_0^H q_x dz = q_x \cdot \phi \text{ and}$$

$$Q_y = \int_0^H q_y dz = q_y \cdot \phi, \quad (8)$$

where the piezometric head, ϕ , is measured from the aquifer base, and where use is again made of the Dupuit-Forchheimer assumption. Equation 8 becomes, with equation 1,

$$Q_x = -k\phi \cdot \frac{\partial \phi}{\partial x} \text{ and } Q_y = -k\phi \cdot \frac{\partial \phi}{\partial y} \quad (9)$$

or

$$Q_x = \frac{-\partial (1/2k\phi^2)}{\partial x} \text{ and } Q_y = \frac{-\partial (1/2k\phi^2)}{\partial y}. \quad (10)$$

The discharge potential, Φ , for unconfined flow is then defined as

$$\Phi = 1/2k\phi^2 + C_u, \quad (11)$$

where again C_u is an arbitrary constant that vanishes from Q_x and Q_y .

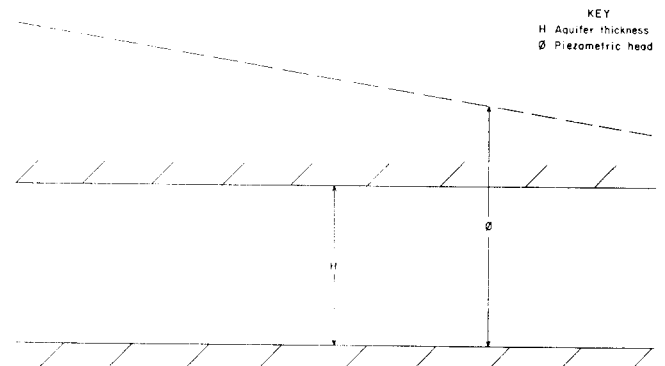


FIGURE 6. - Confined flow setting.

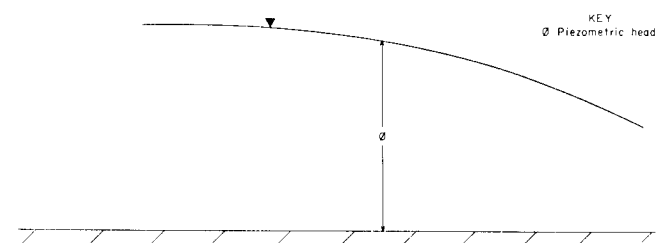


FIGURE 7. - Unconfined flow setting.

Combined Confined and Unconfined Flow

Along the boundary between regions of confined and unconfined flow in figure 8, $\phi = H$, since ϕ is continuous. The constants C_c and C_u can be chosen to ensure that the discharge potential, ϕ , is also continuous at this interregional boundary (28).

Setting $\phi = H$ in equations 6 and 11, continuity of ϕ gives

$$k \cdot H \cdot H = 1/2k\phi^2 + C_u, \quad (12)$$

selecting $C_c = 0$, it follows for C_u that

$$C_u = 1/2kH^2. \quad (13)$$

Thus a discharge potential, ϕ , in a aquifer involving both confined and unconfined flow, may be defined as

$$\phi = \begin{cases} kH\phi & \text{if } \phi \geq H \\ 1/2k\phi^2 + 1/2kH^2 & \text{if } 0 \leq \phi < H \end{cases}. \quad (14)$$

Alternatively, the expression for piezometric head, ϕ , is given as

$$\phi = \begin{cases} \phi/kH & \text{if } \phi \geq kH^2 \\ \sqrt{\frac{\phi - 1/2kH^2}{1/2k}} & \text{if } 1/2kH^2 < \phi < kH^2 \end{cases}. \quad (15)$$

In a Dupuit-Forchheimer model, the continuity equation formulated in terms of discharge vectors becomes

$$\frac{\partial Q_x}{\partial x} + \frac{\partial Q_y}{\partial y} = 0, \quad (16)$$

so that La Place's equation becomes

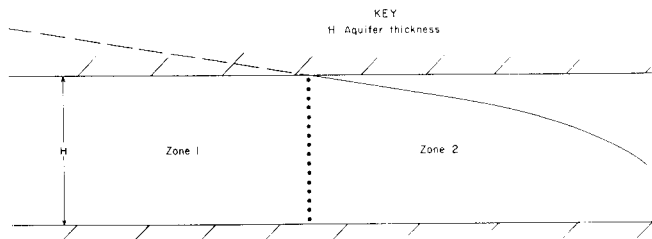


FIGURE 8. - Confined and unconfined flow, combined.

$$\frac{\partial^2 \phi}{\partial x^2} + \frac{\partial^2 \phi}{\partial y^2} = 0, \quad (17)$$

where ϕ is defined by equation 14.

It is noted that the solution to the ground water flow problem formulated in terms of ϕ does not distinguish between confined or unconfined flow conditions. Hence the boundaries between regions of confined and unconfined flow need not be known beforehand. Once ϕ has been determined as a function of location, these flow conditions simply follow from the value of ϕ in equation 15.

ELEMENTARY SOLUTIONS

The solution to a flow problem containing such features as uniform flow, flow toward wells, and discontinuities in the permeability may be obtained by superimposing the elementary solution to each feature. The discharge potential, ϕ , for the combined solution still satisfies equation 17, since equation 17 is linear in ϕ . The following section presents the elementary solutions used in the present model.

Complex Potential Function

An analytic complex function $\Omega = \Omega(z)$ is introduced here as (see references 29 and 30),

$$\Omega(z) = \phi(z) + i\psi(z), \quad (18)$$

where ($z = x + iy$). The real part of this complex potential function, $\text{Re}[\Omega(z)]$, is the discharge potential as given by equation 15 and the imaginary part, $\text{Im}[\Omega(z)]$, is termed the stream function.

The stream function is constant along streamlines, and the total discharge between two streamlines is equal to the difference in their stream function values (see reference 30).

$\phi(z)$ and $\psi(z)$ are related by the Cauchy-Riemann conditions,

$$\frac{\partial \phi}{\partial x} = \frac{\partial \psi}{\partial y} \quad \text{and} \quad \frac{\partial \phi}{\partial y} = -\frac{\partial \psi}{\partial x}. \quad (19)$$

It follows from equations 19 and 17 that both ϕ and ψ are harmonic functions, whereby ψ is termed the conjugate harmonic of ϕ .

Uniform Flow

The complex potential for uniform horizontal flow, $\Omega_f(z)$ (29), is presented here as

$$\Omega_f(z) = V_\gamma H z e^{-i\gamma} + C, \quad (20)$$

where V_γ is the natural ground water flux, [L/T], in a direction, γ , measured with respect to the positive x axis. The constant, C, in equation 20 is arbitrary.

Flow Toward a Well

The complex potential, $\Omega_w(z)$, for a single completely penetrating well at a point, z_o , is presented in ground water flow texts (e.g., reference 29) as

$$\Omega_w(z) = \frac{Q}{2\pi} \ln(z-z_o) + C, \quad (21)$$

where Q is the well strength (discharge rate) [L³/T].

Separating $\Omega_w(z)$ into real and imaginary parts gives

$$\begin{aligned} \phi_w(z) + i\psi_w(z) &= \frac{Q}{2\pi} \ln|z-z_o| \\ &+ \frac{iQ}{2\pi} \arg(z-z_o) + C, \end{aligned} \quad (22)$$

where the imaginary part

$$\psi_w(z) = \frac{Q}{2\pi} \arg(z-z_o), \quad (23)$$

is the stream function for the well. The argument of z is chosen as

$$-\pi \leq \arg(z) \leq \pi.$$

As appears from equation 22, equipotentials are concentric circles around the well, while streamlines are radials from the well. It is noted that the stream function jumps by the amount Q when

crossing the negative axis. This discontinuity in ψ_w for $x < x_o, y = y_o$ is termed the branch cut.

The superposition principle enables a multiple well pattern to be modeled simply as the sum of individual well solutions. The general solution for flow toward n wells then follows from

$$\Omega_w(z) = \sum_{j=1}^n \frac{Q_j}{2\pi} \ln(z-z_j) + C, \quad (24)$$

where z_j is the location and Q_j the strength of the jth well.

Flow Across a Permeability Discontinuity

In figure 9, a cross section of a confined aquifer is depicted containing two zones of different permeability. On the left (-) side, of the dotted vertical the permeability is k_o , and on the right (+) side the permeability is k_1 . Since the piezometric head is continuous on the boundary between k_o and k_1 , it follows from equation 14 that the relation between ϕ_o and ϕ_1 at the permeability discontinuity is

$$\phi_1 = \frac{k_1}{k_o} \cdot \phi_o, \quad (25)$$

where the subscripts in ϕ_o and ϕ_1 , denote the permeability used in equation 14. As seen from equation 25, the potential is discontinuous across the jump in permeability. The discontinuity, $\Delta\phi$, may be expressed in terms of ϕ_o as

$$\Delta\phi = \phi_1 - \phi_o = \left(\frac{k_1 - k_o}{k_o}\right) \cdot \phi_o. \quad (26)$$

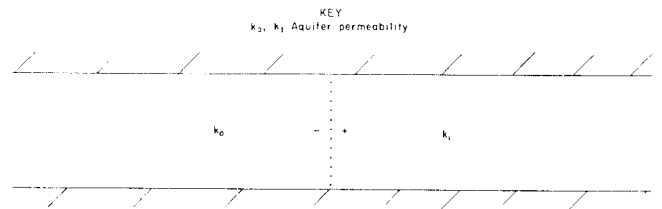


FIGURE 9. - Permeability discontinuity.

In order to model this jump in potential, use is made of line doublets as presented in reference 27 for modeling flow domains containing regions of different permeabilities.

The potential due to a line doublet is discontinuous across the line doublet. This discontinuity in the potential is equal to the doublet strength. Line doublets with varying strengths are distributed along the boundary between zones of different permeability in order to satisfy equation 26. The use of line doublets in the DWATR model is briefly described in the following.

The complex potential due to a line doublet with a second order strength distribution, as given in reference 27, is

$$\Omega_p(z) = -i \frac{S(z)}{2\pi} \ln \left(\frac{z_{\ell}+1-z}{z_{\ell}+1-z} \right) + \mu(z), \quad (27)$$

where S is defined as

$$S(z) = S_{\ell} \left(\frac{z_{\ell}+1-z}{z_{\ell}+1-z_{\ell}} \right) + S_{\ell}+1 \left(\frac{z_{\ell}-z}{z_{\ell}-z_{\ell}+1} \right) - 4\mu_{\ell} \frac{(z-z_{\ell})(z-z_{\ell}+1)}{(z_{\ell}-z_{\ell}+1)^2}, \quad (28)$$

and μ is defined as

$$\mu(z) = \frac{2i\mu_{\ell}}{\pi} \left(\frac{z-1/2(z_{\ell}+z_{\ell}+1)}{z_{\ell}+1-z_{\ell}} \right). \quad (29)$$

In equation 27, z_{ℓ} and $z_{\ell}+1$ are the endpoints of the line doublet. In equation 28, S_{ℓ} and $S_{\ell}+1$ are real numbers representing the strength of the doublet at endpoints z_{ℓ} and $z_{\ell}+1$, and μ_{ℓ} is the parabolic component of strength defined such that the strength at the midpoint between and z_{ℓ} and $z_{\ell}+1$ equals $1/2(S_{\ell} + S_{\ell}+1) + \mu_{\ell}$.

That the real part of equation 27, the potential, is indeed discontinuous across the line doublet, may be seen as follows. If $z = \delta$, where δ is on the line doublet, equation 28 is real, so that the potential, $\Phi_p(\delta)$, becomes

$$\Phi_p(\delta) = \frac{S(\delta)}{2\pi} \cdot \theta, \quad (30)$$

where θ is the imaginary part of the logarithm in equation 27,

$$\theta = \arg \left(\frac{z_{\ell}+1-\delta}{z_{\ell}-\delta} \right). \quad (31)$$

The angle θ is $+\pi$ if δ is selected on the upper side of the line doublet (see figure 10), and $-\pi$ if δ is on the lower side. Consequently the potential, $\Phi_p(\delta)$, in equation 30 jumps by an amount $S(\delta)$ when crossing the line doublet, whereby $S(\delta)$ varies parabolically over the line element.

It may be seen from equation 28 that $S(\delta)$ assumes the values S_{ℓ} , $1/2(S_{\ell}+S_{\ell}+1) + \mu_{\ell}$ and $S_{\ell}+1$ when δ is z_{ℓ} , $1/2(z_{\ell}+z_{\ell}+1)$ and $z_{\ell}+1$, respectively. The potential along each side of a line doublet is plotted in figure 10.

The doublet strength, $S(\delta)$, may be expressed in terms of $\Phi_o(\delta)$ by use of equation 26,

$$S(\delta) = \left(\frac{k_1 - k_o}{k_o} \right) \cdot \Phi_o(\delta). \quad (32)$$

The imaginary part of equation 27, the stream function $\Psi_p(z)$, is continuous everywhere, so that the discharge normal to the line doublet is continuous. Therefore, doublets that model the jump in potential across permeability discontinuities preserve continuity of flow across the boundary.

MODELING FRACTURE ZONES

Zones of concentrated rock fracturing are modeled as discrete zones of high average permeability. Line doublets are distributed end to end along the entire closed boundary of the fracture zone to account for the jump in potential that results from this discontinuity in aquifer permeability.

A fracture flow problem may involve more than one zone of high permeability, furthermore, wells may be located both inside and outside of these zones. Flow resulting from far field conditions is introduced by means of a uniform gradient of flow across the domain of interest.

The uniform flow rates and the well discharges are considered known, but the doublet strengths along discontinuities in permeability are not known in advance. Their values depend on the potential along the doublets as given by equation 32. Imposing the condition of equation 32 at a number of control points along the line doublet results in a set of equations for which the unknown strength parameters may be solved. Once the doublet strengths are determined, the potential in the aquifer can be evaluated as the sum of the potentials due to the uniform flow, all wells and all doublets.

Matrix Equations

Consider the flow domain depicted in figure 11, with permeability k_1 inside the region depicted and k_0 outside. Figure 11 illustrates an idealized fracture zone flow problem in which intersecting zones of rock fracturing are modeled as a single high permeability region. A well is situated at the fracture zone intersection.

Fifty-eight line doublets are used to define the boundary of this high permeability fracture zone. Thus there are 58 unknown strengths, S_ℓ , defined at doublet endpoints, and 58 unknown parabolic strength parameters, μ_ℓ , defined at doublet midpoints. The condition of equation 32 is imposed on all doublet endpoints and midpoints, i.e., on all control points.

This leads to the following 58 equations for line doublet endpoints, δ_j , ($j = 1, 2, \dots, 58$)

$$S_\ell \Lambda_{\ell j} + \mu_\ell \chi_{\ell j} + G_j + \Phi_0 = \left(\frac{k_0}{k_1 - k_0} \right) S_j, \quad (33)$$

$$(\ell = 1, 2, \dots, 58),$$

and the following 58 equations for the line doublet midpoints, δ_j , ($j = 59, 60, \dots, 116$),

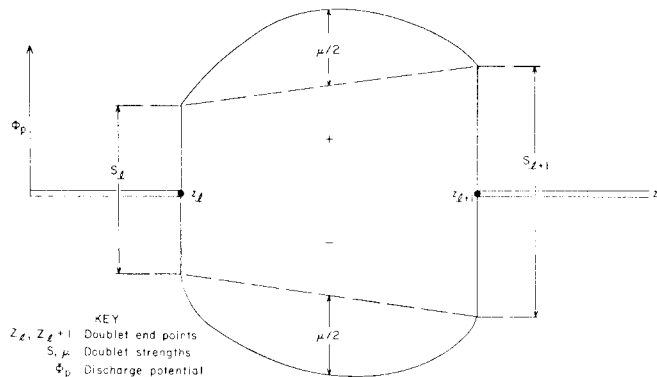


FIGURE 10. - Jump in potential at a line doublet.

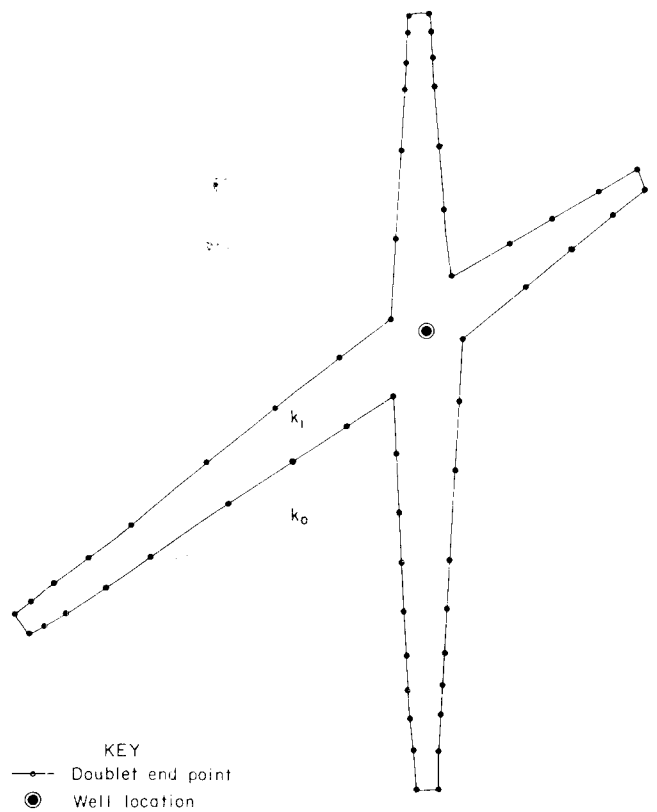


FIGURE 11. - Idealized fracture zone setting.

$$S_\ell \Lambda_{\ell j} + \mu_\ell \chi_{\ell j} + G_j + \Phi_0 = \left(\frac{k_0}{k_1 - k_0} \right) \frac{S_{j-58} + S_{j-57}}{2} + \mu_{j-58}, \quad (34)$$

$$(\ell = 1, 2, \dots, 58),$$

where $S_{59} = S_1$ and $\mu_{59} = \mu_1$.

The coefficient functions $\Lambda_{\ell j}$ and $\chi_{\ell j}$ are defined as

$$\Lambda_{\ell j} = \frac{1}{2\pi} \left[\left(\frac{z_{\ell+1}-\delta_j}{z_{\ell+1}-z_\ell} \right) \cdot \arg \left(\frac{z_{\ell+1}-\delta_j}{z_\ell-\delta_j} \right) - \left(\frac{z_{\ell+1}-\delta_j}{z_{\ell+1}-z_\ell} \right) \cdot \arg \left(\frac{z_\ell-\delta_j}{z_{\ell+1}-\delta_j} \right) \quad (\ell \neq j) \right] \quad (35)$$

and

$$\chi_{\ell j} = \frac{-2}{\pi} \left(\frac{(\delta_j - z_\ell)(\delta_j - z_{\ell+1})}{(z_\ell - z_{\ell+1})^2} \right) \cdot \arg \left(\frac{z_{\ell+1}-\delta_j}{z_\ell-\delta_j} \right). \quad (36)$$

Special care must be taken in calculating Λ_{jj} since the argument function in equation 35 contains a removable singularity. The expression for Λ_{jj} is

$$\Lambda_{jj} = \frac{1}{2\pi} \arg \left(\frac{z_{j+1}-\delta_j}{z_{j-1}-\delta_j} \right). \quad (37)$$

The function G_j contains all known contributions to the potential,

$$G_j = \text{Re} [\Omega_w(\delta_j) + \Omega_f(\delta_j)], \quad (38)$$

where $\Omega_w(\delta_j)$ and $\Omega_f(\delta_j)$ are the complex potentials due to wells and uniform flow.

Equations of the form of equations 33 and 34 contain 116 unknown strength parameters, S_ℓ and μ_ℓ , and an unknown potential, Φ_0 . Specifying the potential Φ^* at a point outside the domain of interest provides the additional equation

$$S_\ell \Lambda_{\ell j} + \mu_\ell \chi_{\ell j} + G_j + \Phi_0 = \Phi^* \quad (j = 117), \quad (39)$$

necessary to solve for the unknown doublet parameters.

These 117 equations may be written in matrix form

$$a_{\ell j} \cdot x_\ell = y_j, \quad (40)$$

where $a_{\ell j}$ becomes, with equations 33 through 39,

$$\begin{aligned} a_{\ell j} &= \Lambda_{\ell j} - \delta_{\ell j} \left(\frac{k_0}{k_1 - k_0} \right) && \text{for } (\ell = 1, 2, \dots, 58), \\ & && (j = 1, 2, \dots, 58) \\ a_{\ell j} &= \chi_{\ell j} && \text{for } (\ell = 59, 60, \dots, 116), \\ & && (j = 1, 2, \dots, 58) \\ a_{\ell j} &= \Lambda_{\ell j} - \delta_{\ell j} \left(\frac{k_0}{k_1 - k_0} \right) - \delta_{\ell, j+1} \left(\frac{k_0}{2(k_1 - k_0)} \right) && \text{for } (\ell = 1, 2, \dots, 58) \\ & && (j = 59, 60, \dots, 117) \\ a_{\ell j} &= \chi_{\ell j} - \delta_{\ell j} \left(\frac{k_0}{k_1 - k_0} \right) && \text{for } (\ell = 59, 60, \dots, 116), \\ & && (j = 59, 60, \dots, 117) \end{aligned} \quad (41)$$

and

$$a_{\ell j} = 1 \quad \text{for } (\ell = 117) \\ (j = 1, 2, \dots, 117),$$

and where $\delta_{\ell j}$ is the Kronecker delta

$$\begin{aligned}\delta_{\ell j} &= 1 \text{ if } \ell = j \text{ and} \\ \delta_{\ell j} &= 0 \text{ if } \ell \neq j.\end{aligned}\quad (42)$$

The vectors x_{ℓ} and y_j in equation 40 are given by

$$\begin{aligned}x_{\ell} &= S_{\ell} \text{ for } (\ell = 1, 2, \dots, 58), \\ x_{\ell} &= \mu_{\ell-58} \text{ for } (\ell = 59, 60, \dots, 116), \\ x_{\ell} &= \phi_0 \text{ for } (\ell = 117),\end{aligned}\quad (43)$$

and

$$y_j = G_j \text{ for } (j = 1, 2, \dots, 117). \quad (44)$$

The solution vector, x_{ℓ} , is obtained in equation 40 by use of Gauss Jordan elimination (see reference 31).

Plotting Piezometric Head Contours

Once the solution vector is known, i.e., once S_{ℓ} and μ_{ℓ} are known, the potential at an arbitrary point z in the domain of interest is obtained from

$$\begin{aligned}\phi(z) &= \text{Re} [\Omega_p(z) + \Omega_w(z) \\ &\quad + \Omega_f(z)] + \Phi_0,\end{aligned}\quad (45)$$

where $\Omega_p(z)$, $\Omega_w(z)$, and $\Omega_f(z)$ are the complex potentials, due respectively to all zones, all wells, and uniform flow.

Piezometric head contours are obtained by first calculating ϕ at a network of points, using equations 45 and 15. A

Program DWATR was developed using the semianalytic method just described. The program was written in Fortran 77 and run on a minicomputer with a 16-bit processor and 1.0 megabyte of internal memory. Virtual memory was used for runs involving more than 150 line doublets.

While streamlines are generated numerically using one of the two Newton-Raphson

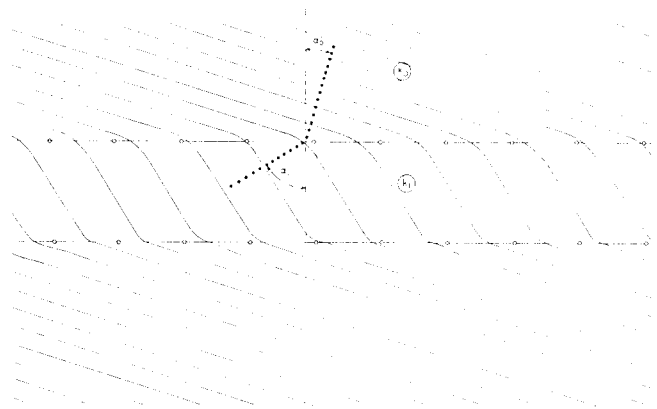


FIGURE 12. - Inhomogeneity in a strip.

cubic spline technique is used to generate contour plots (see reference 32).

Validation

Program DWATR has been validated by solving a problem of uniform confined flow in a homogeneous region of permeability, k_0 , containing a homogeneous infinite strip of permeability, k_1 . The exact solution to this problem is described in reference 33. At the boundary between k_0 and k_1 , the refraction of piezometric contours may be represented as

$$\frac{\tan \alpha_1}{\tan \alpha_0} = \frac{k_1}{k_0}, \quad (46)$$

where α_0 and α_1 are angles indicated in figure 12. The location of doublet endpoints on the boundary between k_0 and k_1 are also indicated. In figure 12, $k_1/k_0 = 5$, $\alpha_0 = 17.5$, and $\alpha_1 = 57.5$. Thus the refraction of contour lines predicted by program DWATR appears to be correct.

PROGRAM DWATR

subroutines incorporated in DWATR, streamline plots (and contour maps) are generated by separate programs. Appendix A describes program modules and input-output (I-O) logical unit numbers.

Streamline data created by DWATR are output to disk I-O units 15 and 17. Contour data are output to I-O units 15 and 13. A significant portion of DWATR's

computation time involves calculating the exact strengths at line doublet control points. For computational efficiency these strengths are output to (and may be reinput from) logical unit 19.

DWATR input parameters and their formats are listed in appendix B. Appendix C is a source listing of the program.

A magnetic tape copy of DWATR, sample I-O data sets, and graphical support programs are all available from the Bureau's Twin Cities (MN) Research Center.

IDEALIZED FRACTURE ZONE SIMULATION

The idealized fracture zone setting depicted in figure 11 serves as the initial application of DWATR. Two intersecting fracture zones are modeled as a single high-permeability region. The ratio of permeabilities inside and outside the region is given by $k_1/k_0 = 1,000$. A well is simulated at the center of the region. Uniform flow is also assumed to occur.

The boundary of the high-permeability region in this figure is composed of 58 line doublets. Doublet strengths are interpolated parabolically between endpoints leading to 116 strength parameters, to be calculated along the boundary.

The accuracy with which line doublets approximate the jump in potential at a permeability zone boundary depends, naturally, on how well a second order doublet approximation represents the actual strength distribution on the boundary. Therefore, selecting the number and spacing of line doublet endpoints is important to obtaining an accurate simulation of a particular flow problem. Too few line doublets along a boundary leads to significant errors of approximation in both ϕ and ψ near the zone boundary. Tracing streamline paths using Newton's method is especially difficult in this case.

In figure 11, doublets are concentrated at the ends of the fracture zone where the gradient in ϕ is steepest. Since strength, S , is proportional to ϕ at the permeability zone boundary, a concentration of doublet control points is often necessary along intervals of the boundary

where equipotential lines are compressed together.

A piezometric surface is developed for the flow problem depicted in figure 11. In figure 13, drawdown of the piezometric surface in the vicinity of the well is clearly influenced by the high permeability fracture zone. The theoretical maximum discharge from this well is limited by the requirement that $\phi > 0$ at the well radius. Maximum discharge is increased by a factor of 2.65 as a result of the fracture zone setting.

APPROPRIATE APPLICATIONS FOR DWATR

The fracture valley settings for which DWATR is appropriate are those where the coal seam is overlain by a single aquifer unit. The aquifer is often confined by a shale layer beneath hilltops and unconfined beneath deeply incised stream valleys. Typically this shallow aquifer is intensely fractured beneath the valley bottom. Numerous fracture traces also cut across the valley bottom, and extend

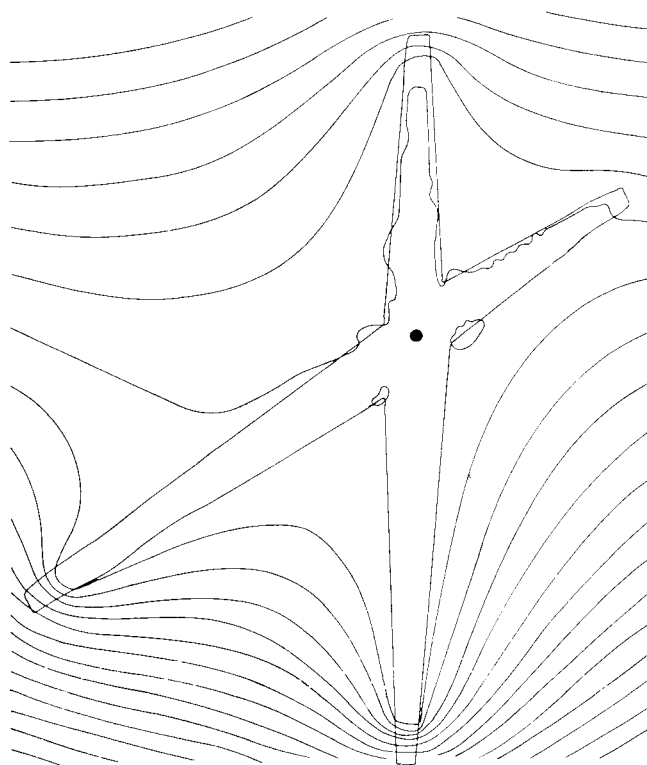


FIGURE 13. - Idealized fracture zone piezometric surface.

hundreds or thousands of feet into the adjacent hills.

Other hydrogeologic features encountered in mine dewatering problems include layered aquifer systems, concentrated surface infiltration to fracture zones, and drainage into nearby underground mine voids. Program DWATR is presently unable to handle these complexities.

These constraints on the application of this model imply that at this stage in its development the model can be used most effectively to aid in conceptual understanding of ground water flow associated with fracture zone well sitings, in addition to providing additional justification for focusing mine dewatering attention on preferred (high permeability) ground water flow paths, such as fracture zones.

Application of DWATR at the Sunshine Mine (West Virginia) dewatering test site was not undertaken until after the dewatering field work had been completed. It is suggested however that hydrology modeling and field dewatering activity be performed more or less concurrently. Conceptual understanding of a dewatering problem increases most when the problem is used in an experimental fashion to discern the relationship between various parameters and the sensitivity of the overall setting to manipulation of parameter values.

Program DWATR may supply an explanation for seemingly anomalous pump test results. It may be used to predict the impact of introducing new wells and it can suggest where additional field data (permeability measures, details of fracture zones, etc.) should be collected in order to fill gaps of understanding.

SUNSHINE MINE DEWATERING SITE

The Sunshine Mine is a small, underground room and pillar operation. The mine is located in the Monongahela River basin in northcentral West Virginia (fig. 14). Geologically it lies almost on the axis of the Kingwood syncline. The valley setting that overlies a portion of the Sunshine Mine workings is known locally as Crab Orchard Run (fig. 15). Most of the ground water inflow problems

at the Sunshine Mine workings occurred in the vicinity of this valley.

The coal seam being mined is the Upper Freeport and the depth to coal beneath Crab Orchard Run averages 110 ft. The Upper Freeport coal is overlain by the Conemaugh Formation and underlain by the

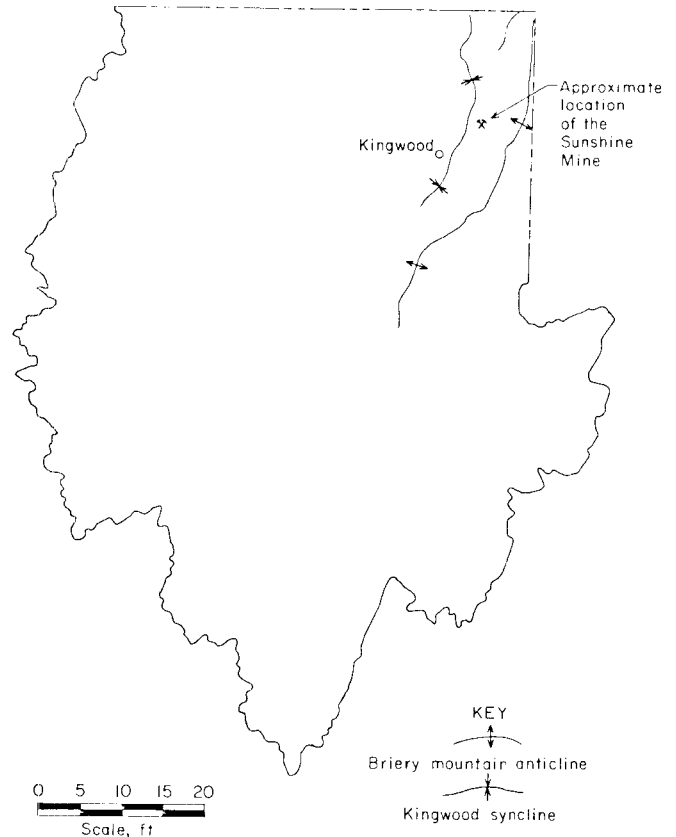


FIGURE 14. - Location of the Sunshine Mine dewatering test site in the Monongahela River basin of West Virginia (3).

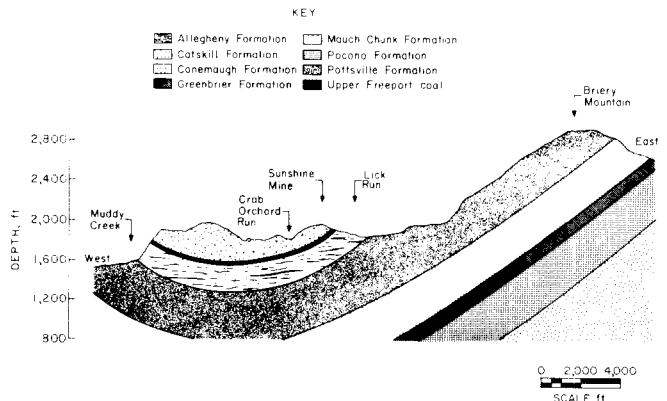


FIGURE 15. - Sunshine Mine location within the Kingwood syncline (3).

Allegheny Formation (3). The Briery Mountain anticline, elevated 1,000 ft above the bottom of Crab Orchard Run and approximately 3 miles east, is believed to be a regional source of recharge for deeper sandstone units below the coal seam, creating an underlying east to west gradient of flow in the Kingwood syncline.

A portion of the topographic map which includes Crab Orchard Run is reproduced in figure 16. Overlain on this map are the Sunshine Mine workings, the photolinear features (fracture traces) that are indicators of high-permeability fracture zones in underlying rock units (35), and the locations of 18 wells and piezometer holes constructed within Crab Orchard Run, as part of this investigation.

Most of the fracture traces are concentrated in the valley bottom, however, five well-defined zones that cut across the valley are also indicated in this figure. More detailed specifications for the wells and piezometer holes annotated on this figure appear in table 3.

Mining company records indicate that the strike of the coal seam is 40° west of north and the dip is to the southwest at 3.4° (6 pct). Geologic cross sections appearing in figures 17 through 19 were constructed from well and core hole data obtained in the vicinity of the mine. In addition to the Upper Freeport coal, these cross sections show the orientation and thickness of a shallow sandstone layer that lies above the coal seam. Figure 16 shows the location of these cross sections in plan view.

Wells labeled 32-45, 32-47, and 32-48 on figure 16 were core holes drilled earlier by the mining company. Water level measurements in these holes were not available.

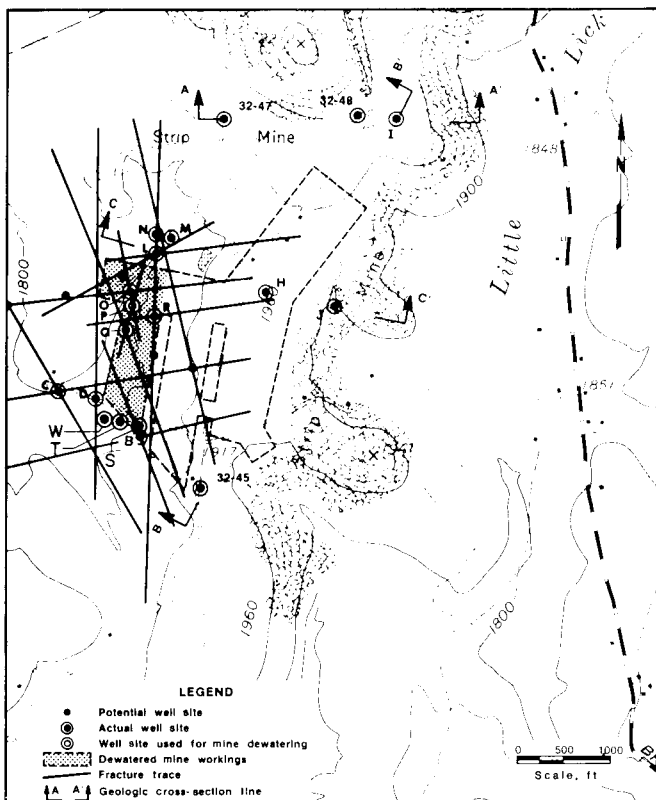


FIGURE 16. - Fracture traces and well locations in the vicinity of Crab Orchard Run (34).

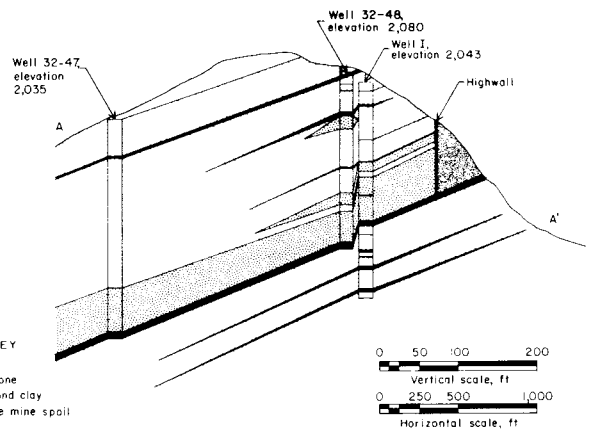


FIGURE 17. - Geologic cross section at AA'.

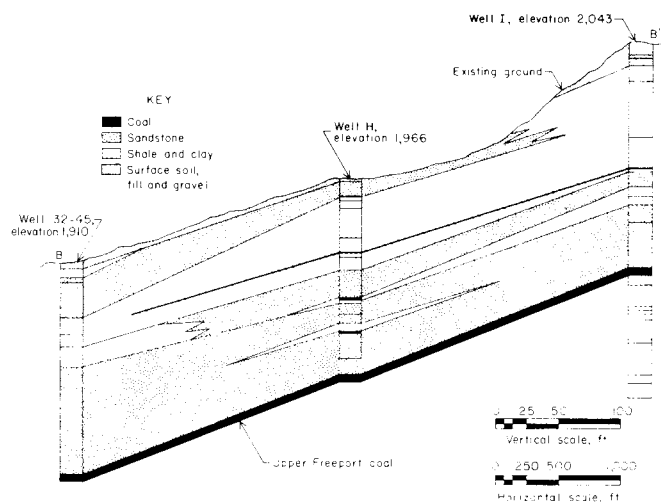


FIGURE 18. - Geologic cross section at BB'.

TABLE 3. - Crab Orchard Run well and aquifer data, feet

Well	Coordinates		Elevation ¹	Well depth	Casing length	Upper Freeport coal elevation	Static water level--		Shallow confined aquifer thickness	Fracture zone status
	x	y					Elevation	Above datum ²		
B.....	50	-2,100	1,800	458	27	1,645	1,756.0	NAP	140	Int.
C.....	-1,750	-1,200	1,777	501	141	1,646	1,711.5	NAP	54	Int.
D.....	-850	-1,350	1,775	454	12	1,652	1,740.2	NAP	111	Single.
H.....	2,700	1,000	1,966	³ 140	8	^e 1,791	1,906.0	218.0	105	None.
I.....	5,300	4,800	2,043	275	174	1,869	1,893.0	NAP	70	Do.
L.....	200	1,800	1,807	314	120	1,708	1,724.0	NAP	99	Int.
M.....	800	2,200	1,811	82	8	^e 1,709	1,802.2	114.2	100	None.
N.....	200	2,200	1,816	200	119	1,714	1,762.9	NAP	102	Single.
O.....	-300	950	1,801	218	9	1,697	1,786.8	NAP	104	Int.
P.....	-250	750	1,795	216	9	1,694	1,786.9	NAP	101	Int.
Q ⁴	-300	200	1,788	³ 112	0	³ 1,688	1,781.5	93.5	100	Int.
R.....	250	500	1,791	220	28	1,698	1,766.0	NAP	93	Int.
S ⁴	100	-2,000	1,807	³ 160	0	1,651	1,760.0	72.0	NA	Single.
T ⁴	-350	-1,850	1,803	³ 140	0	1,648	1,734.2	46.2	NA	None.
W ⁴	-600	-1,750	1,783	^e ³ 140	0	^e 1,650	1,734.6	46.6	NA	Do.
32-45 ⁵ .	1,300	-3,150	1,910	173	0	1,773	NA	NA	90	Do.
32-47 ⁵ .	1,600	4,200	2,035	272	0	1,780	NA	NA	NA	Do.
32-48 ⁵ .	4,500	4,800	2,080	214	0	1,875	NA	NA	86	Do.

^eEstimate. Int Intersection.

¹Wellhead.

²1,688 ft (Upper Freeport coal elevation at well Q).

³Shallow aquifer hole.

⁴Piezometer hole.

⁵Core hole.

NOTE.--All measurements taken in June 1982.

ANALYSIS OF FIELD DATA

The fracture trace analysis indicated that a dense network of fracture zones exists beneath Crab Orchard Run. Ten wells were drilled in this valley, both on and off the fracture traces (see figure 16).

Pumping was performed in each of these wells to obtain a rough measure of a well's sustainable yield and its consequent value for dewatering, however, pump tests to obtain a quantitative measure of permeability involved only four wells, D, O, P, and Q. The results of pump tests performed on this site are summarized in table 4.

The pump test results clearly indicate that most of the ground water flowing to the wells drilled in Crab Orchard Run was coming from the shallow aquifer unit indicated in figures 17 through 19 (34). As can be seen in figure 19, this shallow sandstone unit ranges from 85 to 130 ft thick. It is unconfined in the valley

and confined by an overlying shale layer beneath adjacent hills. Below this aquifer is the 36- to 44-in thick Upper Freeport coal seam, and below the seam is a 5- to 20-ft-thick fireclay layer. Subsequent modeling investigations and mine-aquifer dewatering activity will focus on this shallow sandstone unit.

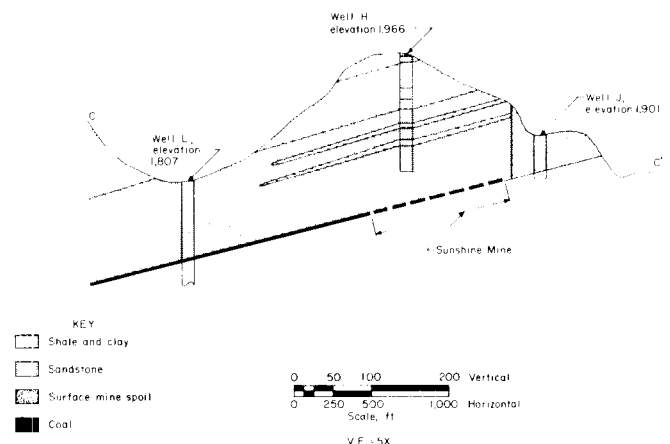


FIGURE 19. - Geologic cross section at CC'.

TABLE 4. - Summary of calculated values of transmissivity, permeability, and storativity from all pump tests (34)

Well		Section of rock	Method	Transmissivity, gpd/ft	Permeability		Storativity
Pumping	Observation				gpd/ft ²	m/h	
D	D	Entire hole.....	Specific capacity estimate, 1 h.	400	NAp	NAp	NAp
D	D	90 to 280 ft.....	Theis recovery method.	31.3	0.16	0.00027	NAp
D	D	75 to 90 ft.....	...do.....	1,193	79.5	.14	NAp
P	Q	Water table aquifer.	Time-drawdown in observation well; Theis fit.	15,916	NAp	NAp	0.008
P	Q	Water table aquifer. Same as above but for upper 32 ft dewatered.	Time-drawdown in observation well; Boulton delayed curve fit.	2.674	NAp	NAp	.001
P	P	Entire saturated hole.	Specific capacity estimate, 1 h.	37,000	NAp	NAp	NAp
P	P	...do.....	...do.....	10,000	NAp	NAp	NAp
O	O	18.58 to 218 ft...	...do.....	19,000	NAp	NAp	NAp
O	O	31.58 to 218 ft...	...do.....	1,300	7.05	.012	NAp
O	O	18.58 to 31.58 ft.	Specific capacity estimate and calculation.	17,700	1,475	2.5	NAp

D Single fracture sited. O,P Fracture intersection sited. Q Observation only.
 NAp Not applicable.

A shallow ground water flow gradient probably runs from the hills just east and north of Crab Orchard Run southwest to the broader southern part of the valley.

The difference in head between wells H and Q (table 4) is used to estimate the rate of ground water flow in this shallow aquifer. With the low (intergranular) permeability values from pump tests at wells D and O (see table 4), uniform flow rates are estimated to range from 8.0 to 330.0 ft/yr (porosity is 0.1).

PARAMETERIZATION OF THE AQUIFER SETTING

For this simulation, the fracture influence on aquifer permeability is assumed to be uniformly distributed throughout the entire thickness of the shallow aquifer, within specified high-permeability zones.

The datum for this problem is the top of the Upper Freeport coal seam at well Q

(elevation 1,688 ft). The coal and underlying shale layers form the bottom confining layer for the shallow aquifer.

High-permeability fracture zones are defined largely according to the valley outline of Crab Orchard Run. However fracture zones that cut across the valley are especially important, because of their orientation with respect to the direction of uniform flow. These fracture zones are individually identified and included within a high-permeability zone. Transverse fractures are assumed to extend for at least 1,000 ft beneath the adjacent hills and they are often the most clearly visible on stereopaired aerial photographs.

In order to accommodate a line doublet representation of fracture zones, and also to reduce the numerical computation associated with streamline tracing, the width of individually identified fracture zones is defined uniformly as 100 ft.

Permeability zones are superimposed on the fracture trace network of Crab Orchard Run, in figure 20. The zone having the highest permeability is designated k_2 . This zone includes the central valley bottom and the individual transverse fracture zones. All those dewatering wells, that had a 24-h sustained yield exceeding 100 gpm were included within this zone (see figure 16).

Specifically, this includes a portion of the valley to the southwest in the vicinity of well C. Well C was the single most productive well drilled during this project, sustaining a 500- to 700-gpm discharge rate for over 8 h.

Well D, although it was barely able to sustain 20 gpm, is located within k_2 , but very close to the boundary. Well D was a compromise location when it was discovered that the fracture intersection just north of it was inaccessible to drilling equipment.

Two other high-permeability regions were also defined, k_1 in the northern part of the valley in the vicinity of wells L, M, and N and k_3 in the southeastern area, near wells B and S. Although fracture zones were believed to be located in these areas of the valley, wells on these sites sustained yields of only 5 to 60 gpm. While this is significantly more than the 1- to 5-gpm yield of a typical domestic well in the area, it indicates that the fracture connection at these sites may be more limited than in the central part of the valley.

At the north end of the valley zone k_1 was defined so as to exclude well M, which was not fracture sited, and which maintained a static level that was 15 to 20 ft higher than other wells in the valley. Otherwise zone k_1 conformed to the valley contour. In the southwest, zone k_3 was defined in order that wells B and S could be included, but wells T and W excluded. The reason for this stems from the much higher static head in shallow well S over that of nearby shallow wells T and W (see table 3). This seems to indicate that natural ground water flow from the northeast is recharging the area around well S much more readily, perhaps via fractures. Static head in well S is

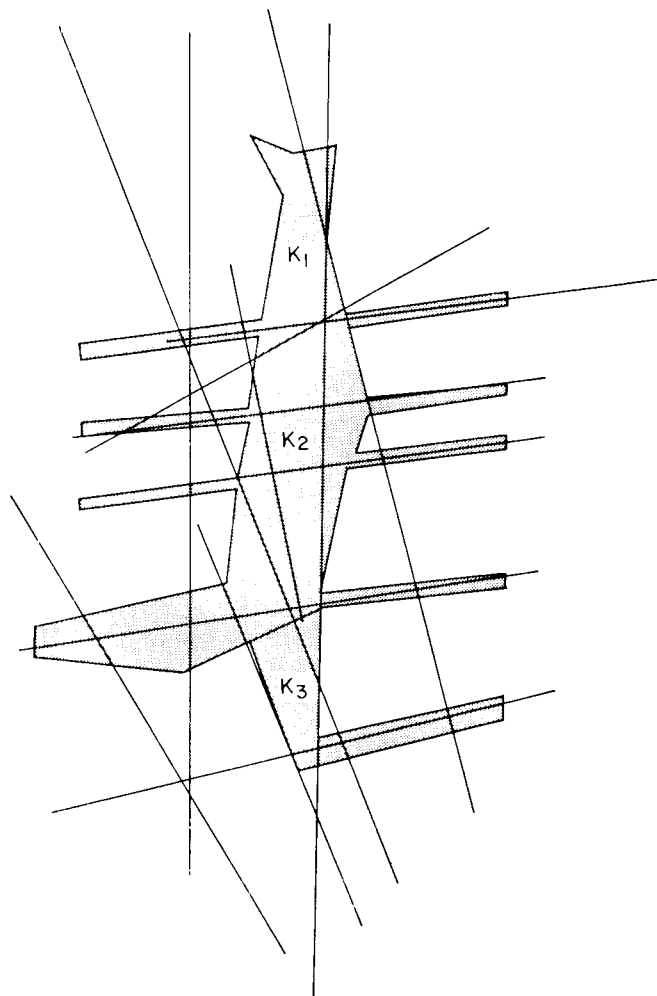


FIGURE 20. - Permeability zone representation of fracture traces near Crab Orchard Run.

nearly the same as that of well B, which is known to be sited on an intersection. Well S is also very near a north-south fracture trace.

Static Background Simulations

Static water level measurements at six shallow well locations in the vicinity of the mine (table 4) were used as criteria for judging the accuracy of a simulation of the shallow aquifer setting, prior to well pumping.

Initially, estimates of permeability used in this simulation were taken from pump test results (34). The surrounding unfractured aquifer, zone k , was assigned a permeability value obtained for the 32- to 218-ft interval of well 0, an interval

that yielded little water during drilling and where little evidence of fracturing was encountered. Zone k_2 was assigned the high permeability value obtained in the 19- to 32-ft interval of well O. This narrow interval supplied most of the well discharge, and in addition, drill logs indicated broken rock at this depth.

All four permeabilities, in addition to the uniform flow rate and the far field boundary head, were then adjusted in order to best fit the available field measurements of static head in the shallow aquifer. After a number of trial and error runs, permeability values and a flow rate were selected that resulted in a reasonable approximation of static conditions observed in six shallow observation wells (see table 3). Table 5 describes these input values.

TABLE 5. - Static background parameter values, gallons per day per square foot

(Uniform flow = 141 ft/yr)

Zone	Pump test results	Range	Selected value
k_1	NA	10- 1,000	250.0
k_2	1,475.0	1,000-10,000	2,500
k_3	NA	10- 1,000	25.0
k	7.05	1- 10	2.5

NA Not available.

The permeability values selected for zones k_1 and k_3 were generally consistent with the results of well pump tests in these zones. Wells in zone k_2 sustained 4-h yields averaging between 300 and 400 gpm, wells L and N in zone k_1 were able to sustain 4-h discharge rates of less than 10 gpm, while well B in zone k_3 sustained a discharge rate of just over 60 gpm for 4 h following drilling.

A comparison of actual and simulated static head values at the six shallow well observation points appears in table 6. Head is measured in feet above the datum (datum = 1,688 ft).

The most difficult data point to fit in this simulation is the observed static head at well S. Field data present three

pieces of information regarding the hydrologic setting of this well that are of interest. First (referring to table 3), the static head at well S is 26 ft higher than at neighboring wells T and W. Second, the head at S is 21 ft lower than at well Q. Third, S showed no measureable response to pumping from well D, while wells T and W responded with 25 ft or more of drawdown (34). As table 6 indicates, the distribution of head values among Q, S, and T in this simulation is only a fair match with the actual values. An interval of (low) permeability, k , between zones k_2 and k_3 might improve the simulated results by inducing a steeper gradient in head between wells Q and S.

TABLE 6. - Actual and simulated static heads; feet above the datum (1,688 ft)

Well	Actual	Simulated
H.....	218	215.0
M.....	115	115
Q^1	95	92
S^1	72	86
T^1	46	56
W^1	47	44

¹A requirement of this simulation is that head be less than 100 ft everywhere in the valley where the aquifer is not confined by an overlying shale layer.

The simulated piezometric surface in the shallow aquifer beneath Crab Orchard Run, prior to dewatering well pumping appears in figure 21. In figure 21, head is measured in feet above the coal seam that is the bottom confining layer of this aquifer.

In general, uniform flow from the northwest results in a gradient in head that is steepest in the low-permeability, k , region surrounding the valley, as in the vicinity of wells H, W, and T.

The gradient is shallower in zone k_1 where the permeability is 10 times greater than k . Within k_2 and k_3 , a very slight gradient is adequate to induce ground water flow at the rate of 141 ft/yr.

At the boundary between k_2 and the surrounding region of permeability k , the gradient is steepest at the tips of the

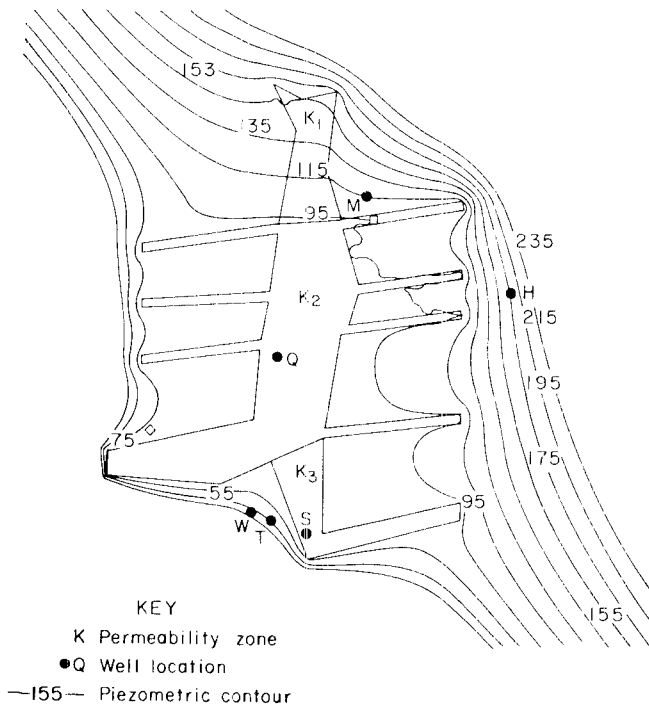


FIGURE 21. - Simulated piezometric surface beneath Crab Orchard Run.

transverse fracture zones, indicating that these fractures concentrate much of the natural ground water flow long before (and after) it has reached the valley bottom.

From a mining standpoint, this means that significant water inflow problems can occur long before mine development has reached beneath the valley bottom. The Sunshine Mine workings are approaching Crab Orchard Run from the east. Therefore, this simulation suggests that the first few mine entries should be aligned with one of the unfractured intervals between transverse fracture zones. This would prevent the mine from interfering prematurely with the dewatering action of wells that are operating in the valley bottom.

The average permeability of a fracture zone, its orientation with respect to the direction of natural ground water flow, and its location with respect to other fracture zones in the flow domain are all important in determining the extent to which uniform ground water flow is calculated by a particular zone. This in turn has implications for future siting of

dewatering wells, since it is generally desirable to site wells within zones that are best able to concentrate the natural flow of ground water in the vicinity of the mine workings.

Simulation of Dewatering Well Operations

A pilot dewatering experiment was conducted at the Sunshine Mine for a 20-day interval in July 1982. The dewatering experiment involved pumping from wells P and R with daily drawdown measurements in P, R, O, and Q (fig. 16).

The effect of dewatering on ground water inflow to the Sunshine Mine workings is described in a later section. Concern here is with the effect of dewatering activity on the fractured aquifer setting of Crab Orchard Run and with the ability of DWATR to adequately simulate these effects.

Certain personnel and equipment constraints were imposed from the beginning on the pumping schedule at the Sunshine Mine. Personnel to operate the system and an electrical generator were available for no more than 4 h/d. Of necessity, therefore, the pumping schedule was intermittent. Although high-capacity pumps were available for maximum discharge during the 2.5 to 3 h that the pumps operated each day, by no means were the wells pumped at maximum 24-h capacity. From July 8 to 28, excepting July 18 and July 23, wells P and R were pumped simultaneously for 2.5 to 3 h/d. Pumps were set at 190 ft in P and 185 ft in R. Both wells were open to aquifers above and below the coal seam. Although the previous pump tests made it evident that the contribution of the lower aquifer to total well discharge was small.

From a modeling standpoint, it is important to know if steady state flow conditions were achieved at some time during this dewatering experiment. Further, since the pumping schedule was intermittent it is necessary to determine if the high intermittent pumping schedule can be approximated, for modeling purposes, as a much lower continuous pumping rate.

Figure 22, which shows the average (over 24 h) pumping rate and the maximum

daily drawdown in pumped wells P and R for each day of the dewatering experiment helps to answer these questions. Although discharge rates from P and R differ by a factor of 10, this figure clearly shows the effect of storage water being withdrawn during the first 2 to 3 days of pumping. Drawdown in well P stabilizes after 4 days of pumping, and in well R after only a single day of pump operation. The decline in pumping rate during the first few days is in response to the increasing depth to water in both well P and R.

Figure 22 shows that after the first 9 days of pumping (July 8-17), drawdown and pumping rates have stabilized in both wells. This drawdown-pumping rate equilibrium is disrupted, however, when pump operations are interrupted on the 18th and again on the 23d. The erratic drawdown and pumping behavior from the 18th onward appear to be the result of these pumping interruptions. Equilibrium appears to have been reestablished only during the last day or two of the experiment.

Figure 23 shows the drawdown response of observation wells O and Q as a result of pumping from P and R. Once again drawdown appears to stabilize after the first 9 days of pumping. Again this steady state condition is disturbed by pump shutdowns on the 18th and 23d of July. Equilibrium is reestablished before the end of the experiment, however.

Despite interruptions in the pumping schedule, steady state pumping rates and drawdown values, for use as input to a steady state dewatering simulation, can with some confidence be abstracted from this 21-day dewatering experiment. The steady-state parameter values in table 7 were abstracted from figures 22 and 23.

TABLE 7. - Steady state dewatering parameter values

Well	Pumping rate, gpm	Drawdown, ft
P.....	8.8-9.8	178.0
R.....	3.7-4.0	170.0
O.....	0	26.0
Q.....	0	14.5

They include the pumping rates selected for DWATR input, and observation well drawdown measurements for comparison of actual and simulated pumping results.

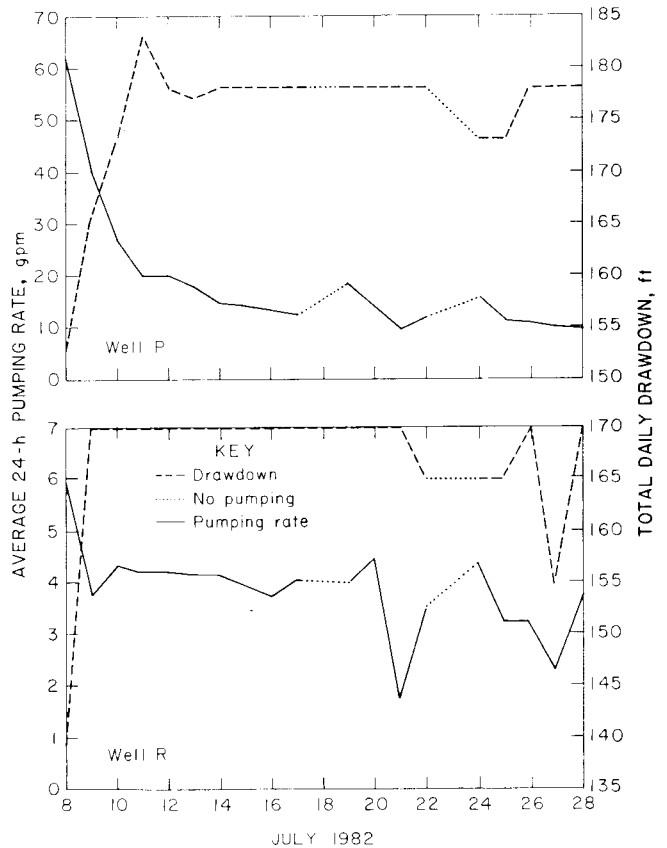


FIGURE 22. - Average pumping and total drawdown, wells P and R.

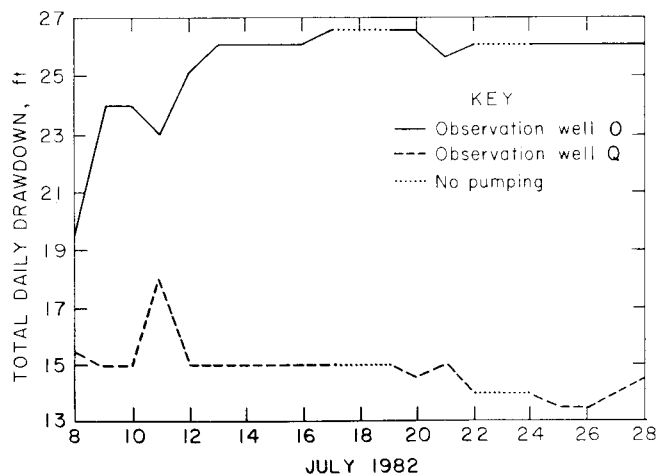


FIGURE 23. - Observation well drawdown (daily total).

Steady state pumping rates for wells P and R range between 8.8 to 9.8 gpm and 3.7 to 4.0 gpm respectively. The range of values reflects the slight downward trend in pumping rate, still apparent at the end of this dewatering experiment. The simulation of steady state dewatering effects is conducted using the minimum pumping rates as inputs.

The first test of this simulation involves a comparison of actual and predicted drawdown of two nearby observation wells. Table 8 summarizes the effect of pumping on observation wells O and Q. While there is close agreement between predicted and actual drawdown at well Q, the results at well O are less consistent. Here, the model has predicted 15 ft of drawdown while field measurements indicate 26 ft. This discrepancy is thought to be due in part at least, to the difference in depth of wells.

While well Q penetrates just the shallow aquifer, O, P, and R all extend more than 100 ft into the confined unit below the Upper Freeport coal seam (see table 4).

Pumping from wells R and P results in a cone of depression in both upper and lower aquifers. Well O, which is open to both upper and lower units, would certainly be affected by reduced head in the lower aquifer. Well Q, which is completed only in the shallow aquifer, would be affected only indirectly by reduced head in the lower aquifer. Thus pumping from wells P and R has a proportionally greater impact on the drawdown in well O than in well Q.

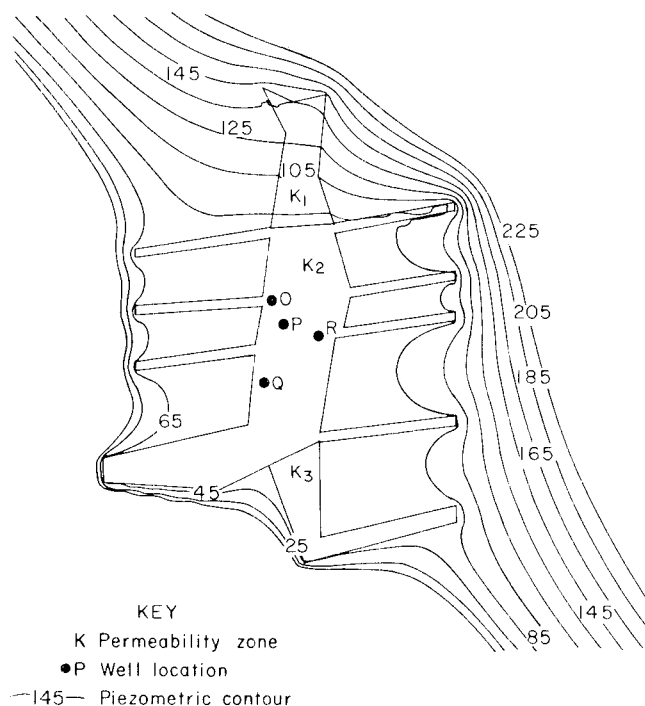


FIGURE 24. - Simulated piezometric surface due to dewatering well pumping.

The shallow aquifer piezometric surface, developed from this dewatering simulation, appears in figure 24. Pumping and observation wells are also annotated on this figure. Comparing this contour map with the one developed for the background simulation (fig. 21) reveals that the net effect of pumping from wells P and R is a head reduction of approximately 10 ft in zone k_2 . Significant drawdown effects are more or less evenly distributed throughout all three permeability zones, although the effect of

TABLE 8. - Well P and R actual (34) and simulated pump test results and effects on observation wells O and Q

Observation well	Actual, June 25, 1982			Simulated	
	Static water level above datum, ¹ ft	Maximum effect of 21 days of pumping (steady state flow)		Pumping rate, gpm	Total drawdown, ft
		Water level above datum, ¹ ft	Total drawdown, ft		
Q.....	95.0	80.5	14.5	0	15.0
O.....	96.0	70.0	26.0	0	15.0
P.....	98.8	-79.2	178.0	8.8	NAP
R.....	78.0	-92.0	170.0	3.7	NAP

NAP Not applicable.

¹1,688 ft (Upper Freeport coal elevation at well Q).

pumping on piezometric surface does not extend far beyond the boundaries of the zones.

Simulation of Alternate Dewatering Well Settings

The maximum dewatering potential of wells P and R is achieved by adjusting the pumping rate so that head at each well radius is zero in relation to the datum (pumps in P and R were set at 190 ft), giving discharge rates of 21 and 9 gpm, respectively.

The piezometric contour in figure 25 was generated using these maximum sustainable pumping rates. As this figure indicates, an additional 10-ft lowering of the piezometric surface beneath Crab Orchard Run could be expected from this maximum pumping rate.

Depending on the direction of future mine development, two other wells (B and C) drilled in Crab Orchard Run may have potential as dewatering sites. Although pumps were never installed in these wells, a simulation of the effects of pumping from wells B and C is included here, primarily to highlight the effect that well locations have on the piezometric surface in this high permeability setting.

Figure 26 is the piezometric surface resulting from this simulation. For comparison purposes, pumping rates selected for these wells are identical to those used to generate figure 25, i.e., C is pumped at 21 gpm, and B at 9 gpm.

As is evident from comparing figures 25 and 26, the location of dewatering wells within zones k_2 and k_3 (given the same pumping rate) has little effect on the resulting piezometric surface within the high permeability zone.

Although modest attempts were made in these simulations to mimic the field observations, by no means does this simulation represent an optimal parameter selection for this problem. Nor is it necessarily the intent of this investigation to generate a site-specific predictor of dewatering affects beneath Crab Orchard Run.

Modeling results are best used to provide insight into the hydrologic

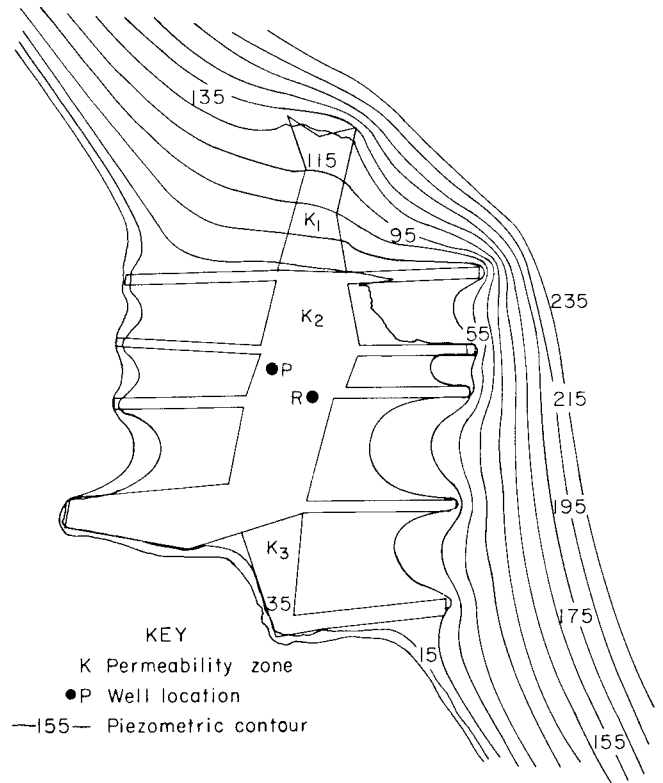


FIGURE 25. - Simulated piezometric surface resulting from maximum sustained pumping.

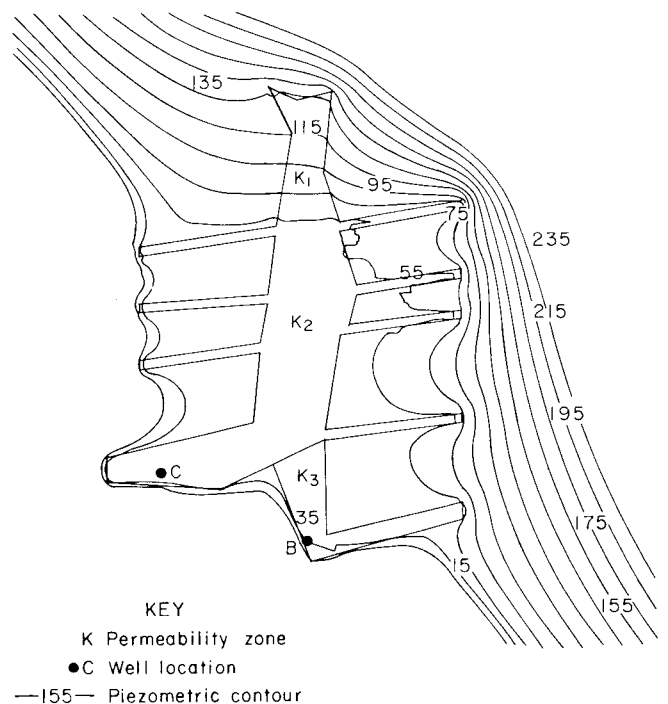


FIGURE 26. - Simulated piezometric surface resulting from sustained pumping of wells B and C.

behavior of high permeability valley settings and their response to dewatering activity. If a modeling investigation is conducted at the same time as the field activity, a good deal more trial and error manipulation of input parameters is justified in attempting to develop a more accurate simulation of the static fracture zone hydrologic setting. Such a model could then be used to guide exploratory drilling and pump testing in order

to better define zones of high permeability in the valley.

The impact of dewatering well operations on inflow to the underground workings of the Sunshine Mine, as they advanced beneath Crab Orchard Run, has thus far not been considered. The mine inflow monitoring program and the in mine results of dewatering activity are presented in the following section.

SUNSHINE MINE DEWATERING FIELD TEST

The Sunshine Mine had a history of severe water problems which included not only high AMD (pH 3.0 to 3.5) treatment costs but also mine water interference with activity at the face. During the time of the dewatering project (October 1981 to August 1982) the mine had only recently opened, and was operating a five-entry development in a single active section. This wet section, which was more or less isolated from the other workings, was experiencing severe mine water interference with continuous miner operation and rubber-tired haulage vehicles. Mine water at the face was entering mainly through roof fractures and roof bolt holes. At the face, mine water was comparatively high quality, however, it became degraded as it was pumped from sump to sump and mixed with water coming from abandoned workings.

The Sunshine Mine workings, superimposed on a topographic map, were shown in figure 16. In that figure, the shaded portion of the workings represents the final development of the active section in this mine during the 9 months of active involvement with this project, January-September 1982.

FRACTURE TRACE ANALYSIS, WELL DRILLING AND DEVELOPMENT

Of the nine fracture-sited wells drilled during this project, three were located more or less on the periphery of future mine development (wells B, C, and D in figure 16). Although two of these wells were capable of sustaining very high yields, they were not used later in the actual mine dewatering operation, due

to a change in mine development plans after the project had begun.

After siting, proposed dewatering wells were surveyed and located on the mine map in order to avoid projected haulageways and to ensure that well sites coincided with future pillar locations.

Eleven wells were drilled as part of this project (ten 6-in wells and one 10-in well). Six wells were drilled on fracture intersections. Two wells were sited on single fractures, and three others were nonfracture sitings. Well depths ranged from 82 to 501 ft (see table 3). An interpreted cross section running along Crab Orchard Run was developed from some of the drill logs and is presented in figure 27.

Initial well development (air surging) to remove drill cuttings wedged in cracks and fractures was inadequate at most drill sites. Consequently, before long-term pump tests could begin, a lengthy interval of remedial well development work was necessary.

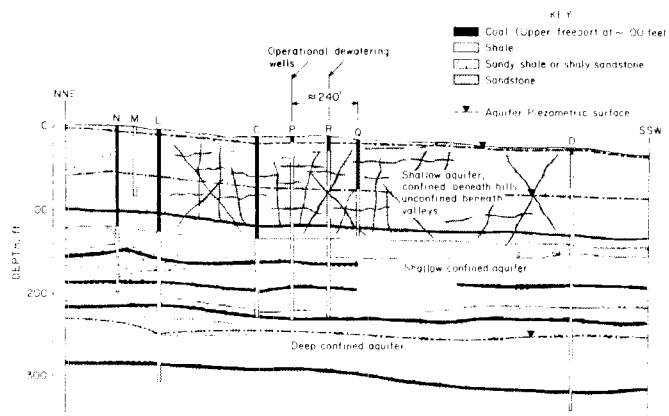


FIGURE 27. - Interpreted geologic cross section along Crab Orchard Run.

IN-MINE DEWATERING RESULTS

The in-mine assessment of dewatering efforts was by necessity limited to intermittent spot measurements of inflow to the wet section, made at various times during the course of the experiment. Inflow to the wet section exceeded 40,000 gpd prior to December 1981, while the section was being actively developed. Because of the high inflow rate and resulting production problems, this section was abandoned in December and all development work stopped. Pumping from this section continued, however.

Three measurements of wet section inflow were made during the period December 1981 to March 1982 prior to dewatering activity of any kind, drilling, pump testing, or scheduled pumping. These measurements indicated that inflow to the wet section had slowly declined after development work was stopped in December. By March, wet section discharge had declined to less than 21,000 gpd.

Well drilling and pump testing of wells L, M, N, O, P, Q, and R, began in mid-May and continued off and on until July 8. Shortly after wells L, M, and N were drilled in late May, the mine foreman reported an abrupt decline in infiltration, in the inactive section, particularly noticeable at point sources (roof bolt holes, etc.) in the mine. By mid-June, wells O, P, Q, and R had been drilled and tested; at this time the mine foreman reported that the water being discharged from the inactive section had decreased to approximately 1,000 to 2,000 gpd.

During June, two visits to the wet section were made to confirm that the previously wet section was now dry and that sump pumps set in the now inactive entries and capable of delivering 75 gpm were operating for only 10 to 20 min/d.

Because of the now apparently dry conditions, mining activity resumed in this section during the last week of June, accompanied by continued reports of dry workings as the entries advanced westward. Renewed mining activity had been underway for 2 weeks before scheduled pumping from dewatering wells P and R was able to begin on July 8.

During the 3 weeks of scheduled well pumping, from July 8 to 28, the apparent trend in mine infiltration was a gradual increase from the initial 1,000 to 2,000 gpd to approximately 6,000 gpd at the end of July. During the entire month, mine workings were expanding to the west beneath Crab Orchard Run.

At the end of July, mine development plans again changed. This time a concern over mine ventilation caused development to proceed in a southerly direction (see figure 16). The dewatering experiment was terminated shortly after this latest change in mine development plans occurred.

One final measurement in mid-August, 2 weeks after all dewatering activity had ceased, indicated that mine discharge from this section (the shaded area in figure 16) had climbed to 19,000 gpd. In early September, the mine foreman indicated that inflow was still increasing, however no further measurements were possible.

The area of mine development from which the underground sump collected mine drainage had expanded from 265,000 ft² at the start of the 21-day dewatering experiment to 540,000 ft² by the end of July. All of this development was in an intensively fractured valley setting.

The quality of water discharged from all dewatering wells was uniformly high (suitable for domestic use) throughout the course of pumping. After an initial flushing, the pH of dewatering well discharge stabilized at 6.5 to 6.8. Iron concentration stabilized at 2.0 to 3.0 mg/L. West Virginia Department of Natural Resources approval was obtained for temporary discharge of this water into a nearby stream without prior treatment. The receiving stream had a pH of 7.5 to 8.0 and total iron of 0.12 mg/L.

ANALYSIS

The Sunshine Mine workings were developed to within 300 ft of the valley bottom before being temporarily abandoned, so it seems unlikely that the piezometric head in the fracture zone beneath Crab Orchard Run was completely unaffected by

drainage into the mine. There is evidence to indicate however that the dewatering influence of the mine was quite limited. For instance, head measurements in the shallow wells of Crab Orchard Run indicated a stable or rising water table throughout April, May, and June. The water level in shallow well Q was less than 10 ft from the surface (see table 3).

Generally speaking, the time-dependent nature of mine inflow and the continuously expanding area of mine workings in active sections makes it difficult to measure the effectiveness of fracture zone dewatering from inside the mine. Before and after comparisons of mine inflow rates are tenuous since there are often a number of factors influencing the measured inflow rate that are difficult to isolate and measure, let alone control.

Measuring in-mine results of dewatering operations at the Sunshine Mine would have been far easier if wells had been developed, and pumping operations begun in January or February when the mine section was inactive, rather than waiting until July when this section had been

reactivated and the mine void was once again expanding.

Considering that mine workings were advancing directly beneath the highly fractured valley setting of Crab Orchard Run during the entire month of July, outflow from this reactivated section remained at a comparatively low level, never exceeding 6,000 gpd during the entire 3-week interval in which scheduled pumping was taking place.

The limited number of in-mine measurements that were made during and after this 21-day experiment points to a significant increase in mine infiltration in early August, after pumping operations were terminated. However, it is not possible to completely isolate the effect of well dewatering from other variables that may have affected the mine inflow rate at this time. For instance, the direction of mine development also changed at about the same time that dewatering operations ended. The alignment of mine workings with the fracture valley setting may have contributed to the increase in mine infiltration during August.

CONCLUSIONS

This investigation has focused attention on fracture zones as an important element of both mine water problems and mine dewatering methods. A number of conclusions, generally having to do with fracture zone involvement in mine inflow, and with the design of mine dewatering operations are possible.

As the in-mine survey and fracture trace studies indicated, high permeability fracture zones ought to be the focus of mine dewatering activity, since they constitute preferred flow paths in the aquifer overlying underground workings. Ground water that is stored within the fracture zone network is water that will likely be released into newly developed and isolated mine workings.

As the flow simulation indicated, zones of fracture concentration are involved in minimizing the number of wells needed to dewater mine workings, since high pumping capacities are more likely when dewatering wells are sited within high permeability zones.

A savings in acid mine drainage treatment costs is possible, since ground water that is intercepted in the fracture zones, before it enters the mine workings, has not yet been degraded by contact with exposed pyritic material in the mine, or by mixing with acidic mine water coming from other workings.

Many of the advantages of fracture zone dewatering impact favorably on mine productivity, in the form of improved working conditions. All of which are most apparent when dewatering activity has reduced inflow to the active areas of mine development. The release of fracture zone storage water at the active face is closely associated with wet section mining conditions.

Ground water flow in fracture zone settings is often complex. Dewatering design activity must be preceded by a conceptual understanding of the various hydrogeologic conditions that influence the pattern of ground water flow in a specific mine-fracture zone setting.

The approach to fracture zone dewatering presented here is oriented toward localized, high inflow mine water problems that arise when mine development is in the vicinity of fracture zones or fracture valley topography. Typical mine water problems for which fracture zone dewatering may be an appropriate solution include, (1) wet sections where the alternatives to water inflow control are unacceptably low productivity or

abandonment, perhaps giving up a sizable piece of coal reserve, (2) mine sections left inactive because of extreme water problems, in which renewed mining activity has once again become necessary (perhaps relatively short-term development for ventilation, water handling, haulage, etc.), or (3) initial entry development for a longwall panel, where the isolated nature of the entry leads to extreme water inflow problems.

REFERENCES

1. W. A. Wahler and Associates. Dewatering Active Underground Coal Mines: Technical Aspects and Cost-Effectiveness (U.S. EPA contract EPA-600/7-79-124). 1979, 151 pp.
2. Robison, T. M. Occurrence and Availability of Ground Water in Ohio County, West Virginia. WV Geol. and Econ. Surv. Bull. 27, 1964, 31 pp.
3. Ward, P. E., and B. M. Wilmoth. Ground Water Hydrology of the Monongahela River Basin in West Virginia. WV Geol. and Econ. Surv. River Basin Bull. 1, 1968, 54 pp.
4. Emrich, G. H., and G. L. Merritt. Effects of Mine Drainage on Ground Water. Ground Water, v. 7, No. 3, 1969, pp. 27-32.
5. Brown, R. L., and R. R. Parizek. Shallow Ground Water Flow Systems Beneath Strip and Deep Coal Mines at Two Sites, Clearfield County, Pennsylvania. Coal Res. Sec., PA State Univ., Coal Res. Sec. Spec. Res. Rep. SK-84, 1971, 74 pp.
6. U.S. Office of Water Research and Technology (Dep. Interior). Use of Fracture Traces in Water Well Location: A Handbook. OWRT TT/82, 1982, 55 pp.
7. Wyrick, G. G., and J. W. Borchers. Hydrologic Effects of Stress Relief Fracturing in an Appalachian Valley. U.S. Geol. Surv. Water-Supply Paper 2177, 1981, 51 pp.
8. Lattman, L. H., and R. R. Parizek. Relationship Between Fracture Traces and the Occurrence of Groundwater in Carbonate Rocks. J. Hydrology, v. 2, 1964, pp. 73-99.
9. U.S. Office of Water Research and Technology (Dep. Interior). Water Well Location by Fracture Trace Mapping. Water Res. Capsule Rep., 1979, 12 pp.
10. Gold, D. P., and R. R. Parizek (eds.). Field Guide to Lineaments and Fractures in Central Pennsylvania: Field Trip Guidebook. PA State Univ., 1976, 75 pp.
11. Siddiqui, S. H., and R. R. Parizek. Hydrogeologic Factors Influencing Well Yields in Folded and Faulted Carbonate Rocks in Central Pennsylvania. Water Resour. Res., v. 7, 1971, pp. 1295-1312.
12. Stoner, J. D. Ground Water Hydrology and Probable Hydrologic Effects of Subsurface Mining in Southwestern Pennsylvania. Pres. at Eastern Conf. of Practical Groundwater Monitoring Consideration for the Mining Industry, NWWA, July 29-30, 1982, 21 pp; available from J. D. Stoner, U.S. Geol. Surv., St. Paul, MN.
13. Lattman, L. H. Technique of Mapping Geologic Fracture Traces and Lineaments on Aerial Photographs. Photogrammetric Eng., v. 84, 1958, pp. 568-576.
14. Petrus, C. A. Investigations of Fracture Traces and Underground Roof Fall Fatalities in the Southern Anthracite Field. M.S. Thesis, PA State Univ., 1979, 126 pp.
15. Paciorek, K. L., and P. F. Kimble. Investigation of Mechanics of Mine Acid Formation (U.S. Dep. of Energy contract ET-78-C-01-8977, Ultra Systems Inc.). March 1980, 132 pp.

16. Suboleski, S. C. Effect of Physical Conditions on Continuous Miner Production in Underground Coal Mines. Ph.D. Thesis, PA State Univ., 1978, 357 pp.
17. Parizek, R. R., and D. R. Buss. Demonstration of the Connector Well Method of Reducing Leakage and Abating Acid Mine Drainage From an Underground Coal Mine, Tioga County, Pennsylvania: Final Rept. for Serv. Contr. EER-130-A, PA Dept. Environ. Resour., Div. of Abandoned Mine Lands, Harrisburg, PA, 1984. In review; for inf. contact Richard Bielicki, PA Dept. Environ. Resour., Harrisburg, PA.
18. Berry, J. K. Elements of Practical Coal Mining. Ch. in Drainage, Soc. Min. Eng. AIME, Littleton, CO, 1973, pp. 155-159.
19. Schubert, J. P. A Hydrogeologic and Numerical Simulation Feasibility Study of Connector Well Dewatering of Underground Coal Mines, Madea, Pennsylvania. Unpublished M.S. Thesis, PA State Univ., 1978, 191 pp.
20. Parizek, R. R. Prevention of Coal Mine Drainage Formation by Well Dewatering. PA State Univ., Coal Res. Sec., Spec. Res. Rep. SR-82, 1971, 73 pp.
21. Parizek, R. R., and E. G. Tarr. Mine Drainage Prevention and Abatement Using Hydrogeological and Geochemical Systems. Paper in Proceedings, Fourth Symposium on Coal Mine Drainage Research, Mellon Inst., Pittsburgh, PA, 1972, pp. 58-82.
22. Narasimhan, T. N. Multidimensional Numerical Simulation of Fluid Flow in Fractured Porous Media. Water Resour. Res., v. 18, No. 4, 1982, pp. 1235-1247.
23. Streltsova-Adams, T. D. Well Hydraulics in Heterogeneous Aquifer Formations. Ch. in Advances in Hydroscience, ed. by V. T. Chow. Academic Press, v. 2, 1978, pp. 357-428.
24. Boulton, N. S., and T. D. Streltsova-Adams. Unsteady Flow to a Pumped Well in an Unconfined Fissured Aquifer. J. Hydrology, v. 37, 1978, pp. 349-363.
25. Wilson, C. R., and P. A. Witherspoon. Steady State Flow in Rigid Networks of Fractures. Water Resour. Res., v. 10, 1974, pp. 328-335.
26. Strack, O. D. L. Analytic Modeling of Flow in a Permeable Fissured Medium. Pacific Northwest Lab. Rep. 4005, Feb. 1982, 79 pp.
27. Strack, O. D. L., and H. M. Haitjema. Modeling Double Aquifer Flow Using a Comprehensive Potential and Distributed Singularities. 2. Solution for Inhomogeneous Permeabilities. Water Resour. Res., v. 17, Oct. 1981, pp. 1551-1560.
28. Strack, O. D. L. Flow in Aquifers With Clay Laminae. a. The Comprehensive Potential. Water Resour. Res., v. 17, Aug. 1981, pp. 985-992.
29. Bear, J. Dynamics of Fluids in Porous Media. Elsevier-North Holland, New York, 1972, 765 pp.
30. Strack, O. D. L., and H. M. Haitjema. Modeling Double Aquifer Flow Using a Comprehensive Potential and Distributed Singularities. 1. Solution for Homogeneous Permeability. Water Resour. Res., v. 17, Oct. 1981, pp. 1535-1549.
31. Abramowitz, M., and I. A. Stegun. Handbook of Mathematical Functions. Dover, 1964, 1046 pp.
32. Tracy, F. T. A Computer Program for Contouring the Output of Finite Element Programs. U.S. Army Corps Eng. Misc. Paper K-74-1, 1974, 26 pp.
33. Verruijt, A. Theory of Ground Water Flow. Gordon and Breach, 1970, 190 pp.
34. Ahnell, G., D. R. Buss, R. M. Cohen, and R. Parizak. Development of a Dewatering System for Controlling Fracture Dominated Inflow for Acid Drainage Abatement, Appendices (contract H0202002, Skelly and Loy). BuMines OFR 109(z)-84, 1984, 212 pp.

APPENDIX A.--DWATR PROGRAM MODULES

<u>Routine</u>	<u>Purpose</u>
DRIVER CONTROL ROUTINES	
DWATR.....	Input-output.
GRID.....	Calculate a grid of Ω values for input to a head contouring program.
SLINE.....	Generate a streamline pattern, by specifying streamline starting locations at wells or elsewhere in the flow region. Select streamline tracing method. Check for permeability zone crossing, normal streamline trace, and termination.
FLOW PROBLEM COMPONENTS	
OMA.....	Determine Ω , the additive solution from flow components, i.e. wells, permeability zones, uniform flow, far field boundary condition.
WELL.....	Determine Ω_w , the solution for the well component of flow. Account for branch cut singularities.
DIPOL.....	Determine Ω_p , the flow solution for discrete permeability zones. Linearly or parabolically interpolate doublet strengths between endpoints. Determine streamline entrance and exit from permeability zones.
DOUBLET STRENGTH	
STGTH.....	Determine line doublet strengths at endpoints subject to internal boundary condition involving permeabilities k_0 and k_1 . Generate n linear equations with n unknown double strengths.
MDPNT.....	Locate line doublet midpoints. Include these coordinates in the array of simultaneous strength equations for parabolic fit.
QUAD.....	Separate first and second order components of doublet strength at the doublet midpoint. Save the parabolic component.
GAUSS.....	Obtain a solution to a set of simultaneous linear equations using Gauss-Jordan (row reduction) procedure.
STREAMLINE ITERATION	
NEWRA.....	Determine z given Ω using Newton's method to iteratively find roots of nonlinear equation; compute error, check convergence on both ϕ and Ψ .
NUMCA.....	Use a variation of Newton's method to trace streamlines, compute error, and check convergence on Ψ only.
MINOR ROUTINES	
DPCHK.....	Check current streamline location for proximity to dipole singularities. Restart streamlines after "stepping over" the singularity.
MXMN.....	Determine maximum and minimum values of z, Ω , and ϕ for plot and contour map program input.
PTOH.....	Convert potential to head. Account for continuous potential across confined and unconfined flow boundaries and continuous ϕ across permeability zone boundaries.
HTOP.....	Convert head to potential.
WELLR.....	Calculate an approach criterion for streamlines near well singularities.
INOUT.....	Determine if z is inside or outside the plot boundary.

DWATR INPUT-OUTPUT FILES

<u>File name</u>	<u>Logical unit number</u>	<u>File name</u>	<u>Logical unit number</u>
User input.....	10	Plotting and contouring (disk).....	15
Printer output.....	6	Streamline plotting (disk).....	17
CRT output.....	1	Doublet strengths (disk)...	19
Head and potential contour grid (disk).....	13	Mass transport-streamline interface (disk).....	14

APPENDIX B.--INPUT VARIABLE DESCRIPTION

INPUT RECORD 1

Variable	Format	Description
IOPT.....	I5	Input-output print option (1 or 0). If IOPT = 1, the program prints iterative streamline data. This option can be used as an aid in selecting proper error bounds, etc., for streamline convergence.
VOPT.....	I5	Mass transport model interface option (1 or 0). If VOPT = 1, an interface file containing streamline data is generated on logical unit 14.
GOPT.....	I5	Grid file option (1 or 0). If GOPT = 1, a grid of head and potential values is generated on logical unit 13 for later contour map construction.
XLO.....	F10.0	Rectangular window boundaries for grid and/or streamline generation, in feet.
YLO.....	F10.0	Do.
XHI.....	F10.0	Do.
YHI.....	F10.0	Do.
ZSPA.....	F10.0	Grid interval on which potential and head values are generated, in feet (ignored if GOPT = 0).

Parameters on input records 1a, 1b, 1c, and 1d are passed to logical unit 14 for input to mass transport program. These four records should be included only if VOPT = 1.

INPUT RECORD 1a

Variable	Format	Description
D.....	E10.5	Molecular diffusion coefficient.
F.....	E10.5	Formation electrical resistivity.
PS.....	E10.5	Average formation particle diameter outside all permeability-porosity zones, in centimeters.
SIGMA...	E10.5	Inhomogeneity factor.
POROS...	E10.5	Porosity outside of all permeability-porosity zones, dimensionless proportion.
RHOS....	E10.5	Rock density outside all permeability-porosity zones, in grams per square centimeter.
ISKP....	15	Interval at which streamline nodes are output to LU 14. If ISKP = 1, all acceptable streamline nodes are output to LU 14. If ISKP = 2, every second node is output. If ISKP = 3, every third node is output, etc.
NZT.....	15	Number of permeability-porosity zones.

INPUT RECORD 1b

Variable	Format	Description
POR(i)...	8E10.5	Porosity inside permeability-porosity zone(i) (8 entries per line).

INPUT RECORD 1c

Variable	Format	Description
P(i)....	8E10.5	Average particle diameter inside permeability-porosity zone(i) (8 entries per line).

INPUT RECORD 1d

Variable	Format	Description
RHO(i)...	8E10.5	Rock density inside permeability-porosity zone(i) (8 entries per line).

INPUT RECORD 2

Variable	Format	Description
ZBND.....	F10.0	Radius of far field, constant head boundary, with center at the origin, in feet.
RHD.....	F10.0	Far field constant head, in feet.

INPUT RECORD 3

Variable	Format	Description ¹
NWL.....	I5	Number of wells ($0 \leq \text{NWL} \leq 10$).
IFLO.....	I5	Uniform ground water flow indicator (1 or 0). If IFLOW = 1, uniform flow exists.
MPT.....	I5	Number of streamline starting locations. A well, with multiple streamlines, is considered 1 starting location ($0 \leq \text{MPT} \leq 100$).
MXPTS...	I5	Maximum number of points per streamline ($\text{MXPTS} \leq 200$).
NZT.....	I5	$ \text{NZT} $ is the number of discrete zones of differing permeability ($0 \leq \text{NZT} \leq 4$). If NZT > 0 doublet strengths are generated and written to a strength file, logical unit 19. If NZT < 0 doublet strengths are read from previously generated strength file, logical unit 19; parameters affecting flow are assumed to be identical to those used in generating the file. If NZT = 0 permeability is uniform throughout the flow domain.
STM.....	I5	Streamline tracing method. STM = 0, Newton-Raphson iterative convergence required on both ϕ and ψ . If STM = 1, unequal ϕ intervals, and iterative convergence required on ψ only.
DEC.....	F10.0	Interval between consecutive streamline points. If STM = 0, DEC is downgradient (+) or upgradient (-) interval in head (ϕ). If STM = 1, DEC is downgradient (+) or upgradient (-) interval in z.
PERM....	F10.0	Homogeneous aquifer permeability, outside all permeability zones, in gallons per day per square foot.
THICK...	F10.0	Aquifer thickness, in feet.
WRDS....	F10.0	Well radius, in feet.
AQ.....	A4	Aquifer type. AQ = CONA upper confining layer is present; AQ = UNCA if no upper confining layer is present.

¹All parenthetic maximum and minimum values are dependent on array size in DWATR.

INPUT RECORD 4¹

Variable	Format	Description
RERR ² ...	F10.0	Absolute error criteria for ϕ convergence.
IERR....	F10.0	Absolute error criteria for ψ convergence. (DWATR calculates a relative error criteria for ϕ and ψ .)
DPJP....	F10.0	The radius of a circle around each doublet singularity, wherein Newton's method is no longer used to calculate succeeding streamline points, in feet.

See footnotes at end of tabulation.

INPUT RECORD 4¹--Continued

Variable	Format	Description
ITRMX...	I5	Maximum number of iterations permitted to achieve convergence criteria.
ALSTP...	F10.0	Minimum value for relaxation parameter α , where $0 < \alpha \leq 1$. If $ALSTP < 0$, α is assigned a fixed value of $ ALSTP $.
LXDWN ² ..	I5	Number of diverging iterations before α is reduced.
LXUP ² ...	I5	Number of converging iterations before α is increased.

¹If MPT = 0, omit this record. ²This parameter is ignored if STM = 1.

MULTIPLE INPUT RECORD 5¹

Variable	Format	Description
XSTRT...	F10.0	Center of a radial pattern of streamline starting points, in feet.
YSTRT...	F10.0	Do.
ANGL....	F10.0	Angular increment in a radial pattern of streamline starts, in degrees.
MLINE...	I5	Number of streamlines in the radial pattern, ($1 \leq MLINE \leq 100$).
RADS....	F10.0	Radius of a circle centered at (XSTRT, YSTRT), upon which MLINE streamline starting points are spaced, at equal intervals.
NUMBR...	I5	Starting point identification number.

¹Number of records of this type must equal MPT, if MPT = 0, omit this record.

MULTIPLE INPUT RECORD 6¹

Variable	Format	Description
XWL.....	F10.0	Coordinate location of a well, in feet.
YWL.....	F10.0	Do.
Q.....	F10.0	Well pumping rate output (+), input (-) in gallons per minute.
NUMW....	I5	Well identification number.

¹Number of records of this type must = NWL, if NWL = 0, omit this record.

MULTIPLE INPUT RECORD 7¹

Variable	Format	Description
ZONE1...	F10.0	Permeability zone identification number.
ZONE2...	F10.0	Permeability inside this zone in gallons per day per square foot.
ZONE3...	F10.0	Number of sides on this polygonal zone boundary. The zone boundary is entered in counterclockwise rotation if $ZONE3 > 0$, and in clockwise rotation if $ZONE3 < 0$ (see input record 8).
ZONE4...	F10.0	Permeability outside the zone (nested zones are permitted), in gallons per day per square foot.
ZONE5...	F10.0	Identification number of the zone outside this permeability zone. If $ZONE5 = 0$ outside permeability is homogeneous.

¹Number of records of this type must equal NZT. Each input record 7 is followed immediately by the appropriate number of input records of type 8.

MULTIPLE INPUT RECORD 8¹

Variable	Format	Description
DPOLEX..	F10.0	Coordinates (x,y) on the boundary of a permeability zone identified by ZONE5. Coordinates must be entered in a <i>counterclockwise</i> rotation. ² Intervening straight line segments form the zone boundary. The last coordinate entered is assumed connected to the first via a straight line. Straight line segments <i>must not</i> intersect.
DPOLEY..	F10.0	

¹Type 8 input records outline a single zone and follow immediately the input record 7 which identifies the permeability zone. Successive combinations of input record 7 and input record 8 designate additional zones. If NZT = 0, input record 7 and input record 8 are omitted.

²Concentric permeability zones are permitted, however successive *interior* zone boundaries must be entered in clockwise, then counterclockwise, then clockwise, etc., rotations. Direction of rotation is indicated by input record 7, ZONE3.

INPUT RECORD 9¹

Variable	Format	Description
ANGL1...	F10.0	Direction of the uniform flow vector. $0 \leq \text{ANGL1} \leq 360$ (respect to positive x axis).
VEL1....	F10.0	Ground water flux in feet per year (velocity = flux/porosity).

¹If IFLOW = 0 omit this record.

APPENDIX C.--DWATR SOURCE LISTING

DWATR4 T=00004 IS ON CR00030 USING 00347 BLKS R=0000

```

0001 FTN7X
0002     BLOCK DATA  DATX
0003 C
0004 C
0005 C
0006     COMMON / CNST / I, PI
0007     COMMON / INPT / IOPT, NZNE, ITER, DPJP, IOMEG
0008     COMMON / ZARG / ARGPO, DODF
0009     COMMON / PJMP / JUMP, MU
0010     COMMON / POLE / ZONE, DPOLE
0011     COMMON / ONED / IFLO, ANGL1, UNFM
0012     COMMON / ZON / LOCZ
0013     COMMON / WELLD / ZBND, RPHI, Q, ZWL, STRT, WRAD, WRDS, NPT, NML,
0014 1     NUMS, NUMW
0015     COMMON / ERRS / RERR, IERR, ITRMX, ALSTP, LXDNW, LXUP
0016     COMMON / CHEM / D, F, P, SIGMA, POR, RHO, ISKP
0017     COMMON / AQF / THICK, AQ, FL, BND
0018     COMMON / LINE / NLINE, STM, DEG, MKPTS
0019     COMMON / IO / LU, PL, GL, AL, JL, IL, TL
0020 C
0021 C
0022     DIMENSION  STRT (100), ZWL (30), Q (30), WRAD (30),
0023 1     NUMS (100, 2), NUMW (30), DPOLE (300), ZONE (4, 7), BND (4),
0024 2     NLINE (100), ARGPO(600), JUMP(300), MU(300), POR (4), P (4),
0025 3     RHO (4)
0026 C
0027     REAL  IERR, JUMP, MU, IOMEG
0028 C
0029     INTEGER  PL, GL, AL, STM, TL
0030 C
0031     COMPLEX  ZWL, I, STRT, BND, DPOLE, DODF, FACT1, FACT2, FACT3,
0032 1 FACT4, CLG
0033 C
0034     END
0035 C
0036 C
0037 C-----
0038 C-----
0039 C
0040 C           BUREAU OF MINES HYDROLOGY MODEL
0041 C
0042 C           1984
0043 C
0044 C     (AN APPROXIMATE ANALYTIC MODEL FOR STEADY STATE, 2-DIMENSIONAL,
0045 C     GROUNDWATER FLOW PROBLEMS INVOLVING WELLS AND UNIFORM FLOW IN
0046 C     AN AQUIFER WITH REGIONS OF INHOMOGENEOUS PERMEABILITY.)
0047 C
0048 C-----
0049 C-----
0050 C
0051 C
0052 $EMA/SIZE/,/VECT/
0053     PROGRAM  DEMAR
0054 C
0055 C     THIS PROGRAM USES A 2 DIMENSIONAL, ANALYTIC ELEMENT APPROACH TO
0056 C     CALCULATE AQUIFER HEAD AND STREAMFLOW LINES RESULTING FROM WELL
0057 C     PUMPING AND UNIFORM FLOW IN A SATURATED AQUIFER CONTAINING DISCRETE
0058 C     ZONES OF DIFFERING PERMEABILITY.  THE SOLUTION DERIVED IS CONTINUOUS

```

```

0059 C   ACROSS CONFINED/UNCONFINED FLOW BOUNDARIES.
0060 C
0061 C   ALL UNITS ARE U.S.  THE DATUM FOR MEASUREMENT OF HEAD IS THE
0062 C   BOTTOM CONFINING LAYER OF THE AQUIFER.
0063 C
0064 C
0065 C
0066 C   COMMON / SIZE / CDEF, CHEM
0067 C   COMMON / VECT / CNST
0068 C   COMMON / CNST / I, PI
0069 C   COMMON / INPT / IOPT, NZNE, ITER, DPJP, IOMEG
0070 C   COMMON / ZARG / ARGPO, DODF
0071 C   COMMON / POLE / ZONE, DPOLE
0072 C   COMMON / PUMP / JUMP, MU
0073 C   COMMON / ONED / IFLO, ANGLI, UNFM
0074 C   COMMON / ZON / LOGZ
0075 C   COMMON / WELLD / ZBND, RPHI, Q, ZWL, STRT, WRAD, WRDS, NPT, NWL,
0076 C   1   NUMS, NUMW
0077 C   COMMON / ERRS / RERR, IERR, ITRMX, ALSTP, LXDWN, LXUP
0078 C   COMMON / IO / LU, PL, GL, AL, JL, IL, TL
0079 C   COMMON / CHEM / D, F, P, SIGMA, POR, RHO, ISKP
0080 C   COMMON / AQF / THICK, AQ, FL, BND
0081 C   COMMON / LINE / NLINE, STM, DEC, MXPTS
0082 C
0083 C
0084 C   DIMENSION  ARGPO (600), BND (4), CHEM (500, 17), CNST
0085 C   1   (300), CDEF (300, 300), DPOLE (300), HDMN (3), HDMX (3),
0086 C   2   JUMP (300), MU (300), NLINE (100), NUMS (100, 2), NUMW
0087 C   3   (30), Q (30), STRT (100), WRAD (30), ZONE (4, 7), ZWL (30),
0088 C   4   ALTR (100), POR (4), P (4), RHO (4)
0089 C
0090 C   CHARACTER*4 AQ,AQFR(3)
0091 C   COMPLEX  BND, CDM, DODF, DODZ, DPOLE, DTRM, FLXVC, I, OMDON,
0092 C   1   OMDEC, OMEGA, OMPRT, OMST, STRT, VELVC, WLTRM, ZWL, Z, FACT1,
0093 C   2   FACT2, FACT3, FACT4, CLG
0094 C   INTEGER  AL, GL, GOPT, PL, STM, VOPT, TL
0095 C   REAL     IERR, JUMP, MU, IOMEG
0096 C
0097 C   DATA  AQFR (2), AQFR (3) / 'CONF','INED' /
0098 C
0099 C   INITIALIZATION.
0100 C
0101 C   PRINTER OUTPUT ON LOGICAL UNIT 6.
0102 C   LU = 6
0103 C
0104 C   STREAMLINE PLOT OUTPUT ON LOGICAL UNIT 17
0105 C   PL = 17
0106 C
0107 C   CONTOUR GRID OUTPUT ON LOGICAL UNIT 13.
0108 C   GL = 13
0109 C
0110 C   AUX. PLOT FILE CONTAINING PLOT SIZE,NO. WELLS,ZONES,COORDS.
0111 C   AND NO. STREAMLINES ON LOGICAL UNIT 15.
0112 C
0113 C   AL = 15
0114 C
0115 C   DOUBLET STRENGTH DATA SAVED ON LOGICAL UNIT 19.
0116 C   JL = 19
0117 C
0118 C   MASS TRANSPORT INTERFACE ON LOGICAL UNIT 14.

```

```

0119 C
0120     TL = 14
0121 C
0122     PI = 3.141592654
0123     I = (0.0, 1.0)
0124     REWIND 10
0125 C
0126 C
0127 C-----
0128 C     READ PRINT OPTIONS CHEMICAL AND GRID OPTIONS AND PLOT SIZE.
0129 C     READ (10, 10) IOPT, VOPT, GOPT, XLO, YLO, XHI, YHI, ZSPA
0130 C-----
0131 C
0132 C
0133 C*****
0134 C     READ CHEM INTERFACE PARAMETERS.
0135 C
0136 C     IF (VOPT .EQ. 0) GO TO 1000
0137 C     READ (10, 20) D, F, PS, SIGMA, POROS, RHOS, ISKP, NZT
0138 C     IF (NZT .GT. 0) READ (10, 25) (POR (IZNE), IZNE = 1, NZT)
0139 C     IF (NZT .GT. 0) READ (10, 25) (P (IZNE), IZNE = 1, NZT)
0140 C     IF (NZT .GT. 0) READ (10, 25) (RHO (IZNE), IZNE = 1, NZT)
0141 C*****
0142 C
0143 C
0144     1000 CONTINUE
0145 C
0146 C-----
0147 C     READ FAR FIELD HEAD BOUNDARY CONDITION.
0148 C     READ (10, 30) ZBND, RHD
0149 C-----
0150 C
0151 C
0152 C     A NEGATIVE WELL RADIUS (WRDS) WILL INVOKE THE OPTIONAL WELL
0153 C     APPROACH CRITERIA I.E. HEAD(Z) .LT. HEAD(WELL RADIUS).
0154 C
0155 C
0156 C-----
0157 C     READ NO.WELLS,STREAMLINES,UNIFORM FLOW,MAX.PTS.,NO.PERM.ZONES,
0158 C     STREAM.TRAC.METH.,DEC IN HEAD,BACKGRND.PERM.,AQ.THICK.,WELL RAD.,
0159 C     AQ.TYPE
0160 C     READ (10, 40) NWL, IFLO, MPT, MXPTS, NZT, STM, DEC, PERM, THICK,
0161 C     1  WRDS, AQ
0162 C-----
0163 C
0164 C     REMIND ALL DATA FILES
0165 C
0166 C     IF (MPT .GT. 0) REMIND PL
0167 C     IF (MPT .GT. 0 .OR. GOPT .GT. 0) REMIND AL
0168 C     IF (NZT .NE. 0) REMIND JL
0169 C     IF (GOPT .GT. 0) REMIND GL
0170 C     IF (VOPT .GT. 0) REMIND TL
0171 C
0172 C     SPECIFY PLOT BOUNDARIES.
0173 C
0174 C     BND (1) = CMPLX (XLO, YLO)
0175 C     BND (2) = CMPLX (XHI, YLO)
0176 C     BND (3) = CMPLX (XHI, YHI)
0177 C     BND (4) = CMPLX (XLO, YHI)
0178 C

```

```

0179      XMID = (XHI + XLO) / 2
0180      YMID = (YHI + YLO) / 2
0181      XSID = XHI - XLO
0182      YSID = YHI - YLO
0183  C
0184      NZPLS = IABS (NZT)
0185      NZNE = NZPLS + 1
0186  C
0187  C      IF NO STREAMLINES SKIP INPUT.
0188  C
0189      IF (MPT .EQ. 0) GO TO 1030
0190  C
0191  C
0192  C      MIN. WELL RADIUS AT SINGULARITIES.
0193  C
0194      IF (WRDS .LT. .0001) WRDS = .0001
0195  C
0196  C
0197  C-----
0198  C      READ ERROR CRITERIA FOR ITERATIVE METHS, MAX. ITERATION, LOW. ALP
0199  C      BOUND, LOWER AND UPPER RELAX. CRITERIA.
0200  C
0201  C      THE Z SPACING METHOD REQUIRES ONLY (IERR) ENTRY, OTHER
0202  C      PARAMETERS ARE IGNORED.
0203  C
0204      READ (10, 50) RERR, IERR, DPJP, ITRNK, ALSTP, LXDWN, LXUP,
0205 1  IRALT
0206  C-----
0207  C      DEVELOP RADIAL STREAMLINE PATTERN AROUND EACH INJECTION WELL
0208  C      IF (RADS) = WELL RADIUS.
0209      NPT = 0
0210  C
0211      DO 1020 IPT = 1, MPT
0212  C      (NLINE) STREAMLINE STARTING POINTS ARE LOCATED ON A CIRCLE
0213  C      CENTERED AT (XSTRT, YSTRT) WITH RADIUS (RADS).
0214  C
0215  C
0216  C-----
0217  C      READ STREAMLINE STARTING POINTS, ANGLE, NO. LINES, RADIUS, PT.NO.
0218  C      READ (10, 60) XSTRT, YSTRT, ANGL, MLINE, RADS, NUMBR
0219  C-----
0220  C
0221  C
0222      IF (RADS .LT. .001) RADS = .001
0223      ANGL = ANGL * PI / 180.
0224  C
0225      DO 1010 ILINE = 1, MLINE
0226      THETA = ILINE * ANGL
0227      NPT = NPT + 1
0228      NLINE (NPT) = MLINE
0229      STRT (NPT) = CMPLX (XSTRT + RADS * COS (THETA), YSTRT + RADS
0230 1 * SIN (THETA))
0231      NUMS (NPT, 1) = NUMBR
0232      ALTR (NPT) = IERR
0233 1010      CONTINUE
0234  C
0235 1020      CONTINUE
0236  C
0237      IF (IRALT .LE. 0) GO TO 1027
0238      DO 1025 IRA = 1, IRALT

```

```

0239 C -----
0240 C     AS AN ALTERNATIVE, SPECIFY A N-R CONVERGENCE CRITERIA ON PSI
0241 C     FOR INDIVIDUAL STREAMLINES. THIS IS USEFUL FOR PROBLEMS
0242 C     WHERE SOME LINES ARE COMPRESSED CLOSE TOGETHER
0243 C     (STRONGER CRITERIA) AND SOME ARE SPACED FAR APART
0244 C     (WEAKER CRITERIA).
0245 C     READ (10, 15) IPT, ALTR (IPT)
0246 C -----
0247 C     1025     CONTINUE
0248 C     1027     CONTINUE
0249 C
0250 C
0251 C     1030     CONTINUE
0252 C
0253 C     IF (NML .LE. 0) GO TO 1050
0254 C     DO 1040 IWL = 1, NML
0255 C
0256 C
0257 C -----
0258 C     READ WELL LOCATION, PUMPING RATE AND WELL NO.
0259 C     READ (10, 70) ZWL (IWL), Q (IWL), NUMW (IWL)
0260 C -----
0261 C
0262 C
0263 C     1040     CONTINUE
0264 C
0265 C     1050     CONTINUE
0266 C
0267 C     INPUT DOUBLET PARAMETERS.
0268 C
0269 C     MAXIMUM 5 ZONES, 10 DIPOLES (SIDES) PER ZONE.
0270 C     ZONE(I,1) = ZONE NUMBER (I).
0271 C     ZONE(I,2) = PERM. INSIDE ZONE(I).
0272 C     ZONE(I,3) = NUMBER OF SIDES ON THE ZONE(I) POLYGON.
0273 C     IF > 0 COUNTER-CLOCKWISE ROTATION
0274 C     IF < 0 CLOCKWISE ROTATION
0275 C     ZONE(I,4) = ZONE(I,4) = PERM. OUTSIDE ZONE.
0276 C     ZONE(I,5) = OUTSIDE ZONE NUMBER (I)
0277 C     ZONE(I,6) = CUMULATIVE ZONE INDEX (START)
0278 C     ZONE(I,7) = CUMULATIVE ZONE INDEX (END)
0279 C
0280 C     DPOLE(I) = COMPLEX COORDINATE X+IY OF LINE DIPOLE ENDPOINTS.
0281 C     I = PERMEABILITY ZONE NUMBER (ZONE(I,1)).
0282 C     J = LINE DIPOLE (ENDPOINT) NUMBER.
0283 C
0284 C     A CLOSED POLYGONAL BOUNDARY IS GENERATED ACCORDING TO THE
0285 C     SEQUENCE IN WHICH ENDPOINTS ARE READ IN. THE CLOSING BOUNDARY
0286 C     IS OBTAINED BY CONNECTING DPOLE(1) WITH DPOLE(N).
0287 C     (N) DIPOLE ENDPOINTS FORMING A CLOSED POLYGON ARE ENTERED IN
0288 C     COUNTER CLOCKWISE ROTATION IF THEY FORM AN OUTER-MOST ZONE
0289 C     BOUNDARY. SUCCESSIVE INTERIOR ZONE BOUNDARIES ARE ENTERED IN
0290 C     CLOCKWISE, THEN COUNTERCLOCKWISE, THEN CLOCKWISE ETC. ROTATION.
0291 C
0292 C     IF (NZT .EQ. 0) GO TO 1070
0293 C
0294 C     DO 1060 IZNE = 1, NZPLS
0295 C
0296 C -----
0297 C     READ PERM. ZONE PARAMETERS.
0298 C     READ (10, 80) (ZONE (IZNE, L), L = 1, 5)

```

```

0299 C-----
0300 C
0301 C     DEFAULT OUTSIDE PERM IS BACKGROUND.
0302 C         IF (ZONE (IZNE, 5) .LE. 0.0) ZONE (IZNE, 4) = PERM
0303 C         IF (ZONE (IZNE, 5) .LE. 0.0) ZONE (IZNE, 5) = NZNE
0304 C
0305 C     DETERMINE ZONE BOUNDARY INDICIES.
0306 C
0307 C         IF (IZNE .GT. 1) GO TO 1065
0308 C         ZONE (IZNE, 6) = 1.
0309 C         ZONE (IZNE, 7) = ABS (ZONE (IZNE, 3))
0310 C         GO TO 1075
0311 C 1065     ZONE (IZNE, 6) = ZONE (IZNE-1, 6) + ABS (ZONE (IZNE-1, 3))
0312 C         ZONE (IZNE, 7) = ZONE (IZNE-1, 7) + ABS (ZONE (IZNE, 3))
0313 C 1075     CONTINUE
0314 C
0315 C         NPOL1 = ZONE (IZNE, 6)
0316 C         NPOL2 = ZONE (IZNE, 7)
0317 C
0318 C
0319 C-----
0320 C     READ ZONE BOUNDARYS.
0321 C         READ (10, 30) (DPOLE (IPOL), IPOL = NPOL1, NPOL2)
0322 C-----
0323 C
0324 C
0325 C-----
0326 C     READ DOUBLET STRENGTHS FROM PREVIOUS I-D-E-N-T-I-C-A-L RUN.
0327 C
0328 C         IF (NZT .LT. 0) READ (JL, 90) (JUMP (IPOL), MU (IPOL),
0329 C 1         IPOL = NPOL1, NPOL2)
0330 C-----
0331 C
0332 C
0333 C 1060     CONTINUE
0334 C
0335 C     IF NO PERM. ZONES.
0336 C
0337 C 1070     ZONE (NZNE, 1) = NZNE
0338 C         ZONE (NZNE, 2) = PERM
0339 C         ZONE (NZNE, 4) = PERM
0340 C         POR (NZNE) = POROS
0341 C         P (NZNE) = PS
0342 C         RHO (NZNE) = RHOS
0343 C         LOCZ = NZNE
0344 C
0345 C
0346 C-----
0347 C     READ ONE DIMENSIONAL FLOW DIRECTION AND AND FLUX.
0348 C     FLUX = VELOCITY * POROSITY.
0349 C     IF (IFLO .GT. 0) READ (10, 30) ANGL1, FLUX
0350 C-----
0351 C
0352 C
0353 C     ECHO AQUIFER TYPE AND OTHER INPUT PARAMETERS.
0354 C
0355 C     AQFR(1) = ' '
0356 C     IF (AQ .EQ. 'CONA') AQFR (1) = ' '
0357 C     IF (AQ .EQ. 'UNCA') AQFR (1) = ' UN'
0358 C     WRITE (LU, 110) (AQFR (L), L = 1, 3), THICK, ZBND, RHD, DEC,

```

```

0359      1  RERR, IERR, XMID, YMID, XSID, YSID
0360      C
0361      C
0362      WRITE (LU, 120) (AQFR (L), L = 1, 3), PERM
0363      C
0364      IF (NZT .EQ. 0) GO TO 1090
0365      C
0366          DO 1080  IZNE = 1, NZPLS
0367          WRITE (LU, 130) ZONE (IZNE, 2), ZONE (IZNE, 1)
0368          NPOL1 = ZONE (IZNE, 6)
0369          NPOL2 = ZONE (IZNE, 7)
0370          WRITE (LU, 140) (DPOLE (IPOL), IPOL = NPOL1, NPOL2)
0371      1080  CONTINUE
0372      1090  CONTINUE
0373      C
0374      IF (IFLO .LE. 0) GO TO 1100
0375      WRITE (LU, 150) FLUX, ANGL1
0376      C
0377      C
0378      C
0379      1100  CONTINUE
0380      IF (NZT .LT. 0) WRITE (LU, 160)
0381      C
0382      C
0383      IF (NWL .LE. 0) GO TO 1110
0384      WRITE (LU, 170)
0385      WRITE (LU, 180) (NUMW (IWL), ZWL (IWL), Q (IWL), IWL = 1, NWL)
0386      C
0387      C
0388      C
0389      C
0390      1110  CONTINUE
0391      C
0392      C      DEFAULT BOUNDARIES.
0393      IF (ZLIM .EQ. 0.0) ZLIM = ZBND
0394      C
0395      C      EXTRINSIC PERM AND 1-D FLOW CONVERTED TO (FT./HR.).
0396      C
0397          PERM = PERM * 3600.0 / 646315.0
0398          FLUX = FLUX / 365.0 / 24.0
0399          DO 1120  IZNE = 1, NZNE
0400          ZONE (IZNE, 2) = ZONE (IZNE, 2) * 3600.0 / 646315.0
0401          ZONE (IZNE, 4) = ZONE (IZNE, 4) * 3600.0 / 646315.0
0402      1120  CONTINUE
0403      C
0404      C      ONE-D. FLOW CONVERTED TO RADIANS, ESTABLISH 1-D BOUNDARY HEAD.
0405      ANGL1 = ANGL1 * 2.0 * PI / 360.
0406      UNFM = THICK * FLUX
0407      C
0408      C      PUMPING RATE CONVERTED TO (CU.FT./HR.)
0409      C
0410          DO 1130  IWL = 1, NWL
0411      1130  Q (IWL) = Q (IWL) / 7.4805 * 60.0
0412      C
0413      C      DETERMINE BOUNDARY PHI.
0414      C
0415      CALL HTOP (RPHI, RHD, PERM, THICK)
0416      C
0417      C      CALL DIPOLE STRENGTH ROUTINES
0418      LP = 2

```

```

0419 C
0420 C   LINEAR INTERPOLATION.
0421 C   IF (NZT .GT. 0 .AND. LP .LT. 2) CALL STGTH (IHD, RPHI, LP)
0422 C
0423 C   LINEAR AND SECOND ORDER INTERPOLATION
0424 C   IF (NZT .GT. 0 .AND. LP .GE. 2) CALL NDPNT (NZNE, IHD, RPHI, LP)
0425 C
0426 C
0427 C   IF NZT .LT. 0 STRENGTHS WERE OBTAINED FROM A PREVIOUS RUN.
0428 C
0429 C   NZT = NZPLS
0430 C
0431 C
0432 C   GENERATE A STREAMLINE PATTERN.
0433 C
0434 C   IF (MPT .NE. 0) CALL SLINE (HDMN, HDMX, VOPT, IFLAG, ICT1, ALTR)
0435 C
0436 C   GENERATE A GRID OF HEAD VALUES FOR CONTOURING.
0437 C
0438 C   IF (GOPT .NE. 0) CALL GRID (ZSPA, HDMN, HDMX, IFLAG, ICT2)
0439 C
0440 C   IF (GOPT .EQ. 0 .AND. MPT .EQ. 0) GO TO 1170
0441 C
0442 C   WRITE TO AUXILIARY PLOTTING FILE.
0443 C
0444 C   WRITE (AL, 190) XLO, YLO, XHI, YHI, ZSPA
0445 C   WRITE (AL, 200) NWL, NZT
0446 C   IF (NWL .LE. 0) GO TO 1145
0447 C
0448 C       DO 1140 IWL = 1, NWL
0449 C       WRITE (AL, 210) IWL, ZWL (IWL)
0450 C 1140   CONTINUE
0451 C
0452 C 1145  IF (NZT .LE. 0) GO TO 1165
0453 C       NTOT = ZONE (NZT, 7)
0454 C
0455 C       WRITE (AL, 210) NTOT
0456 C
0457 C       DO 1160 IZNE = 1, NZT
0458 C       NPOL = ABS (ZONE (IZNE, 3))
0459 C       NPOL1 = ZONE (IZNE, 6)
0460 C       NPOL2 = ZONE (IZNE, 7)
0461 C       WRITE (AL, 210) NPOL
0462 C
0463 C       DO 1160 IPOL = NPOL1, NPOL2
0464 C       WRITE (AL, 210) IZNE, DPOLE (IPOL)
0465 C 1160   CONTINUE
0466 C
0467 C 1165  CONTINUE
0468 C       WRITE (AL, 190) (HDMX (IH), IH = 1, 3)
0469 C       WRITE (AL, 190) (HDMN (IH), IH = 1, 3)
0470 C       WRITE (AL, 200) ICT1, ICT2
0471 C
0472 C 1170  CONTINUE
0473 C
0474 C
0475 C
0476 C   10  FORMAT ( 3I5, 5F10.0 )
0477 C   15  FORMAT ( I5, F10.0 )
0478 C   20  FORMAT ( 6E10.5, 2I5 )

```

```

0479      25  FORMAT (8E10.5)
0480      30  FORMAT ( 2F10.0 )
0481      40  FORMAT ( 6I5, 4F10.0, A4 )
0482      50  FORMAT ( 3F10.0, I5, F10.0, 3I5 )
0483      60  FORMAT ( 3F10.0, I5, F10.0, I5)
0484      70  FORMAT ( 3F10.0, I5 )
0485      80  FORMAT ( 5F10.0 )
0486      90  FORMAT ( 2E15.9 )
0487     110  FORMAT ( ///1X, 3A4, " AQUIFER THICKNESS ",F10.2, " (FEET)",/
0488           1   1X, "BOUNDARY COND. (RADIUS)",F10.2, " (FEET)"/1X,
0489           2   "BOUNDARY COND. (HEAD)"F10.2," (FEET)"/1X,"DECREMENT IN HEAD"
0490           3   ,F10.5, /1X, "ERROR CRITERIA: (PHI)" E10.5, " (PSI) "
0491           4   E10.5, /1X, "EVALUATION BOUNDARY (CTR.", F8.2, 1X, F8.2,
0492           5   ", SIDES", F10.2, " BY", F10.2, " )(FEET)" )
0493     120  FORMAT ( //1X, 3A4, 1X, " AQUIFER PERMEABILITY",//1X,
0494           1   10H(BOUNDARY), F10.4, 1X, 11H(GL/DY/FT2) // )
0495     130  FORMAT(1X,"PERM. INSIDE ", F10.4, 1X,11H(GL/DY/FT2) //1X,
0496           1   "ZONE",1X,F5.0,5X,23HBOUNDARY COORDS. (FEET) ,5X,
0497           2   23HBOUNDARY COORDS. (FEET) ,/25X, 5H(X,Y) ,23X, 5H(X,Y) )
0498     140  FORMAT ( 15X, 2F10.2 , 8X, 2F10.2 )
0499     150  FORMAT ( //1X, 18HUNIFORM (1-D) FLUX, 1X, F10.5, 1X, 7HFT./YR.,
0500           1   1X, 14HAT AN ANGLE OF, F5.1, 1X, 8HDEGREES. )
0501     160  FORMAT ( //1X, 41H( DOUBLET STRENGTHS INPUT FROM A PREVIOUS ,
0502           1   15HIDENTICAL RUN. ) )
0503     170  FORMAT ( /// 19X 32HWELL LOCATIONS AND PUMPING RATES//1X,
0504           1   8HWELL NO., 5X, 7HX-COORD 6X, 7HY-COORD , 2X, "PUMPING RATE (",
0505           2   "GAL/MIN)", 3X, 8HZONE NO. / )
0506     180  FORMAT ( /1X, I4, 5X, F10.2, 3X, F10.2, 3X, F10.2 )
0507     190  FORMAT ( 5E15.7 )
0508     200  FORMAT ( 2I4 )
0509     210  FORMAT ( I4, 2E15.7 )
0510  C
0511      END
0512  C
0513  C
0514  C
0515      SUBROUTINE  GRID (ZSPA, HDMN, HDMX, IFLAG, ICT)
0516  C
0517  C      CALCULATE A GRID OF OMEGA VALUES FOR HEAD CONTOUR MAPPING.
0518  C
0519  C
0520      COMMON / CNST / I, PI
0521      COMMON / INPT / IOPT, NZNE, ITER, DPJP, IOMEG
0522      COMMON / POLE / ZONE, DPOLE
0523      COMMON / ZON / LOCZ
0524      COMMON / WELLD / ZBND, RPHI, Q, ZWL, STRT, WRAD, WRDS, NPT, NWL,
0525           1   NUMS, NUMW
0526      COMMON / IO / LU, PL, GL, AL, JL, IL, TL
0527      COMMON / AQF / THICK, AQ, FL, BND
0528  C
0529  C
0530      DIMENSION BND (4), DPOLE (300), HDMN (3), HDMX (3), NUMS (100,
0531           1   2), NUMW (30), Q (30), STRT (100), WRAD (30), ZHD (4), ZONE (4,
0532           2   7), ZWL (30)
0533  C
0534      REAL  IOMEG
0535  C
0536      INTEGER  AL, GL, PL, TL
0537  C
0538      COMPLEX  BND, DODZ, DPOLE, I, OMCON, OMDEC, OMEGA, OMPRT, STRT,

```

```

0539      1  ZSTR, ZWL, Z, D20DZ
0540  C
0541      ICT = 0
0542  C
0543  C      ESTABLISH GRID BOUNDARIES.
0544      IXEND = REAL (BND (2) - BND (4)) / ZSPA
0545      IYEND = AIMAG (BND (4) - BND (2)) / ZSPA
0546      ZSTR = BND (4)
0547  C
0548      NZT = NZNE - 1
0549      IHD = 1
0550  C
0551  C      BEGIN COLUMN AND ROW LOOPS.
0552  C
0553      DO 1040 IY = 1, IYEND
0554  C
0555          DO 1030 IX = 1, IXEND
0556  C
0557  C      FIND EACH Z.
0558  C
0559          Z = ZSTR + CMPLX ((IX - 1) * ZSPA, - (IY - 1) * ZSPA)
0560  C
0561  C      OMIT Z VALUES TOO NEAR SINGULARITIES.
0562  C
0563          IF (NZT .LE. 0) GO TO 1005
0564  C
0565          DO 1000 IZNE = 1, NZT
0566              NPOL1 = ZONE (IZNE, 6)
0567              NPOL2 = ZONE (IZNE, 7)
0568  C
0569              DO 1000 IPOL = NPOL1, NPOL2
0570                  IF (CABS (Z - DPDL (IPOL)) .GT. .50) GO TO 1000
0571                  HD = - 99.0
0572                  OMEGA = ( - 99.0, - 99.0)
0573                  GO TO 1020
0574  C      1000      CONTINUE
0575  C
0576  C      1005      CONTINUE
0577  C
0578          IF (NWL .LE. 0) GO TO 1015
0579  C
0580          DO 1010 IWL = 1, NWL
0581              IF (CABS (Z - ZWL (IWL)) .GT. .50) GO TO 1010
0582              HD = - 99.0
0583              OMEGA = ( - 99.0, - 99.0)
0584              GO TO 1020
0585  C      1010      CONTINUE
0586  C
0587  C      1015      CONTINUE
0588  C
0589  C
0590      ICT = ICT + 1
0591  C
0592  C      CALCULATE OMEGA(Z).
0593  C
0594          CALL DMA (Z, OMCON, OMEGA, DODZ, D20DZ, IFLAG, IHD, NZNE)
0595          ROMEQ = REAL (OMEGA)
0596  C
0597  C      CALCULATE HEAD.
0598          CALL PTOH (ROMEQ, HD, ZONE (LOC2, 2))

```

```

0599 C
0600     ZHD (1) = HD
0601     ZHD (2) = REAL (Z)
0602     ZHD (3) = AIMAG (Z)
0603 C
0604 C     FIND MIN. AND MAX. VALUES FOR PLOTTING LATER.
0605 C
0606     CALL MXMN (ZHD, HDMN, HDMX, ICT)
0607 C
0608 C
0609 C     WRITE TO GRID FILE
0610 C
0611     1020     WRITE (GL, 10) IX, IY, Z, HD, OMEGA
0612 C     PRINT STATUS ON DISPLAY TERMINAL.
0613     WRITE (1, 20) IX, IY
0614     1030     CONTINUE
0615     WRITE (1, 30) IY
0616     1040     CONTINUE
0617 C
0618     IZERO = 0
0619     WRITE (GL, 10) IZERO
0620 C
0621     RETURN
0622 C
0623 C
0624 C
0625     10 FORMAT ( '2I4, 5E15.7 ' )
0626     20 FORMAT ( 'GRID ROW AND COLUMN...', 2I5 )
0627     30 FORMAT ( 'GRID COLUMN COMPLETED...', I5 )
0628 C
0629     END
0630 C
0631 C
0632 C
0633     SUBROUTINE SLINE (HDMN, HDMX, VOPT, IFLAG, ICT, ALTR)
0634 C
0635 C     CALCULATE A STREAMLINE PATTERN USING ONE OF TWO ITERATIVE METHODS
0636 C
0637 C
0638     COMMON / CNST / I, PI
0639     COMMON / INPT / IOPT, NZNE, ITER, DPJP, IOMEG
0640     COMMON / POLE / ZONE, DPOLE
0641     COMMON / ZON / LOCZ
0642     COMMON / WELLD / ZBND, RPHI, Q, ZWL, STRT, WRAD, WRDS, NPT, NWL,
0643     1     NUMS, NUMW
0644     COMMON / ERRS / RERR, IERR, ITRMX, ALSTP, LXDWN, LXUP
0645     COMMON / IO / LU, PL, GL, AL, JL, IL, TL
0646     COMMON / CHEM / D, F, P, SIGMA, POR, RHO, ISKP
0647     COMMON / AQF / THICK, AQ, FL, BND
0648     COMMON / LINE / NLINE, STM, DEC, MXPTS
0649 C
0650 C
0651     DIMENSION BND (4), DPOLE (300), HDMN (3), HDMX (3), HEAD (4,
0652     1     200), NLINE (100), NUMS (100, 2), NUMW (30), Q (30), STRT
0653     2     (100), WRAD (30), ZONE (4, 7), ZWL (30), ALTR (100), POR (4),
0654     3     P (4), RHO (4)
0655 C
0656 C
0657     COMPLEX BND, CDM, DODZ, DPOLE, FLXVC, I, OMCON, OMDEC, OMEGA,
0658     1     OMPRT, OMST, STRT, VELVC, ZWL, Z, D2ODZ

```

```

0659      INTEGER    AL, GL, PL, STM, VOPT, TL
0660      REAL        IERR, IOMEG
0661 C
0662      DATA      POND, ZERO / 4HPOND, 4HZERO /
0663 C
0664 C      BEGIN STREAMLINE DEVELOPMENT
0665 C
0666 C      PRINT HEADERS.
0667 C      WRITE (LU, 10)
0668 C
0669 C      IF (STM .EQ. 1) WRITE (LU, 20)
0670 C      IF (STM .EQ. 0) WRITE (LU, 30)
0671 C
0672 C      ICT = 0
0673 C      ICTM = 0
0674 C
0675 C      BEGIN EACH STREAMLINE HERE.
0676 C
0677 C      DO 1100 IPT = 1, NPT
0678 C      ICT = ICT + 1
0679 C      ICTM = ICTM + 1
0680 C      IHD = 1
0681 C      IHDM = 1
0682 C      ITER = 0
0683 C      Z = STRT (IPT)
0684 C
0685 C      CALCULATE STARTING HEAD.
0686 C      CALL OMA (Z, OMCON, OMEGA, DODZ, D2ODZ, IFLAG, IHD, NZNE)
0687 C
0688 C      OMST = OMCON
0689 C
0690 C      CALCULATE RELATIVE ERROR CRITERIA FOR IM(OMEGA).
0691 C      IF (IPT .EQ. 1) RELE = ABS (AIMAG (OMCON))
0692 C      IERR = ALTR (IPT) * RELE
0693 C
0694 C      HEAD (2, IHD) = REAL (Z)
0695 C      HEAD (3, IHD) = AIMAG (Z)
0696 C      ROMEG = REAL (OMEGA)
0697 C      IOMEG = AIMAG (OMEGA)
0698 C
0699 C      CALL PTOH (ROMEG, HEAD (1, IHD), ZONE (LOCZ, 2))
0700 C
0701 C      CALL MXMN (HEAD (1, IHD), HDMN, HDMX, ICT)
0702 C
0703 C      TERMINATE STREAMLINE IF PONDING OR ZERO HEAD.
0704 C      IF (FL .EQ. POND) GO TO 1090
0705 C
0706 C      CHEMICAL INTERFACE OPTION.
0707 C      IF (VOPT .EQ. 0) GO TO 1000
0708 C      MINUS = - 1
0709 C      CALL STMVL (HEAD (1, IHD), OMEGA, Z, DODZ, D2ODZ, ICTM, IHDM,
0710 C      1 IPT, MINUS, ZONE (LOCZ, 2))
0711 C      1000 CONTINUE
0712 C
0713 C      HEAD (4, IHD) = IPT
0714 C
0715 C      WRITE TO PLOTTING FILE.
0716 C      WRITE (PL, 70) (HEAD (IH, IHD), IH = 1, 4)
0717 C
0718 C      PRINTER OUTPUT

```

```

0719      WRITE (LU,40)
0720      WRITE (LU,50)
0721      WRITE (LU,60)
0722      WRITE (LU, 80) IPT, IHD, OMEGA, DODZ, HEAD (1, IHD)
0723      WRITE (LU,51)
0724      WRITE (LU,61)
0725      WRITE (LU, 81) (HEAD (IH, IHD), IH = 2,3), FL, ITER, LOOZ
0726  C
0727  C      BEGIN LOOP FOR SUCCESSIVE STREAMLINE POINTS.
0728  C
0729 1010      IHD = IHD + 1
0730      IHDM = IHDM + 1
0731      ITER = 0
0732      LOOZ = LOOZ
0733  C
0734  C      CHECK STREAMLINE APPROACH TO WELLS, STOP IF WITHIN
0735  C      WELL RADIUS.
0736  C
0737      IF (IFLAG .LE. 0) GO TO 1020
0738      IF (CABS (Z - ZWL (IFLAG)) .GE. ABS (WRDS)) GO TO 1020
0739      IF (DEC * Q (IFLAG) .GT. 0) GO TO 1050
0740  C
0741 1020      CONTINUE
0742  C
0743  C
0744  C      SELECT STREAMLINE TRACING METHOD, NEWTONS METHOD WITH CONVERGENCE
0745  C      ON BOTH PHI AND PSI OR ON PSI ALONE.
0746  C
0747  C      (1). ALLOW PHI INTERVAL BETWEEN STREAMLINE POINTS TO VARY.
0748  C          ITERATE ON PSI ONLY.
0749  C
0750      IF (STM .EQ. 1) CALL NUMCA (DEC, DODZ, D2ODZ, Z, OMCON, OMEGA,
0751 1 IFLAG, IHD)
0752  C
0753  C
0754      IF (STM .NE. 0) GO TO 1030
0755  C
0756  C      (2). FIX THE PHI INTERVAL, ITERATE ON BOTH PHI AND PSI.
0757  C
0758  C      MAINTAIN A CONTINUOUS OMEGA VARIABLE FOR NEWTON ITERATION AND
0759  C      COMPUTING CONVENIENCE.
0760  C      CONTINUOUS OMEGA (OMCON OR OMDEC).
0761  C
0762      HD = HEAD (1, 1) - (IHD - 1) * DEC
0763      IF (HD .LE. 0.0) GO TO 1075
0764      CALL HTOP (ROMEG, HD, ZONE (NZNE, 2), THICK)
0765      OMDEC = CMPLX (ROMEG, AIMAG (OMST))
0766  C
0767      CALL NEWRA (OMDEC, DODZ, D2ODZ, Z, OMCON, OMEGA, IFLAG, IHD)
0768  C
0769  C
0770 1030      CONTINUE
0771  C
0772  C      CHECK TO SEE IF PERM. ZONE BOUNDARY WAS CROSSED.
0773  C
0774      IF (LOOZ .NE. LOOZ) WRITE (LU, 90) LOOZ, LOOZ
0775  C
0776      ROMEG = REAL (OMEGA)
0777      CALL PTOH (ROMEG, HEAD (1, IHD), ZONE (LOOZ, 2))
0778  C

```

```

0779 C      CHECK FOR PONDING OR ZERO HEAD.
0780      IF (FL .EQ. POND) GO TO 1090
0781      IF (FL .EQ. ZERO .AND. STM .EQ. 0) GO TO 1090
0782 C
0783 C      HEAD(1,I) = HYDRAULIC HEAD (FT.)
0784 C      HEAD(2,I) = X-COORD. (FT.)
0785 C      HEAD(3,I) = Y-COORD. (FT.)
0786 C      HEAD(4,I) = STREAMLINE NUMBER.
0787 C
0788      HEAD (2, IHD) = REAL (Z)
0789      HEAD (3, IHD) = AIMAG (Z)
0790      HEAD (4, IHD) = IPT
0791 C
0792      CALL MXMN (HEAD (1, IHD), HDMN, HDMX, ICT)
0793 C
0794 C
0795 C      WRITE TO PLOTTING FILE, BUT FIRST LABEL BACKTRACKING
0796 C      STREAMLINE POINTS.
0797 C
0798      IF (IHD .EQ. 2) HGRAD = HEAD (1, 1)
0799      IBACK = 1
0800      IF (DEC .GT. 0) GO TO 1045
0801      IF (HEAD (1, IHD) .LE. HGRAD) GO TO 1047
0802      IF (IFLAG .EQ. -2) GO TO 1048
0803      HGRAD = HEAD (1, IHD)
0804 1048      IBACK = 0
0805      GO TO 1047
0806 C
0807 1045      IF (HEAD (1, IHD) .GE. HGRAD) GO TO 1047
0808      IF (IFLAG .EQ. -2) GO TO 1049
0809      HGRAD = HEAD (1, IHD)
0810 1049      IBACK = 0
0811 1047      CONTINUE
0812 C
0813      WRITE (LU,40)
0814      WRITE (PL, 70) (HEAD (IH, IHD), IH = 1, 4), IFLAG, IBACK
0815      WRITE (LU,50)
0816      WRITE (LU,60)
0817      WRITE (LU, 80) IPT, IHD, OMEGA, DODZ, HEAD (1, IHD)
0818      WRITE (LU,51)
0819      WRITE (LU,61)
0820      WRITE (LU, 81) (HEAD (IH, IHD), IH = 2,3), FL, ITER, LOCZ
0821 C
0822      ICT = ICT + 1
0823      ICTM = ICTM + 1
0824 C
0825 C      CALCULATE STREAMLINE VELOCITY AND FLUX FOR KINETIC CHEMICAL
0826 C      MODEL INTERFACE.
0827 C
0828      IF (VOPT .EQ. 0) GO TO 1040
0829      IF (IHD .EQ. 1) GO TO 1041
0830      IF (MOD(IHD, ISKP) .NE. 0) GO TO 1042
0831 1041      IF (IFLAG .EQ. -2 .OR. IBACK .EQ. 1) GO TO 1042
0832 C
0833      CALL STMVL (HEAD (1, IHD), OMEGA, Z, DODZ, D2ODZ, ICTM, IHDM,
0834 1      IPT, MINUS, ZONE (LOCZ, 2))
0835 C
0836      GO TO 1040
0837 1042      ICTM = ICTM - 1
0838      IHDM = IHDM - 1

```

```

0839 1040 CONTINUE
0840 C
0841 C CHECK FOR ABNORMAL STREAMLINE TRACE.
0842 C
0843 C IF (IFLAG .GE. 0) GO TO 1060
0844 C
0845 C STAGNANT STREAMLINE
0846 C
0847 C IF (IFLAG .EQ. - 1) WRITE (LU, 100) IPT
0848 C IF (IFLAG .EQ. - 1) GO TO 1090
0849 C
0850 C MAXIMUM ITERATIONS WITHOUT CONVERGENCE
0851 C
0852 C IF (IFLAG .EQ. - 2) WRITE (LU, 110) IPT
0853 C IF (IFLAG .EQ. - 2) GO TO 1060
0854 C
0855 C DIPOLE ENDPOINT IN THE STREAMLINE PATH.
0856 C
0857 C IF (IFLAG .EQ. - 4) WRITE (LU, 170) IPT
0858 C IF (IFLAG .EQ. - 4) GO TO 1090
0859 C
0860 C
0861 C STREAMLINE AT WELL.
0862 C
0863 1050 HEAD (1, IHD) = - 999999.99
0864 HEAD (2, IHD) = REAL (ZWL (IFLAG))
0865 HEAD (3, IHD) = AIMAG (ZWL (IFLAG))
0866 HEAD (4, IHD) = IPT
0867 NUMS (IPT, 2) = NUMW (IFLAG)
0868 ICT = ICT + 1
0869 C
0870 C WRITE TO PLOTTING FILE.
0871 C
0872 C WRITE (PL, 70) (HEAD (IH, IHD), IH = 1, 4)
0873 C WRITE (LU, 120) IHD, (HEAD (IH, IHD), IH = 1, 4)
0874 C GO TO 1100
0875 1060 CONTINUE
0876 C
0877 C CHECK PLOT BOUNDARIES.
0878 C
0879 C CALL INOUT (BND, 2, IT)
0880 C IF (IT .NE. 0) GO TO 1070
0881 C WRITE (LU, 130) IPT
0882 C GO TO 1090
0883 C
0884 C ZERO HEAD
0885 C
0886 1075 WRITE (LU, 180) IPT
0887 C GO TO 1090
0888 1070 CONTINUE
0889 C
0890 C MAX. STREAMLINE POINTS.
0891 C
0892 C IF (IHD .LT. MXPTS) GO TO 1010
0893 C WRITE (LU, 140) IPT
0894 1090 NUMS (IPT, 2) = - 7
0895 1100 CONTINUE
0896 C
0897 1110 CONTINUE
0898 C

```

```

0899 C RESCALE LAST STREAMLINE FOR CHEM FILE AND TRANSFER CHEM. DATA
0900 C TO OUTPUT DEVICE (LOGICAL UNIT 14).
0901 C
0902 IF (VOPT .EQ. 0) GO TO 1120
0903 MINUS = - 2
0904 ICTM = ICTM + 1
0905 CALL STMVL (DM, CDM, CDM, CDM, CDM, ICTM, IHDM, IPT, MINUS, DM)
0906 1120 CONTINUE
0907 C
0908 WRITE (LU, 150) ICT
0909 ENDSL = - 47.
0910 WRITE (PL, 160) ENDSL
0911 C
0912 RETURN
0913 C
0914 C
0915 C
0916 10 FORMAT ( ///, 1X, 80(1H*), /, 21X, 22HSTREAMLINE DEVELOPMENT )
0917 20 FORMAT ( 21X, 23H(VARIABLE PHI INTERVAL), /// )
0918 30 FORMAT ( 21X, 20H(FIXED PHI INTERVAL), /// )
0919 40 FORMAT ( 1X, 80 ( 1H- ) )
0920 50 FORMAT ( /, 2X, 10HSTREAMLINE, 2X, 5HPOINT, 3X, 3HPHI, 10X,
0921 1 3HPSI, 5X, 11HD(PHI)/D(X), 2X, 11HD(PHI)/D(Y), 5X, 4HHEAD)
0922 51 FORMAT ( /6X 7HX COORD, 4X, 7HY COORD, 2X, 11HCONF./UNCF., 2X,
0923 1 "N.R. ITER", 1X, 4HZONE )
0924 60 FORMAT ( 6X, 3HNO., 6X, 3HNO., 25X, 11HD(PHI)/D(X), 3X,
0925 1 12H-D(PHI)/D(X), 2X, 6H(FEET) )
0926 61 FORMAT ( 29X, 4HFLOW )
0927 70 FORMAT ( 4E15.5, 2I5 )
0928 80 FORMAT ( 2X, I5, 4X, I5, 4 (1X, E12.5), 1X, F10.2 )
0929 81 FORMAT ( 1X, F10.2, 1X, F10.2, 7X , A4, 3X, I5, 3X, I5)
0930 90 FORMAT ( 1X, 15HSTREAMLINE HAS , 17HCROSSED BOUNDARY
0931 1 15HFROM PERM. ZONE, I5, 13H TO PERM ZONE, I5, 1H. )
0932 100 FORMAT ( 1X, 10HSTREAMLINE, I5, 1X, 10HTERMINATED, 1X
0933 1 13HD(OMEGA)/D(Z) 1X 22HIS APPROXIMATELY ZERO. )
0934 110 FORMAT ( 1X, 22H--WARNING-- STREAMLINE, I5, 1X, 9HFAILED TO, 1X,
0935 1 45HCONVERGE AT THIS POINT AFTER MAX. ITERATIONS. )
0936 120 FORMAT ( 8X, I5, 33X, F10.2, 1X, F10.2, 3X, F10.2, 2X, F10.2 )
0937 130 FORMAT ( 1X, 10HSTREAMLINE, I5, 24H TERMINATED AT BOUNDARY )
0938 140 FORMAT ( 1X, 10HSTREAMLINE, I5, 29H TERMINATED AFTER MAX. NO. OF
0939 1 5HPTS./ / )
0940 150 FORMAT ( 1X, I5, 30H RECORDS OF STREAMLINE OUTPUT )
0941 160 FORMAT ( 45X, E15.5 )
0942 170 FORMAT ( 1X, 10HSTREAMLINE, I5, 1X, 13HTERMINATED AT, 1X,
0943 1 18HDIPOLE SINGULARITY)
0944 180 FORMAT ( 1X, 10HSTREAMLINE, I5, 1X, 15HTERMINATED WITH, 1X
0945 1 10HZERO HEAD. )
0946 C
0947 END
0948 C
0949 C
0950 C
0951 SUBROUTINE OMA (Z, OMCON, OMEGA, DODZ, D2ODZ, MKWL, IHD, NZNE)
0952 C
0953 C THIS ROUTINE DETERMINES THE ADDATIVE EFFECT OF ALL HYDROLOGIC
0954 C COMPONENTS IN THE FLOW DOMAIN.
0955 C
0956 C
0957 COMMON / CNST / I, PI
0958 COMMON / ZARG / ARGPO, DODF

```

```

0959      COMMON / WELLD / ZBND, RPHI, Q, ZWL, STRT, WRAD, WRDS, NPT, HML,
0960      1  NUMS, NUMW
0961      COMMON / ONED / IFLO, ANGL1, UNFM
0962      COMMON / POLE / ZONE, DPOLE
0963      COMMON / ZON / LOCZ
0964      COMMON / IO / LU, PL, GL, AL, JL, IL, TL
0965      C
0966      C
0967      DIMENSION ARGPO (600), DPOLE (300), NUMS (100, 2), NUMW
0968      1  (30), Q (30), STRT (100), WRAD (30), ZONE (4, 7), ZWL (30)
0969      C
0970      COMPLEX  DODZ, DODZ, DOLD, DOWL, DPOLE, I, OMCON, OMEGA, OMLD,
0971      1  OMWL, STRT, ZWL, Z, ONEFL, BND1, D2ODZ, D2WL, D2LD
0972      INTEGER  AL, GL, PL, TL
0973      C
0974      OMEGA = (0.0, 0.0)
0975      DODZ = (0.0, 0.0)
0976      D2ODZ = (0.0, 0.0)
0977      C
0978      C  DETERMINE WELL CONTRIBUTION TO OMEGA.
0979      C
0980      IF (NWL .LE. 0) GO TO 1000
0981      CALL WELL (Z, OMWL, DOWL, D2WL, MXWL, IHD)
0982      OMEGA = OMEGA + OMWL
0983      DODZ = DODZ + DOWL
0984      D2ODZ = D2ODZ + D2WL
0985      1000  CONTINUE
0986      C
0987      C
0988      C  ADD ONE DIMENSIONAL FLOW TO OMEGA AND DODZ SUBJECT TO BOUNDARY
0989      C  CONDITION THAT WHEN Z = ZBND* $\cos(\text{ANGL}) + I \sin(\text{ANGL})$ ,  $\text{OMEGA}(10) = 0$ .
0990      C
0991      IF (IFLO .EQ. 0) GO TO 1010
0992      BND1 = ZBND * (COS (ANGL1) + I * SIN (ANGL1))
0993      ONEFL = UNFM * (COS (ANGL1) - I * SIN (ANGL1)) * (Z - BND1)
0994      OMEGA = OMEGA + ONEFL
0995      C
0996      DODZ = DODZ + UNFM * (COS (ANGL1) - I * SIN (ANGL1))
0997      C
0998      1010  CONTINUE
0999      C
1000      C
1001      C  DETERMINE PERM. ZONE CONTRIBUTION TO OMEGA.
1002      C
1003      IF (NZNE .LE. 1) GO TO 1020
1004      CALL DIPOL (Z, OMLD, DOLD, D2LD, IHD, NZNE)
1005      OMEGA = OMEGA + OMLD + RPHI
1006      DODZ = DODZ + DOLD
1007      D2ODZ = D2ODZ + D2LD
1008      C
1009      OMCON = CMPLX (ZONE (NZNE, 2) / ZONE (LOCZ, 2) * REAL (OMEGA),
1010      1  AIMAG (OMEGA))
1011      C
1012      GO TO 1030
1013      C
1014      C  ADD BOUNDARY HEAD (POTENTIAL) IF NOT ALREADY DONE ABOVE.
1015      C
1016      1020  OMEGA = OMEGA + RPHI
1017      OMCON = OMEGA
1018      1030  CONTINUE

```

```

1019 C
1020 C
1021     RETURN
1022 C
1023 C
1024     END
1025 C
1026 C
1027 C
1028     SUBROUTINE WELL (Z, OMWL, DOWL, D2WL, MXWL, IHD)
1029 C
1030 C     THIS ROUTINE CALCULATES COMPLEX POTENTIAL (OMEGA) AT A
1031 C     GIVEN X,Y COORDINATE (Z), RESULTING FROM WELL PUMPING.
1032 C
1033 C
1034     COMMON / CNST / I, PI
1035     COMMON / ZON / LOCZ
1036     COMMON / WELLD / ZBND, RPHI, Q, ZWL, STRT, WRAD, WRDS, NPT, NWL,
1037 1     NUMS, NUMW
1038     COMMON / IO / LU, PL, GL, AL, JL, IL, TL
1039 C
1040 C
1041     DIMENSION IWIND (30), LSARG (30), NUMS (100, 2), NUMW (30), Q
1042 1     (30), STRT (100), WRAD (30), ZWL (30)
1043 C
1044     COMPLEX    CMLG, DOWL, DTRM, D1, D2, D3, I, OMWL, STRT, WLTRM,
1045 1     ZWL, Z, D2WL, D2TR
1046     INTEGER    AL, GL, PL, TL
1047     REAL       LSARG
1048 C
1049     OMWL = (0.0, 0.0)
1050     DOWL = (0.0, 0.0)
1051     D2WL = (0.0, 0.0)
1052     WLMX = 0.0
1053     MXWL = 0
1054 C
1055 C     LOOP FOR EACH WELL.
1056 C
1057     DO 1030 IWL = 1, NWL
1058 C
1059 C     DETERMINE THE ADDITIVE EFFECT OF EACH WELL ON THE POINT (Z).
1060 C
1061     QPI = Q (IWL) / (2.0 * PI)
1062     CMLG = CLOG ((Z - ZWL (IWL)) / ZBND)
1063 C
1064 C     ARBITRARILY, MAKE THE BRANCH CUT PARALLEL TO POS. X AXIS.
1065 C
1066     IF (AIMAG (CMLG) .LT. 0.0) CMLG = CMPLX (REAL (CMLG), AIMAG
1067 1     (CMLG) + 2.0 * PI)
1068     IF (IHD .NE. 1) GO TO 1000
1069     IWIND (IWL) = 0
1070     GO TO 1010
1071 C
1072 C     IF STREAMLINE CROSSES THE BRANCH CUT COUNTERCLOCKWISE THEN
1073 C     ADD 2PI FOR CONTINUITY OF ARG(Z).
1074 C
1075 1000     IF (LSARG (IWL) - AIMAG (CMLG) .GT. PI) IWIND (IWL) = IWIND
1076 1     (IWL) + 1
1077 C
1078 C     IF STREAMLINE CROSSES BRANCH CLOCKWISE, SUBTRACT 2PI.

```

```

1079 C
1080     IF (LSARG (IWL) - AIMAG (CMLG) .LT. - PI) IWIND (IWL) = IWIND
1081     (IWL) - 1
1082 1010     LSARG (IWL) = AIMAG (CMLG)
1083 C
1084 C     REVISE IM(OMEGA) ACCORDINGLY.
1085 C
1086     CMLG = CMPLX (REAL (CMLG), AIMAG (CMLG) + IWIND (IWL) * 2.0 *
1087     PI)
1088     WLTRM = QPI * CMLG
1089 C
1090 C     CHECK WELL APPROACH.
1091 C
1092     IF (CABS (Z - ZWL (IWL)) .LT. WRDS) MXWL = IWL
1093 1020     CONTINUE
1094     OMWL = OMWL + WLTRM
1095 C
1096 C     CALCULATE D(OMEGA)/D(Z) FOR ITERATION SCHEME. NOTE, WLTRM IS
1097 C     COMPLEX HERE BECAUSE INDIVIDUAL STREAMLINES ARE SPECIFIED.
1098 C
1099     DTRM = QPI / (Z - ZWL (IWL))
1100     D2TR = -QPI / (Z - ZWL (IWL)) ** 2
1101     DOWL = DOWL + DTRM
1102     D2WL = D2WL + D2TR
1103 1030     CONTINUE
1104 C
1105     RETURN
1106 C
1107 C
1108     END
1109 C
1110 C     .....
1111 C
1112     SUBROUTINE NEWRA (DCDV, DERIV, D2DDZ, INDV, DEPV, DEPV2, IFLAG,
1113     1     IHD)
1114 C
1115 C     CALCULATE X AND Y (Z) GIVEN PHI AND PSI (OMEGA) USING NEWTONS
1116 C     METHOD TO ITERATIVELY FIND THE ROOTS OF A NON-LINEAR EQUATION.
1117 C     A RELAXATION PARAMETER (ALPHA) IS AUTOMATICALLY INCREASED OR
1118 C     DECREASED TO SPEED CONVERGENCE.
1119 C
1120 C     NEWTONS METHOD REQUIRING CONVERGENCE ON BOTH PHI AND PSI IS
1121 C     GENERALLY NOT PRACTICAL IF STREAMLINE PATHS ARE SHARPLY AFFECTED
1122 C     BY RADICAL DIFFERENCES IN PERMEABILITY.
1123 C     THIS ITERATIVE SCHEME IS INTENDED PRIMARILY FOR USE IN COUPLING
1124 C     THE HYDROLOGY OUTPUT WITH NUMERICAL MODELS OF MASS AND/OR
1125 C     CHEMICAL TRANSPORT ALONG STREAMLINES. (EG. INSITU LEACHING)
1126 C
1127     COMMON / CNST / I, PI
1128     COMMON / ZON / LOCZ
1129     COMMON / INPT / IOPT, NZNE, ITER, DPJP, IOMEG
1130     COMMON / ZARG / ARGPO, DDDF
1131     COMMON / ONED / IFLO, ANGL1, UNFM
1132     COMMON / ERRS / RERR, IERR, ITRMX, ALSTP, LXDWN, LXUP
1133     COMMON / ID / LU, PL, GL, AL, JL, IL, TL
1134 C
1135 C
1136     DIMENSION ARGPO (600), LCIND (5)
1137 C
1138     COMPLEX     BESTD, BESTI, BESTV, BEST2, DCDV, DEPV2, DEPV, DEP1,

```

```

1139      1  DERIV, DIFF, DODF, INDV, I, LCIND, LSDIF, OLDER, OLDV, TINDV,
1140      2  D2ODZ
1141      INTEGER  AL, GL, PL, RELAX, TL
1142      REAL     IANG, IDIFF, IERR, IMNDF, IOMEG, MINER
1143  C
1144      IFLAG = 0
1145      ALPHA = 1.0
1146      RELAX = 0
1147      LAX = 0
1148      IF (IHD .EQ. 2) LCIND = INDV
1149  C
1150  C  PREVIOUS STREAMLINE POINT IS INITIAL ESTIMATE FOR NEXT POINT.
1151  C
1152      DEPI = DEPV
1153      LSDIF = DEPV - DCDV
1154      SPAC = REAL (LSDIF)
1155      MINER = 9.0E9
1156  C
1157  C  CALCULATE RELATIVE ERROR FOR RE(OMEGA).
1158  C  UPDATE REAL ERROR CRITERIA AT EACH NODE.
1159  C
1160      RELR = ABS (RERR * REAL (DCDV))
1161  C
1162      IF (IOPT .EQ. 0) GO TO 990
1163      WRITE (LU,11)
1164      WRITE (LU,10) RELR, IERR
1165  C
1166  C  CHECK FOR D(OMEGA)/D(Z) = 0.
1167  990  IF (CABS (DERIV) .LE. RERR) GO TO 1120
1168  C
1169  1000  CONTINUE
1170      ITER = ITER + 1
1171      OLDV = DEPV
1172      OLDER = DERIV
1173  1010  CONTINUE
1174  C
1175  C  CALCULATE A TENTATIVE NEW POINT (Z) ON THE STREAMLINE USING
1176  C  NEWTONS FORMULA AND PREVIOUS STREAMLINE POINT AS INITIAL GUESS.
1177  C
1178      TINDV = INDV - ALPHA * (OLDV - DCDV) / OLDER
1179  C
1180  C  CALCULATE OMEGA AT THIS TENTATIVE Z.
1181  C
1182      CALL OMA (TINDV, DEPV, DEPV2, DERIV, D2ODZ, IFLAG, IHD, NZNE)
1183  C
1184  C  CHECK PROXIMITY TO DIPOLE SINGULARITIES.
1185  C
1186      CALL DPCHK (TINDV, LCIND, OMCON, OMEGA, SPAC, IERR,
1187  1  IFLAG, ISING, IHD, IZ)
1188      IF (ISING .NE. 0) GO TO 1155
1189  C
1190  C  CALCULATE DIFFERENCE BETWEEN CALCULATED OMEGA AND DESIRED.
1191  C
1192      DIFF = DEPV - DCDV
1193      RDIFF = REAL (DIFF)
1194      IDIFF = AIMAG (DIFF)
1195  C
1196  C
1197      IF (IOPT .NE. 0) WRITE (LU, 20) TINDV, DIFF, ALPHA, RELAX, LAX
1198  C

```

```

1199 C      CHECK CONVERGENCE REQUIREMENT ON PHI AND PSI.
1200 C
1201 1020 IF (ABS (RDIFF) .LE. RELR .AND. ABS (IDIFF) .LE. IERR)
1202     1 GO TO 1115
1203     IF (ABS (RDIFF) .LT. RELR .OR. RDIFF * REAL (LSDIF) .GT. 0.0) GO
1204     1 TO 1030
1205 C
1206 C      ALTER RELAXATION PARAMETERS AS NEEDED.
1207 C
1208     RELAX = RELAX + 1
1209     LAX = 0
1210     GO TO 1040
1211 1030 LAX = LAX + 1
1212 C
1213 1040 IF (ABS (IDIFF) .LT. IERR .OR. IDIFF * AIMAG (LSDIF) .GT.
1214     1 0.0) GO TO 1050
1215     RELAX = RELAX + 1
1216     LAX = 0
1217     GO TO 1060
1218 1050 LAX = LAX + 1
1219 1060 IF (RELAX .LE. LXDMN) GO TO 1070
1220     IF (ALPHA .LE. ALSTP) GO TO 1070
1221 C
1222 C      IF NEWTONS ITER. IS DIVERGING REDUCE ALPHA (RELAXATION PARAMETER)
1223 C      AND CHOOSE AN INTERIOR Z AS NEXT GUESS. NOTE THAT ALPHA IS NOT
1224 C      AFFECTED BY PHI OR PSI DIVERGENCE WHILE THEY MEET THEIR
1225 C      INDIVIDUAL ERROR CRITERIA.
1226 C
1227     LAX = 0
1228     RELAX = 0
1229     ALPHA = ALPHA / 2.0
1230     GO TO 1080
1231 C
1232 C      COMPARE CALCULATED VALUE OF OMEGA TO DESIRED VALUE, IF CLOSE
1233 C      ENOUGH STOP ITERATING.
1234 C
1235 1070 IF (LAX .LT. LXUP) GO TO 1080
1236     IF (ALPHA .LT. 1.0) ALPHA = ALPHA * 2.0
1237     LAX = 0
1238     RELAX = 0
1239 C
1240 1080 INDV = TINDV
1241     LSDIF = DIFF
1242 C
1243 C      RETAIN THE BEST ESTIMATES IN CASE MAX. ITER. BOUND IS REACHED.
1244 C
1245     RELER = CABS (CPLX (RDIFF / RELR, IDIFF / IERR))
1246     IF (RELER .GE. MINER) GO TO 1090
1247     MINER = RELER
1248     BESTI = TINDV
1249     BESTD = DEPV
1250     BESTV = DERIV
1251     BEST2 = DEPV2
1252     LOCB = LOCZ
1253 1090 CONTINUE
1254 C
1255 C      STOP IF MAX. ITERATION LIMIT IS EXCEEDED.
1256 C
1257     IF (ITER .GT. ITRMX) GO TO 1100
1258     GO TO 1000

```

```

1259 1100 WRITE (LU, 30)
1260 C
1261 C BEST ESTIMATE BECOMES NEXT STREAMLINE POINT. PRINT WARNING.
1262 C
1263 TINDV = BESTI
1264 DEPV = BESTD
1265 DERIV = BESTV
1266 DEPV2 = BEST2
1267 LOCZ = LOCB
1268 IFLAG = -2
1269 GO TO 1155
1270 C
1271 C STREAMLINE POINT HAS BEEN FOUND. SAVE THE LAST FIVE POINTS.
1272 C
1273 1115 IF (IZ .GT. 4) GO TO 1140
1274 IZ = IZ + 1
1275 GO TO 1130
1276 1140 DO 1150 KZ = 1,4
1277 1150 LCIND (5 - KZ) = LCIND (6 - KZ)
1278 1130 LCIND (IZ) = TINDV
1279 C
1280 1155 INDV = TINDV
1281 C DEPV = DCOV
1282 C
1283 C CHECK FOR D(OMEGA)/D(Z) APPROX. EQUAL TO ZERO.
1284 C
1285 C IF (CABS (DERIV) .LE. RERR) GO TO 1120
1286 C
1287 C RETURN
1288 C
1289 1120 IFLAG = - 1
1290 C
1291 C RETURN
1292 C
1293 C
1294 C
1295 10 FORMAT ( / 5X, 7HX-COORD , 5X, 7HY-COORD , 3X, 13HREAL CONVERG.
1296 1 4X, 12HIM. CONVERG. 2X, 5HALPHA, 2X, 5HRELAX, 2X, 7HRESTORE )
1297 11 FORMAT( /1X, " REL. ERROR CRITERIA (REAL", F7.6, " IM. ", F7.6, 1H) )
1298 20 FORMAT ( 2X, F10.2, 2X, F10.2, 2X, E12.5, 5X, E12.5, 3X, F5.3, 2
1299 1 (1X, 15) )
1300 30 FORMAT ( 8X, 43HNEWTON ITER. LIMIT EXCEEDED FOR THIS POINT. )
1301 C
1302 C END
1303 C
1304 C .....
1305 C .....
1306 C
1307 C SUBROUTINE NUMCA (SPAC, DODZ, D2ODZ, Z, OMCON, OMEGA, IFLAG,
1308 1 IHD)
1309 C
1310 C STREAMLINE TRACING USING NEWTONS METHOD, WITH CONVERGENCE
1311 C REQUIRED OF PSI ALONE. A RELAXATION PARAMETER IS INCLUDED
1312 C TO SPEED CONVERGENCE.
1313 C THIS ITERATIVE SCHEME GUARANTEES NEITHER EQUAL Z NOR EQUAL
1314 C PHI SPACING OF STREAMLINE NODES.
1315 C
1316 C
1317 C COMMON / INPT / IOPT, NZNE, ITER, DPJP, IOMEG
1318 C COMMON / CNST / I, PI

```

```

1319      COMMON / ZON / LOCZ
1320      COMMON / ERRS / RERR, IERR, ITRMX, ALSTP, LXDMN, LXUP
1321      COMMON / IO / LU, PL, GL, AL, JL, IL, TL
1322 C
1323 C
1324      DIMENSION LCIND (5)
1325 C
1326      COMPLEX  BESTC, BESTD, BESTO, BESTZ, CWZ, DODZ, I, LCIND, NEWZ,
1327 i  OMCON, OMEGA, WZ, WZ1, WZ2, Z1, Z2, Z
1328      INTEGER  AL, GL, PL, TL
1329      REAL     IERR, IMDIF, IOMEG, MINER
1330 C
1331      MINER = 9.E9
1332      IFLAG = 0
1333      ALPHA = 1.0
1334 C
1335      IF (IHD .NE. 2) GO TO 990
1336      IZ = 1
1337      LCIND (1) = Z
1338      ISING = 0
1339      990 CONTINUE
1340 C
1341 C      NEGATIVE ALSTP ALLOWS INITIAL ALPHA LESS THAN 1.
1342 C      (USEFUL WHEN STREAMLINE CONVERGENCE IS DIFFICULT)
1343 C
1344      IF (ALSTP .LT. 0.0) ALPHA = ABS(ALSTP)
1345 C
1346 C
1347      IF (IOPT .EQ. 0) GO TO 991
1348      WRITE (LU,11) IERR
1349      WRITE (LU,10)
1350 C      RELR = ABS(RERR * REAL(OMEGA))
1351 C
1352 C      OBTAIN ENDPOINT OF STREAMLINE TANGENT VECTOR OF LENGTH (SPAC).
1353 C
1354      991 WZ = (- 1.0, 0.0) * DODZ
1355      CWZ = CABS (WZ) / WZ
1356      NEWZ = Z + SPAC * CABS (WZ) / WZ
1357 C      ITERATE ALONG THE EQUIPOTENTIAL PASSING THROUGH NEWZ TO
1358 C      OBTAIN THE DESIRED PSI VALUE.
1359 C
1360      DO 1030 ITER = 1, ITRMX
1361 C
1362      CALL OMA (NEWZ, OMCON, OMEGA, DODZ, D2ODZ, IFLAG, IHD, NZNE)
1363 C
1364 C      CHECK STREAMLINE PROXIMITY TO DIPOLE ENDPOINT SINGULARITIES.
1365 C
1366      CALL DPCHK (NEWZ, LCIND, OMCON, OMEGA, SPAC, IERR, IFLAG,
1367 i  ISING, IHD, IZ)
1368      IF (ISING .NE. 0) GO TO 1045
1369 C
1370 C      STREAMLINE POINT OK.
1371 C
1372      WZ = (- 1.0, 0.0) * DODZ
1373      IMDIF = IOMEG - AIMAG (OMEGA)
1374 C
1375 C      CHECK FOR CONVERGENCE ON PSI ONLY.
1376 C
1377      AERR = ABS (IMDIF)
1378      IF (AERR .LT. IERR) GO TO 1035

```

```

1379 C
1380 C     CONVERGENCE NOT GOOD ENOUGH, FIND A NEW Z.
1381 C
1382 C     IF (IOPT .NE. 0) WRITE (LU, 20) NEWZ, IMDIF, ALPHA
1383 C
1384 C
1385 C     RETAIN BEST GUESS SO FAR.
1386 C
1387 C     IF (AERR .GE. MINER) GO TO 1000
1388 C     MINER = AERR
1389 C     BESTZ = NEWZ
1390 C     BESTO = OMEGA
1391 C     BESTD = DODZ
1392 C     BESTL = OMCON
1393 C     LOCB = LOCZ
1394 C
1395 C     ALTER RELAXATION PARAMETER AS NEEDED.
1396 C
1397 C 1000 CONTINUE
1398 C     IF (ITER .LE. 1) GO TO 1005
1399 C     Z2 = Z1
1400 C     Z2ER = Z1ER
1401 C     W22 = W21
1402 C 1005 Z1 = NEWZ
1403 C     Z1ER = IMDIF
1404 C     W21 = W2
1405 C     IF (ITER .LE. 1) GO TO 1010
1406 C     IF (Z1ER * Z2ER .GT. 0.0 .OR. ABS(Z2ER) .GT. ABS(Z1ER))
1407 C 1     GO TO 1010
1408 C     IF (ALPHA .LE. ABS(ALSTP)) GO TO 1010
1409 C     ALPHA = ALPHA / 2.0
1410 C     Z1 = Z2
1411 C     Z1ER = Z2ER
1412 C     W21 = W22
1413 C
1414 C     CALCULATE A NEW ESTIMATE OF Z.
1415 C
1416 C 1010 NEWZ = Z1 - ALPHA * I * Z1ER / W21
1417 C
1418 C 1030 CONTINUE
1419 C
1420 C     NEXT POINT NOT FOUND AFTER MAX. ITERATIONS.
1421 C     SO USE BEST EST. SO FAR.
1422 C
1423 C     NEWZ = BESTZ
1424 C     OMEGA = BESTO
1425 C     DODZ = BESTD
1426 C     OMCON = BESTC
1427 C     LOCZ = LOCB
1428 C     IFLAG = - 2
1429 C     GO TO 1045
1430 C
1431 C     NEXT POINT FOUND.  SAVE THE LAST FIVE STREAMLINE POINTS.
1432 C
1433 C 1035 IF (IZ .GT. 4) GO TO 1050
1434 C     IZ = IZ + 1
1435 C     GO TO 1040
1436 C
1437 C 1050 DO 1060 KZ = 1,4
1438 C 1060 LCIND (5 - KZ) = LCIND (6 - KZ)

```

```

1439 C
1440   1040 LCIND (IZ) = NEWZ
1441   1045 Z = NEWZ
1442 C
1443 C   CHECK FOR MIN. DODZ
1444 C
1445 C   IF (CABS (DODZ) .LE. RERR) IFLAG = - 1
1446 C
1447 C   RETURN
1448 C
1449 C
1450 C
1451   10 FORMAT ( / 5X, 7HX-COORD, 5X, 7HY-COORD, 3X, 15HPSI CONVERGENCE,
1452   1   5X, 5HRELAX )
1453   11 FORMAT ( / 1X, " REL. ERROR CRITERIA ON PSI ", F7.6 )
1454   20 FORMAT ( F10.2, 3X, F10.2, 5X, E12.6, 7X, F5.3, / )
1455 C
1456 C   END
1457 C
1458 C   .....
1459 C   .....
1460 C
1461 C   SUBROUTINE DPCHK (NEWZ, LCIND, DMCON, OMEGA, SPAC, IERR, IFLAG,
1462   1   ISING, IHD, IZ)
1463 C
1464 C   CHECK CURRENT STREAMLINE COORD. FOR PROXIMITY TO DIPOLE
1465 C   SINGULARITIES.
1466 C
1467 C
1468 C   COMMON / ZON / LOCZ
1469 C   COMMON / INPT / IDPT, NZNE, ITER, DPJP, IOMEG
1470 C   COMMON / CNST / I, PI
1471 C   COMMON / POLE / ZONE, DPOLE
1472 C   COMMON / WELLD / ZBND, RPHI, Q, ZWL, STRT, WRAD, WRDS, NPT, NWL,
1473   1   NUMS, NUMW
1474 C   COMMON / LINE / NLINE, STM, DEC, MXPTS
1475 C   COMMON / IO / LU, PL, GL, AL, JL, IL, TL
1476 C
1477 C
1478 C   DIMENSION DPOLE (300), ZONE (4, 7), STRT (100), ZWL (30),
1479   1   Q (30), WRAD (30), NUMS (100, 2), NUMW (30), LCIND(5), NLINE(100)
1480 C
1481 C   COMPLEX   DODZ, DPOLE, I, NEWZ, DMCON, OMEGA, Z, ZGSS2,
1482   1   ZGSS, ZWL, STRT, LCIND, D2DODZ
1483 C   INTEGER   AL, GL, PL, STM, TL
1484 C   REAL      IOMEG, IERR, IOM2, IOMM, IMDF
1485 C
1486 C   NZT = NZNE - 1
1487 C
1488 C   CHECK ALL DIPOLE ENDPOINTS.
1489 C
1490 C   DO 1000 IZNE = 1, NZT
1491 C     NPOL1 = ZONE (IZNE, 6)
1492 C     NPOL2 = ZONE (IZNE, 7)
1493 C
1494 C     DO 1000 IPOL = NPOL1, NPOL2
1495 C       IF (CABS (NEWZ - DPOLE (IPOL)) .GT. DPJP) GO TO 1000
1496 C
1497 C   A DIPOLE SINGULARITY IS IN THE PATH OF THIS STREAMLINE COORD.
1498 C

```

```

1499          WRITE (LU, 10) NEWZ
1500 C
1501 C          ORIENT A CIRCLE AROUND THE DOUBLET ENDPOINT.  USE ONE OF THE
1502 C          LAST FIVE Z COORDS. TO DETERMINE THE RADIUS OF THE CIRCLE.
1503 C          PRIOR STREAMLINE POINTS ARE CHOSEN (INCREASING THE RADIUS
1504 C          OF THE CIRCLE) IF THE NEWTON ITERATION FAILS REPEATEDLY AT ONE
1505 C          DIPOLE SINGULARITY.
1506 C
1507          IF (IZ .LE. 0) GO TO 1080
1508          Z = LCIND (IZ)
1509          IZ = IZ - 1
1510          ARGZ = AIMAG (CLOG (Z - DPOLE (IPOL)))
1511          IF (ARGZ .LT. 0) ARGZ = ARGZ + 2.0 * PI
1512          RAD = CABS (Z - DPOLE (IPOL))
1513          IF (RAD .GT. 5.*DEC) GO TO 1080
1514 C
1515 C          CHECK FOR WELLS INSIDE THE DIPOLE CIRCLE.  IF THERE, CHECK
1516 C          STREAMLINES THAT TERMINATE AT THE WELL RADIUS.
1517 C
1518          DO 1020 IWL = 1, NWL
1519          WLRD = CABS (ZWL (IWL) - DPOLE (IPOL))
1520          IF (WLRD .GE. RAD) GO TO 1020
1521          ZGSS = ZWL (IWL) + WRDS
1522          CALL OMA (ZGSS, OMCON, OMEGA, DODZ, D2ODZ, MXWL, IHD, NZNE)
1523          IOM2 = AIMAG (OMCON)
1524          IOMM = AIMAG (OMCON) - Q (IWL)
1525          IF ((IOMEG - IOM2) * (IOMEG - IOMM) .GT. 0.0) GO TO 1020
1526 C
1527 C          THE PSI VALUE IS FOUND AT A WELL RADIUS.
1528 C
1529          IFLAG = IWL
1530          GO TO 1060
1531 1020          CONTINUE
1532 C
1533 C          LOCATE A STARTING RIGHT BOUND ON THE CIRCLE.  STARTING ANGLE
1534 C          IS DETERMINED BY LAST Z + 1 DEGREE.
1535 C
1536          ANGL = ARGZ + PI / 180.0
1537          ZGSS2 = DPOLE (IPOL) + RAD * (COS (ANGL) + I * SIN (ANGL))
1538          CALL OMA (ZGSS2, OMCON, OMEGA, DODZ, D2ODZ, MXWL, IHD, NZNE)
1539          IOMM = AIMAG (OMEGA)
1540 C
1541 C          TRAVERSE THE PERIMETER OF THE CIRCLE IN 10 DEGREE (OR LESS)
1542 C          INCREMENTS, IN ORDER TO BOUND THE PSI VALUE.
1543 C
1544          IBND = 0
1545          TEN = PI / 18.
1546 1050          ANG2 = ANGL
1547          IF (ANG2 + TEN .GE. ARGZ + 2.0 * PI) TEN = PI / 180.
1548          IOM2 = IOMM
1549          IF (IBND .GT. 0) IBND = IBND + 1
1550 C
1551 C          IF PSI IS BOUNDED, HALVE THE LAST ANGLE INCREMENT AND
1552 C          CALCULATE A NEW PSI VALUE.
1553 C
1554 1030          ANGL = ANG2 + TEN / (2.0 ** IBND)
1555          IF (ANGL .GE. ARGZ + 2.0 * PI) GO TO 1080
1556          ZGSS = DPOLE (IPOL) + RAD * (COS (ANGL) + I * SIN (ANGL))
1557          CALL OMA (ZGSS, OMCON, OMEGA, DODZ, D2ODZ, MXWL, IHD, NZNE)
1558          IOMM = AIMAG (OMEGA)

```

```

1559 C
1560 C
1561 C      CHECK IF PSI IS BOUNDED.
1562 C
1563 C      IMDF = IOMEG - IOMM
1564 C      IF (<<IOMEG - IOM2> * IMDF .GT. 0) GO TO 1050
1565 C
1566 C      PSI HAS BEEN BOUNDED, CHECK ERROR IN PSI ESTIMATE.
1567 C
1568 C      IF (ABS (IMDF) .LE. IERR) GO TO 1060
1569 C      IBND = IBND + 1
1570 C      IF (IBND .GT. 10) GO TO 1090
1571 C      GO TO 1030
1572 C
1573 C      NEW Z HAS BEEN FOUND.
1574 C
1575 C      1060      NEWZ = ZGSS
1576 C      GO TO 1010
1577 C
1578 C      ONLY ONE PSI VALUE FOUND ON THE DIPOLE CIRCLE.  TERMINATE
1579 C      THE STREAMLINE.
1580 C
1581 C      1080      NEWZ = Z
1582 C      WRITE (LU, 20)
1583 C      IFLAG = -4
1584 C      GO TO 1010
1585 C
1586 C      UNABLE TO MEET SPECIFIED CONVERGENCE CRITERIA
1587 C
1588 C      1090      NEWZ = Z
1589 C      IFLAG = -2
1590 C
1591 C      1010      CONTINUE
1592 C      ISING = IPOL
1593 C
1594 C      RETURN
1595 C
1596 C      1000      CONTINUE
1597 C      ISING = 0
1598 C
1599 C      RETURN
1600 C
1601 C
1602 C
1603 C
1604 C      10  FORMAT ( 1X, 30HDIPOLE SINGULARITY ENCOUNTERED, 1X,
1605 C      1    29HIN STREAMLINE PATH AT COORDS., 2F9.2 )
1606 C      20  FORMAT ( 1X, 28HUNABLE TO LOCATE NEXT COORD.,1X,
1607 C      1    22HSTREAMLINE TERMINATES.)
1608 C
1609 C      END
1610 C
1611 C      .....
1612 C      .....
1613 C
1614 C      SUBROUTINE  MXMN (ZHD, HDMN, HDMX, ICT)
1615 C
1616 C      DETERMINE MAX AND MIN VALUES OF STREAMLINE COORDS AND HEAD.
1617 C
1618 C

```

```

1619      COMMON / IO / LU, PL, GL, AL, JL, IL, TL
1620 C
1621 C
1622      DIMENSION HDMN (3), HDMX (3), ZHD (4)
1623 C
1624      INTEGER  AL, GL, PL, TL
1625      IF (ICT .GT. 1) GO TO 1010
1626 C
1627      DO 1000  IH = 1, 3
1628          HDMX (IH) = - 9.E9
1629      1000  HDMN (IH) = 9.E9
1630 C
1631      1010  DO 1020  IH = 1, 3
1632          IF (ZHD (IH) .LT. HDMN (IH)) HDMN (IH) = ZHD (IH)
1633          IF (ZHD (IH) .GT. HDMX (IH)) HDMX (IH) = ZHD (IH)
1634      1020  CONTINUE
1635 C
1636      RETURN
1637 C
1638 C
1639      END
1640 C
1641 C .....
1642 C
1643 C
1644      SUBROUTINE PTOH (RMEG, HD, PERM)
1645 C
1646 C      CONVERT POTENTIAL TO HEAD.  NOTE, THAT PHI IS CONTINUOUS ACROSS
1647 C      CONFINED/UNCONFINED FLOW BOUNDARY.
1648 C
1649 C
1650      COMMON / IO / LU, PL, GL, AL, JL, IL, TL
1651      COMMON / AQF / THICK, AQ, FL, BND
1652 C
1653 C
1654      DIMENSION BND (4)
1655 C
1656      CHARACTER*4 AQ
1657      COMPLEX  BND
1658      INTEGER  AL, GL, PL, TL
1659      REAL  KBND
1660 C
1661      DATA  ZERO, POND, UNCF, CONF, CONA / 4HZERO, 4HPOND, 4HUNCF,
1662 1 4HCONF, 4HCONA /
1663 C
1664      KBND = PERM * THICK ** 2
1665 C
1666 C      CHECK IF CONFINED OR UNCONFINED FLOW.
1667 C
1668      IF (RMEG .GE. KBND) GO TO 1010
1669      IF (RMEG .GE. .5 * KBND) GO TO 1000
1670 C
1671 C      IF AQUIFER IS UNSATURATED, SET HEAD=0
1672 C
1673      WRITE (LU, 10)
1674      FL = ZERO
1675      HD = 0.0
1676 C
1677      RETURN
1678 C

```

```

1679 C      IF FLOW IS UNCONFINED AT THIS POINT USE THIS EXPRESSION FOR HEAD.
1680 C
1681   1000 HD = ABS (SQRT (2.0 * ROMEQ / PERM - THICK ** 2))
1682      FL = UNCF
1683 C
1684      RETURN
1685 C
1686 C      IF HEAD EXCEEDS AQUIFER THICKNESS, CHECK TO BE SURE THAT THE
1687 C      AQUIFER HAS AN UPPER CONFINING LAYER, IF NOT SURFACE PONDING
1688 C      EXISTS AND THIS SOLUTION BREAKS DOWN, TERMINATE STREAMLINE.
1689 C
1690   1010 IF (AQ .EQ. 'CONA') GO TO 1020
1691      FL = POND
1692      WRITE (LU, 20)
1693 C
1694      RETURN
1695 C
1696   1020 HD = ROMEQ / (PERM * THICK)
1697      FL = CONF
1698 C
1699      RETURN
1700 C
1701 C
1702 C
1703      10 FORMAT ( 8X, 42HAQUIFER PUMPED TO ZERO HEAD AT THIS POINT. )
1704      20 FORMAT ( 8X, 43HHEAD EXCEEDS UNCONFINED AQUIFER THICKNESS,
1705      1 23HSTREAMLINE TERMINATED. )
1706 C
1707      END
1708 C
1709 C .....
1710 C
1711      SUBROUTINE HTOP (PHI, HD, PERM, THICK)
1712 C
1713 C      CONVERT HEAD TO POTENTIAL. NOTE, CHECK FOR CONFINED OR
1714 C      UNCONFINED FLOW.
1715 C
1716 C
1717      COMMON / IO / LU, PL, GL, AL, JL, IL, TL
1718 C
1719 C
1720 C      UNCONFINED FLOW.
1721 C
1722      INTEGER AL, GL, PL, TL
1723      IF (HD .LE. THICK) PHI = .5 * PERM * (THICK ** 2 + HD ** 2)
1724 C
1725 C      CONFINED FLOW.
1726 C
1727      IF (HD .GT. THICK) PHI = PERM * THICK * HD
1728 C
1729      RETURN
1730 C
1731      END
1732 C
1733 C .....
1734 C
1735      SUBROUTINE INOUT (BND, Z, IT)
1736 C
1737 C      DETERMINE IF Z IS INSIDE OR OUTSIDE OF PLOT BOUNDARY.
1738 C

```

```

1739 C
1740 COMMON / IO / LU, PL, GL, AL, JL, IL, TL
1741 C
1742 C
1743 DIMENSION BND (4)
1744 C
1745 COMPLEX BND, Z
1746 INTEGER AL, GL, PL, TL
1747 IT = 0
1748 BIO = 0.0
1749 C
1750 DO 1000 IB = 1, 4
1751 IBP = IB + 1
1752 IF (IB .EQ. 4) IBP = 1
1753 BIO = BIO + AIMAG (CLOG ((Z - BND (IBP)) / (Z - BND (IB))))
1754 1000 CONTINUE
1755 C
1756 IT = BIO
1757 C
1758 RETURN
1759 C
1760 C
1761 END
1762 C
1763 C
1764 C
1765 SUBROUTINE DIPOL (Z, OMLD, DOLD, D2LD, IHD, NZNE)
1766 C
1767 THIS ROUTINE CALCULATES THE COMPLEX POTENTIAL RESULTING
1768 FROM ONE OR MORE LINE DIPOLES PLACED ON THE BOUNDARYS BETWEEN
1769 AQUIFER REGIONS HAVING DISCRETELY DIFFERENT PERMEABILITIES.
1770 C
1771 THE DIPOLE STRENGTH (S) IS THE LIMIT AS H GOES TO ZERO,
1772 AND Q GOES TO INFINITY OF Q*H, AT RATES
1773 SUCH THAT THE PRODUCT Q*H REMAINS CONSTANT. I.E. AS
1774 H GOES TO ZERO, Q GOES TO INFINITY AS 1/H.
1775 C
1776 C
1777 C
1778 COMMON / CNST / I, PI
1779 COMMON / ZARG / ARGPO, DODF
1780 COMMON / POLE / ZONE, DPOLE
1781 COMMON / PJMP / JUMP, MU
1782 COMMON / ZON / LOCZ
1783 COMMON / IO / LU, PL, GL, AL, JL, IL, TL
1784 C
1785 C
1786 CALCULATE OMEGA FOR ARBITRARY POINTS (Z), USING THE PREVIOUSLY
1787 CALCULATED DIPOLE STRENGTHS (S) AS ENTRIES IN THE COMPLEX
1788 POTENTIAL EXPRESSION.
1789 C
1790 DIMENSION ARGPO (600), DPOLE (300), JUMP (300),
1791 1 MU (300), OMDP (2), WIND (3), ZONE (4, 7)
1792 C
1793 COMPLEX CLG, DODF, DOLD, DPARB, DPAR1, DPAR2, DPOLE, DPRFA,
1794 1 DPRFB, FACT1, FACT2, FACT3, FACT4, I, OMDP, OMLD, OMZN, OPREF,
1795 2 PARB, TERMP, TERM1, TERM2, TERM3, Z, D2LD, DPAR0, DPAR3, DPAR4
1796 INTEGER AL, GL, OZNE, PLS, PLUS, PL, TL
1797 REAL JUMP, MU
1798 C

```

```

1799      DMLD = (0.0, 0.0)
1800      DOLD = (0.0, 0.0)
1801      D2LD = (0.0, 0.0)
1802      NZT = NZNE - 1
1803  C
1804      DO 1010 IZNE = 1, NZT
1805          DMZN = (0.0, 0.0)
1806          WIND (IZNE) = 0.0
1807          NPOL1 = ZONE (IZNE, 6)
1808          NPOL2 = ZONE (IZNE, 7)
1809  C
1810      DO 1000 IPOL = NPOL1, NPOL2
1811          PLUS = IPOL + 1
1812          IF (IPOL .EQ. NPOL2) PLUS = NPOL1
1813          PLS = NPOL2 + IPOL
1814  C
1815  C      CALCULATE AND ASSEMBLE THE DOUBLET EXPRESSION.
1816  C
1817          FACT1 = Z - DPOLE (PLUS)
1818          FACT2 = DPOLE (PLUS) - DPOLE (IPOL)
1819          FACT3 = Z - DPOLE (IPOL)
1820          FACT4 = - FACT2
1821          TERM1 = FACT1 / FACT4
1822          TERM2 = FACT3 / FACT2
1823          TERM3 = FACT1 / FACT3
1824          TERMP = (Z - (DPOLE (PLUS) + DPOLE (IPOL)) / 2.0) / FACT2
1825          RCLG = REAL (CLOG (TERM3))
1826          ACLG = AIMAG (CLOG (TERM3))
1827  C
1828  C      TWO BRANCH CUTS ARE ASSOCIATED WITH EACH LINE DIPOLE,
1829  C      ONE AT EACH DIPOLE ENDPOINT. BRANCH CUTS ARE SITUATED SO THAT
1830  C      THE BRANCH FROM ENDPOINT Z(J+1) OVERLIES THE LINE DIPOLE AND
1831  C      BRANCHES FROM BOTH Z(J+1) AND Z(J) OVERLAP AT THE RIGHT
1832  C      OF THE LINE DIPOLE.
1833  C
1834  C
1835  C      CALCULATE OMEGA PREFIX.
1836  C
1837          OPREF = - I / (2.0 * PI) * (JUMP (IPOL) * TERM1 + JUMP
1838 1      (PLUS) * TERM2)
1839  C
1840  C      CALCULATE ANGLE MADE BY TENTATIVE Z AND ADJACENT BRANCH CUTS.
1841  C      POSITIVE ORIENTATION.
1842  C
1843          ARGPO (IPOL) = AIMAG (CLOG (- FACT3)) - AIMAG (CLOG
1844 1      (FACT2))
1845          ARGPO (PLS) = AIMAG (CLOG (- FACT1)) - AIMAG (CLOG
1846 1      (FACT2))
1847  C
1848          IF (ARGPO (PLS) .LE. 0.0) ARGPO (PLS) = ARGPO
1849 1      (PLS) + 2.0 * PI
1850          IF (ARGPO (IPOL) .LE. 0.0) ARGPO (IPOL) = ARGPO
1851 1      (IPOL) + 2.0 * PI
1852  C
1853  C      CALCULATE CONTINUOUS LINE DIPOLE (IPOL-PLS) ARGUMENT
1854  C      IN ZONE (IZNE).
1855  C
1856          CLG = CMPLX (RCLG, ARGPO (PLS) - ARGPO (IPOL))
1857  C
1858  C      DETERMINE IF PERM. ZONE BOUNDARY WAS CROSSED.

```

```

1859 C
1860 C   IF THE ANGLES MADE BY Z AND ZONE IZNE DOUBLET ENDPOINTS
1861 C   SUM TO 2PI THEN Z LIES WITHIN ZONE IZNE, IF THEY SUM TO 0
1862 C   Z LIES OUTSIDE.
1863 C
1864 C       WIND (IZNE) = WIND (IZNE) + AIMAG (CLG)
1865 C
1866 C   CALCULATE THE PARABOLIC COMPONENT OF DOUBLET STRENGTH.
1867 C   STRENGTH IS INTERPOLATED USING A PARABOLIC FIT, BETWEEN
1868 C   ENDPOINTS. THE STRENGTH IS AN EXACT FIT AT THE MIDPOINT.
1869 C
1870 C       PARB = MU (IPOL) * ( - 2.0 * I / PI ) * (TERM1 * TERM2 *
1871 1   CLG - TERMP)
1872 C
1873 C   ADD LINEAR AND SECOND ORDER TERMS.
1874 C
1875 C       OMDP (1) = OPREF * CLG + PARB
1876 C
1877 C   CUMULATIVE POTENTIAL FOR ONE ZONE.
1878 C
1879 C       OMZN = OMZN + OMDP (1)
1880 C
1881 C   CALCULATE D(OMEGA)/D(Z) FOR THE DIPOLE TERMS.
1882 C   D(OMEGA)/D(Z) IS CONTINUOUS EXCEPT AT BRANCH CROSSINGS.
1883 C
1884 C       DPRFA = I / (2.0 * PI) * (JUMP (IPOL) / FACT4 + JUMP
1885 1   (PLUS) / FACT2)
1886 C       DPRFB = FACT3 ** 2 - FACT1 ** 2
1887 C
1888 C       DPAR0 = FACT3 + FACT1
1889 C       DPAR1 = DPAR0 / FACT2 ** 2
1890 C       DPAR2 = FACT3 * FACT1
1891 C       DPARB = MU (IPOL) * (2.0 * I / PI)
1892 C       DPAR3 = FACT3 / FACT1
1893 C       DPAR4 = FACT4 / FACT1 ** 2
1894 C
1895 C       DOLD = DOLD + DPRFA * (CLG + DPRFB / DPAR2)
1896 1   + DPARB * (DPAR1 * CLG + 2.0 / FACT2)
1897 C
1898 C       D2LD = D2LD + DPRFA * (DPAR3 * DPAR4 +
1899 1   (2.0 * DPAR2 * FACT2 - DPRFB * DPAR0) / DPAR2 ** 2)
1900 2   + DPARB * (2.0 / (FACT2 ** 2) * CLG + DPAR1 * DPAR3 * DPAR4)
1901 1000   CONTINUE
1902 C
1903 C   CUMULATIVE POTENTIAL FOR ALL ZONES.
1904 C
1905 C   IWND = WIND(IZNE)
1906 C   IF (IWND .NE. 0) OMZN = CMPLX(-REAL(OMZN),AIMAG(OMZN))
1907 C       OMLD = OMLD + OMZN
1908 1010   CONTINUE
1909 C
1910 C   DETERMINE THE PERM. ZONE LOCATION OF THE CURRENT (TENTATIVE) (Z).
1911 C   Z MAY LIE INSIDE A ZONE THAT IS ITSELF CONTAINED WITHIN ANOTHER
1912 C   ZONE.
1913 C
1914 C       LOCZ = NZNE
1915 C
1916 C       DO 1020 IZNE = 1, NZT
1917 C       IWND = WIND (IZNE)
1918 C       IF (IWND .EQ. 0) GO TO 1020

```

```

1919         OZNE = ZONE (IZNE, 5)
1920         WIND (OZNE) = 0.0
1921         LOCZ = IZNE
1922 1020     CONTINUE
1923 C
1924         RETURN
1925 C
1926 C
1927         END
1928 C
1929 C .....
1930 C
1931 *EMA/SIZE//VECT/
1932         SUBROUTINE STGTH (IHD, RPHI, LP)
1933 C
1934 C     THIS ROUTINE SOLVES (N) LINEAR EQUATIONS WITH (N) UNKNOWNNS
1935 C     TO DETERMINE THE STRENGTH (DELTA PHI) OF (N) LINE DIPOLE
1936 C     ENDPPOINTS FORMING THE BOUNDARY BETWEEN TWO OR MORE AQUIFER
1937 C     ZONES WITH DISCRETELY DIFFERENT PERMEABILITIES.
1938 C
1939 C
1940 C
1941         COMMON / SIZE / COEF, CHEM
1942         COMMON / VECT / CNST
1943         COMMON / POLE / ZONE, DPOLE
1944         COMMON / INPT / IOPT, NZNE, ITER, DPJP, IOMEG
1945         COMMON / PJMP / JUMP, MU
1946         COMMON / CNST / I, PI
1947         COMMON / DNED / IFLO, ANGL1, UNFM
1948         COMMON / ZON / LOCZ
1949         COMMON / IO / LU, PL, GL, AL, JL, IL, TL
1950 C
1951 C
1952         DIMENSION CHEM (500, 17), CNST (300), COEF (300, 300),
1953 1         DPOLE (300), JUMP (300), MU (300), ZONE (4, 7)
1954 C
1955         COMPLEX CL, CLG, DODZ, DPOLE, FACT1, FACT2, FACT3, FACT4,
1956 1         FACT5, FACT6, I, OMCON, OMEGA, TERM1, TERM2, TERM3, TERM4,
1957 2         TERMS, Z, D2ODZ
1958         INTEGER AL, ER, GL, PLUS, PL, TL
1959         REAL JUMP, MU, IOMEG
1960 C
1961         ITER = 0
1962         ITFLG = 0
1963         WRITE (1, 40)
1964 C
1965         DO 1000 IPOL = 1, 300
1966 C
1967         DO 1000 JPOL = 1, 300
1968 1000     COEF (JPOL, IPOL) = 0.0
1969 C
1970 C     CALCULATE THE BOUNDARY CONDITION AT EVERY DIPOLE ENDPPOINT,
1971 C     I.E. DIPOLE STRENGTH (S) = (K - K1)/K * PHI. THIS CONDITION
1972 C     IS DEVELOPED FROM THE FUNCTION RELATING PHI AND HEAD AND
1973 C     FROM THE ASSERTION THAT AT THE ZONE BOUNDARY HEAD IS CONSTANT BUT
1974 C     PERM. CHANGES FROM K TO K1.
1975 C
1976         NZT = NZNE - 1
1977 C
1978         DO 1090 IZNE = 1, NZT

```

```

1979      NIPL1 = ZONE (IZNE, 6)
1980      NIPL2 = ZONE (IZNE, 7)
1981 C
1982 C      RATIO OF PERMS. INSIDE AND OUTSIDE.
1983 C
1984      PFUNC = ZONE (IZNE, 4) / (ZONE (IZNE, 2) - ZONE (IZNE, 4))
1985 C
1986 C      IF ZONE BOUNDARY IS ENTERED IN CLOCKWISE ROTATION, ORIENTATION
1987 C      IS REVERSED.
1988 C
1989      IF (ZONE (IZNE, 3) .LT. 0.0)
1990 1      PFUNC = -ZONE (IZNE, 2) / ZONE (IZNE, 4) * PFUNC
1991 C
1992 C      CALCULATE DIPOLE STRENGTH, LOOP ONCE FOR EACH DIPOLE.
1993 C
1994 C      DIPOLE STRENGTHS ARE DETERMINED BY SIMULTANEDOUSLY SOLVING
1995 C      THE N REAL POTENTIAL EQUATIONS (ONE FOR EACH DIPOLE HENCE
1996 C      ONE FOR EACH S(J), J=1...N ), WITH THE ABOVE CONDITION.
1997 C
1998      DO 1080 IPOL = NIPL1, NIPL2
1999      MINUS = IPOL - 1
2000      IF (MINUS .LT. NIPL1) MINUS = NIPL2
2001      PLUS = IPOL + 1
2002      IF (PLUS .GT. NIPL2) PLUS = NIPL1
2003 C
2004 C      THE POTENTIAL EXPRESSION FOR THE TWO DIPOLES IN
2005 C      PERMEABILITY ZONE (IZNE) AND ADJACENT TO
2006 C      (IPOL) INDIVIDUALLY CONTAIN TERMS WHICH BECOME INFINITE
2007 C      AS Z APPROACHES Z(J) (THE DIPOLE). HOWEVER, COLLECTIVELY
2008 C      THESE TERMS CANCEL EACH OTHER, LEAVING A SINGLE FINITE
2009 C      LOG TERM WHICH IS HERE COMBINED WITH THE ZONE BOUNDARY COND.
2010 C
2011      FACT5 = DPOLE (IPOL) - DPOLE (PLUS)
2012      FACT6 = DPOLE (IPOL) - DPOLE (MINUS)
2013      TERM4 = FACT5 / FACT6
2014 C
2015 C      THE REAL PART OF THIS EXPRESSION INVOLVES AN ARGUMENT.
2016 C
2017      ARG = AIMAG (CLOG (TERM4))
2018 C
2019 C      ENSURE ARG HAS A SIGN OPPOSITE THAT OF OTHER INTERIOR ANGLES.
2020 C
2021      IF (ARG .GT. 0.0) ARG = ARG - 2.0 * PI
2022 C
2023      ARG4 = PFUNC - 1.0 / (2.0 * PI) * ARG
2024      IF (ABS (ARG4) .LE. 1.0E - 10) ARG4 = SIGN (1.0E - 10, ARG4)
2025 C
2026 C      BEGIN CALCULATING THE COEFFICIENTS FOR THE N SIMULTANEOUS
2027 C      EQUATIONS INVOLVING THE N UNKNOWN STRENGTHS (S). THE
2028 C      DIAGONAL OF THIS MATRIX IS -1.
2029 C
2030 C
2031      COEF (IPOL, IPOL) = -1.0
2032 C
2033 C      INCLUDE IN REAL(OMEGA) THE CONTRIBUTION DUE TO A CONSTANT HEAD
2034 C      BOUNDARY, WELLS AND UNIFORM FLOW.
2035 C      NOTE THAT CNST INVOLVES Z(IPOL)
2036 C      OTHER OMEGA AND THE BOUNDARY PHI.
2037 C
2038 C

```

```

2039          NOPOL = 0
2040 C
2041          CALL OMA (DPOLE (IPOL), OMC0N, OMEGA, D0DZ, D20DZ, MKWL, IHD,
2042 1  NOPOL)
2043 C
2044          CNST (IPOL) = - REAL (OMEGA) / ARG4
2045 C
2046 C          CALCULATE THE COEFFICIENTS OF THE DIPOLE STRENGTH MATRIX.
2047 C          INCLUDE ALL PERMEABILITY ZONES (ALL DIPOLES) IN THE MATRIX.
2048 C
2049          DO 1070 JZNE = 1, NZT
2050          NJPOL = ABS (ZONE (JZNE, 3))
2051          NJPL1 = ZONE (JZNE, 6)
2052          NJPL2 = ZONE (JZNE, 7)
2053          IF (ZONE (JZNE, 1) .NE. ZONE (JZNE, 1)) GO TO 1030
2054          NCT = NJPOL - 2
2055 C
2056 C          CALCULATE THE S MATRIX COEFFICIENTS FOR THOSE DIPOLES ON
2057 C          THE BOUNDARY OF PERMEABILITY ZONE (JZNE).
2058 C          LOOP N-2 TIMES SINCE TWO ADJACENT DIPOLES ARE OMITTED.
2059 C
2060          DO 1020 JCT = 1, NCT
2061          JPOL = JCT + IPOL
2062          IF (JPOL .GT. NJPL2) JPOL = JPOL - NJPOL
2063          MINUS = JPOL - 1
2064          IF (MINUS .LT. NJPL1) MINUS = NJPL2
2065          PLUS = JPOL + 1
2066          IF (PLUS .GT. NJPL2) PLUS = NJPL1
2067 C
2068 C          CHECK FOR COINCIDENT DIPOLES WITHIN ZONE (JZNE), I.E. SLOTS.
2069 C
2070          IF (DPOLE (IPOL) .EQ. DPOLE (PLUS)) GO TO 1020
2071          IF (DPOLE (IPOL) .NE. DPOLE (JPOL)) GO TO 1010
2072          FACT5 = DPOLE (JPOL) - DPOLE (PLUS)
2073          FACT6 = DPOLE (JPOL) - DPOLE (MINUS)
2074          TERMS = FACT5 / FACT6
2075          CLG = CLOG (TERMS)
2076 C
2077 C          COEF. OF STRENGTH FOR COINCIDENT ENDPOINT WITHIN ZONE (JZNE).
2078 C
2079          COEF (JPOL, IPOL) = REAL ( - I / (2.0 * PI) * CLG)
2080 1 / ARG4
2081 C
2082          GO TO 1020
2083 1010          FACT1 = DPOLE (IPOL) - DPOLE (PLUS)
2084          FACT2 = DPOLE (JPOL) - DPOLE (PLUS)
2085          FACT3 = DPOLE (IPOL) - DPOLE (JPOL)
2086          FACT4 = - FACT2
2087          TERM1 = FACT1 / FACT2
2088          TERM2 = FACT3 / FACT4
2089          TERM3 = FACT1 / FACT3
2090          CLG = CLOG (TERM3)
2091 C
2092 C          COEFFICIENT OF STRENGTH S(J) FOR ENDPOINT(I) IN ZONE (JZNE).
2093 C
2094 C
2095          COEF (JPOL, IPOL) = COEF (JPOL, IPOL) -
2096 1 REAL (I / (2.0 * PI) * TERM1 * CLG) / ARG4
2097 C
2098 C          COEFFICIENT OF STRENGTH S(J+1) FOR ENDPOINT (I) IN ZONE (JZNE).

```

```

2099 C
2100 C     NOTE THAT ALL COEF. ARE REAL SINCE DIPOLE CAUSES JUMP IN
2101 C     REAL(OMEGA).
2102 C
2103 C           COEF (PLUS, IPOL) = COEF (PLUS, IPOL) -
2104 1     REAL (I / (2.0 * PI) * TERM2 * CLG) / ARG4
2105 C
2106 1020           CONTINUE
2107 C
2108 C           GO TO 1060
2109 C
2110 C     CALCULATE THE S MATRIX COEFFICIENTS FOR THOSE DIPOLES THAT ARE
2111 C     ON THE BOUNDARIES OF OTHER PERMEABILITY ZONES.
2112 C     (ALL DIPOLES MUST BE INCLUDED IN THE STRENGTH MATRIX).
2113 C
2114 1030           DO 1050 JPOL = NJPL1, NJPL2
2115 C           MINUS = JPOL - 1
2116 C           IF (MINUS .LT. NJPL1) MINUS = NJPL2
2117 C           PLUS = JPOL + 1
2118 C           IF (PLUS .GT. NJPL2) PLUS = NJPL1
2119 C
2120 C     CHECK FOR COINCIDENT LINE DIPOLES IN OTHER ZONES
2121 C     OMIT INFINITE TERMS (SINCE THEY CANCEL EACH OTHER OUT)
2122 C     FROM CALCULATION OF STRENGTH COEFFICIENT. THE FINITE PORTION
2123 C     IS CALCULATED HERE.
2124 C
2125 C           IF (DPOLE (IPOL) .EQ. DPOLE(PLUS)) GO TO 1050
2126 C           IF (DPOLE (IPOL) .NE. DPOLE (JPOL)) GO TO 1040
2127 C           FACT5 = DPOLE (JPOL) - DPOLE(PLUS)
2128 C           FACT6 = DPOLE (JPOL) - DPOLE (MINUS)
2129 C           TERMS = FACT5 / FACT6
2130 C           CLG = CLOG (TERMS)
2131 C
2132 C     COEF. OF STRENGTH (S<J>) FOR COINCIDENT ENDPOINT (I) IN ZONE
2133 C     (JZNE). ONE TERM ONLY.
2134 C
2135 C
2136 C           COEF (JPOL, IPOL) = REAL ( - I / (2.0 * PI) * CLG)
2137 1     / ARG4
2138 C           GO TO 1050
2139 C
2140 C     DIPOLES NOT COINCIDENT.
2141 1040           FACT1 = DPOLE (IPOL) - DPOLE(PLUS)
2142 C           FACT2 = DPOLE (JPOL) - DPOLE(PLUS)
2143 C           FACT3 = DPOLE (IPOL) - DPOLE (JPOL)
2144 C           FACT4 = - FACT2
2145 C           TERM1 = FACT1 / FACT2
2146 C           TERM2 = FACT3 / FACT4
2147 C           TERM3 = FACT1 / FACT3
2148 C           CLG = CLOG (TERM3)
2149 C
2150 C     COEF. OF STRENGTH S<J> FOR ENDPOINT I IN ZONE (JZNE).
2151 C
2152 C           COEF (JPOL, IPOL) = COEF (JPOL, IPOL) -
2153 1     REAL (I / (2.0 * PI) * TERM1 * CLG) / ARG4
2154 C
2155 C     COEF. OF STRENGTH S<J+1> FOR ENDPOINT I IN ZONE (JZNE).
2156 C
2157 C           COEF (PLUS, IPOL) = COEF (PLUS, IPOL) -
2158 1     REAL (I / (2.0 * PI) * TERM2 * CLG) / ARG4

```

```

2159 C
2160 1050      CONTINUE
2161 C
2162 1060      CONTINUE
2163 C
2164 1070      CONTINUE
2165 C
2166 1080      CONTINUE
2167 C
2168 1090      CONTINUE
2169 C
2170 C      ISUM ROWS IN THE S MATRIX.
2171 C      ISUM = ZONE (NZT, 7)
2172 C
2173 C      SOLVE THE N LINEAR EQUATIONS INVOLVING N UNKNOWN DIPOLE
2174 C      STRENGTHS (S(J), J=1,..N) USING GAUSSIAN ELIMINATION MATRIX SOLVER.
2175 C
2176 C      CALL GAUSS (ISUM, ER)
2177 C
2178 C      REPACK THE POTENTIAL JUMP FOR EACH DIPOLE.
2179 C
2180 1100      CONTINUE
2181 C
2182 C      WRITE (LU, 10)
2183 C
2184 C      DO 1130 IZNE = 1, NZT
2185 C      NIPL1 = ZONE (IZNE, 6)
2186 C      NIPL2 = ZONE (IZNE, 7)
2187 C
2188 C      DO 1120 IPOL = NIPL1, NIPL2
2189 C
2190 C      JUMP (IPOL) = CNST (IPOL)
2191 C      IF (IZNE .GE. 2) JUMP (IPOL) = - CNST (IPOL)
2192 C
2193 C      IMPOL = IPOL
2194 C      IF (LP .LE. 1) GO TO 1110
2195 C      IF (MOD (IPOL, 2) .EQ. 0) GO TO 1120
2196 C      IMPOL = (IPOL + 1) / 2
2197 C
2198 C      SAVE STRENGTH VALUES.
2199 C
2200 1110      WRITE (JL, 20) JUMP (IPOL)
2201 C
2202 C      WRITE (LU, 30) IZNE, IMPOL, DPOLE (IPOL), JUMP (IPOL)
2203 1120      CONTINUE
2204 1130      CONTINUE
2205 C
2206 C      RETURN
2207 C
2208 C
2209 C
2210 10  FORMAT ( /// 29X, 17HDOUBLET STRENGTHS, //, 32X, 11H(ENDPOINTS),
2211 1  //, 2X, 8HZONE NO., 3X, 11HDOUBLET NO., 9X, 12HCOORDS.(X,Y),
2212 2  9X, 17HJUMP IN POTENTIAL )
2213 20  FORMAT ( 2E15.9 )
2214 30  FORMAT ( 1X, 15, 7X, 15, 3X, 2E12.5, 7X, E15.7 )
2215 40  FORMAT ( 'SETTING UP DOUBLET STRENGTH MATRIX' )
2216 C
2217 C      END
2218 C

```

```

2219 C .....
2220 C
2221 C     SUBROUTINE MDPNT (NZNE, IHD, RPHI, LP)
2222 C
2223 C     CALCULATE EXACT STRENGTH AT ENDPOINTS AND MIDPOINT
2224 C     OF EACH LINE DOUBLET BOUNDARY SEGMENT.
2225 C
2226 C     COMMON / IO / LU, PL, GL, AL, JL, IL, TL
2227 C     COMMON / POLE / ZONE, DPOLE
2228 C
2229 C
2230 C     DIMENSION DPOLE (300), ZONE (4, 7)
2231 C
2232 C     COMPLEX  DPOLE
2233 C     INTEGER  AL, GL, PL, TL
2234 C     NZT = NZNE - 1
2235 C
2236 C     DO 1020  IZNE = NZT, 1, -1
2237 C         NPOL1 = ZONE (IZNE, 6)
2238 C         NPOL2 = ZONE (IZNE, 7)
2239 C
2240 C     INSERT SPACE FOR MIDPOINT COORD.
2241 C
2242 C         DO 1000  IPOL = NPOL2, NPOL1, -1
2243 C             1000  DPOLE (2 * IPOL - 1) = DPOLE (IPOL)
2244 C
2245 C     INSERT MIDPOINT COORD.
2246 C
2247 C         ZONE (IZNE, 3) = ZONE (IZNE, 3) * 2
2248 C         ZONE (IZNE, 6) = ZONE (IZNE, 6) * 2.0 - 1.0
2249 C         ZONE (IZNE, 7) = ZONE (IZNE, 7) * 2.0
2250 C         MPOL1 = ZONE (IZNE, 6)
2251 C         MPOL2 = ZONE (IZNE, 7)
2252 C
2253 C         DO 1010  IPOL = MPOL1, MPOL2, 2
2254 C             IPLS1 = IPOL + 1
2255 C             IPLS2 = IPOL + 2
2256 C             IF (IPLS2 .GT. MPOL2) IPLS2 = MPOL1
2257 C             DPOLE (IPLS1) = (DPOLE (IPLS2) + DPOLE (IPOL)) / 2.0
2258 C             1010  CONTINUE
2259 C
2260 C
2261 C     1020  CONTINUE
2262 C
2263 C     CALCULATE SIMULTANEOUS EXACT STRENGTHS AT ENDPOINTS AND MIDPOINTS.
2264 C
2265 C     CALL STGTH (IHD, RPHI, LP)
2266 C
2267 C     SEPARATE NONLINEAR COMPONENTS.
2268 C
2269 C     IF (LP .GE. 2) CALL QUAD (NZT)
2270 C
2271 C     RETURN
2272 C
2273 C
2274 C     END
2275 C
2276 C     .....
2277 C
2278 C     SUBROUTINE QUAD (NZT)

```

```

2279 C
2280 C   CALCULATE PARABOLIC COMPONENT OF DOUBLET STRENGTH AT EACH
2281 C   DOUBLET MIDPOINT.
2282 C
2283 C
2284 C   COMMON / POLE / ZONE, DPOLE
2285 C   COMMON / PJMP / JUMP, MU
2286 C   COMMON / IO / LU, PL, GL, AL, JL, IL, TL
2287 C
2288 C
2289 C   DIMENSION DPOLE (300), JUMP (300), MU (300), ZONE (4, 7)
2290 C
2291 C   COMPLEX   DPOLE
2292 C   INTEGER   AL, GL, PL, TL
2293 C   REAL      JUMP, MU
2294 C
2295 C   REWIND JL
2296 C
2297 C   WRITE (LU, 10)
2298 C
2299 C       DO 1020 IZNE = 1, NZT
2300 C
2301 C           MPOL1 = ZONE (IZNE, 6)
2302 C           MPOL2 = ZONE (IZNE, 7)
2303 C
2304 C               DO 1000 IPOL = MPOL1, MPOL2, 2
2305 C                   IPLS = IPOL + 2
2306 C                   IF (IPOL + 1 .EQ. MPOL2) IPLS = MPOL1
2307 C
2308 C   LINEARLY APPROXIMATED STRENGTH AT MIDPOINT.
2309 C
2310 C       STMID = (JUMP (IPOL) + JUMP (IPLS)) / 2.0
2311 C
2312 C
2313 C   THE DISCREPANCY BETWEEN ACTUAL JUMP AND LINEARLY APPROXIMATED
2314 C   STRENGTH IS THE COMPONENT (MU) TO BE ADDED TO (S) AT THE
2315 C   MIDPOINT AND INTERPOLATED QUADRATICALLY BETWEEN THE ENDPOINTS.
2316 C
2317 C       IMPOL = IPOL + 1
2318 C       IM2 = IMPOL / 2
2319 C       MU (IPOL) = JUMP (IMPOL) - STMID
2320 C
2321 C       WRITE (LU, 30) IZNE, IM2, DPOLE (IM2), MU (IPOL)
2322 C   1000   CONTINUE
2323 C
2324 C   1020   CONTINUE
2325 C
2326 C       DO 1030 IZNE = 1, NZT
2327 C           ZONE (IZNE, 3) = ZONE (IZNE, 3) / 2.0
2328 C           ZONE (IZNE, 6) = (ZONE (IZNE, 6) + 1) / 2.0
2329 C           ZONE (IZNE, 7) = ZONE (IZNE, 7) / 2.0
2330 C
2331 C   RESTORE DIPOLE, AND STRENGTH ARRAYS.  SAVE STRENGTH VALUES.
2332 C
2333 C       NPOL1 = ZONE (IZNE, 6)
2334 C       NPOL2 = ZONE (IZNE, 7)
2335 C
2336 C       DO 1010 IPOL = NPOL1, NPOL2
2337 C           JUMP (IPOL) = JUMP (2 * IPOL - 1)
2338 C           MU (IPOL) = MU (2 * IPOL - 1)

```

```

2339          WRITE (JL, 20) JUMP (IPOL), MU (IPOL)
2340 1010      DPOLE (IPOL) = DPOLE (2 * IPOL - 1)
2341 C
2342 1030      CONTINUE
2343 C
2344 C
2345          RETURN
2346 C
2347 C
2348 C
2349 10      FORMAT ( ///, 31X, 11H(MIDPOINTS), //, 1X, 8HZONE NO., 3X,
2350 1      11HDOUBLET NO., 7X, 11HCOORDS(X,Y), 8X, 22HINCREMENT IN POTENTI
2351 2AL , /, 44X, 15H(PARABOLIC FIT) )
2352 20      FORMAT ( 2E15.9 )
2353 30      FORMAT ( 1X, 15, 7X, 15, 5X, 2E12.5, 5X, E12.5 )
2354 C
2355          END
2356 C
2357 C
2358 C
2359 *EMA/SIZE/,/VECT/
2360          SUBROUTINE GAUSS (MIN, ER)
2361 C
2362 C          OBTAIN A SOLUTION TO A SET OF SIMULTANEOUS LINEAR EQUATIONS
2363 C          OF THE FORM AX=B.
2364 C          DESCRIPTION OF PARAMETERS:
2365 C          I = ROW
2366 C          J = COLUMN
2367 C          COEF(I,J) = MATRIX OF COEFFICIENTS
2368 C          CNST(J)  = COLUMN OF CONSTANTS
2369 C          = SOLUTION ARRAY
2370 C          METHOD:
2371 C          ROW REDUCTION USING THE GAUSS-JORDAN PROCEDURE
2372 C
2373 C
2374 C
2375          COMMON / SIZE / COEF, CHEM
2376          COMMON / VECT / CNST
2377          COMMON / IO / LU, PL, GL, AL, JL, IL, TL
2378 C
2379 C
2380          DIMENSION CHEM (500, 17), CNST (300), COEF (300, 300), COLI (300)
2381 C
2382          INTEGER AL, ER, GL, PL, TL
2383          MINUS = MIN - 1
2384          TOL = 1.0E - 10
2385          ER = 0
2386          WRITE (1, 40)
2387 C
2388 C          PIVOTING IS NOT NECESSARY WITH THIS MATRIX SINCE THE DIAGONAL
2389 C          ELEMENT IS ALWAYS THE LARGEST IN THE ROW.
2390 C
2391          DO 1020 I = 1, MINUS
2392 C
2393          DO 1025 IROW = I, MIN
2394 1025      COLI (IROW) = COEF (IROW, I)
2395 C
2396 C          CHECK FOR SINGULAR MATRIX
2397 C
2398          IF (ABS (COLI (I)) .GT. TOL) GO TO 1000

```

```

2399          ER = 1
2400          WRITE (LU, 10)
2401          GO TO 1070
2402 C
2403 C      ELIMINATE VARIABLES
2404 C
2405 1000      JJ = I + 1
2406 C
2407          DO 1010 J = JJ, MIN
2408          CFIJ = COEF (I, J)
2409          CNST (J) = CNST (J) - CFIJ * CNST (I) / COLI (I)
2410 C
2411          DO 1010 N = I, MIN
2412          K = MIN - N + 1
2413          COEF (K, J) = COEF (K, J) - CFIJ * COLI (K) / COLI (I)
2414 1010      CONTINUE
2415 C
2416          WRITE (1, 20) I
2417 1020      CONTINUE
2418 C
2419 C      BACK SOLUTION
2420 C
2421          DO 1050 II = 1, MINUS
2422          I = MIN - II + 1
2423 C
2424          DO 1030 IROW = 1, I
2425 1030      COLI (IROW) = COEF (IROW, I)
2426 C
2427          DO 1040 JJ = 2, I
2428          J = I - JJ + 1
2429          CFIJ = COEF (I, J)
2430          CNST (J) = CNST (J) - CFIJ * CNST (I) / COLI (I)
2431 C
2432          DO 1040 K = J, I
2433          COEF (K, J) = COEF (K, J) - CFIJ * COLI (K) / COLI (I)
2434 1040      CONTINUE
2435 C
2436          WRITE (1, 30) I
2437 1050      CONTINUE
2438 C
2439 C      SOLVE FOR CNST
2440 C
2441          DO 1060 J = 1, MIN
2442 1060      CNST (J) = CNST (J) / COEF (J, J)
2443 C
2444 1070      RETURN
2445 C
2446 C
2447 C
2448 10      FORMAT ( //, 1X, 29HSINGULAR MATRIX - NO SOLUTION, / )
2449 20      FORMAT ( 'UPPER TRIANGULAR...IN COLUMN', I5 )
2450 30      FORMAT ( 'BACK SOLUTION...IN COLUMN', I5 )
2451 40      FORMAT ( 'BEGIN GAUSS ELIMINATION PROCEDURE' )
2452 C
2453      END
2454 C
2455 C
2456 $EMAP/SIZE//,VECT/
2457      SUBROUTINE STMVL (HEAD, OMEGA, Z, DDDZ, D2DDZ, ICT, IHD, IPT,
2458 1      MINUS, PERM)

```

```

2459 C
2460 C   FOR EACH POINT ON THE STREAMLINE
2461 C   THIS ROUTINE CALCULATES FLUID FLUX (SPECIFIC DISCHARGE),
2462 C   VELOCITY (VEL=FLUX/POROSITY) AND THEIR DERIVATIVES ANALYTICALLY
2463 C   FROM D(OMEGA)/D(Z) AND D2(OMEGA)/D2(Z) USING CAUCHY REIMANN
2464 C   CONDITIONS.  THESE VALUES ARE USED IN A CONVECTION
2465 C   DIFFUSION GEOCHEMICAL MODEL.
2466 C
2467 C
2468 C   COMMON / SIZE / COEF, CHEM
2469 C   COMMON / VECT / CNST
2470 C   COMMON / CNST / I, PI
2471 C   COMMON / WELLD / ZBND, RPHI, Q, ZWL, STRT, WRAD, WRDS, NPT, NUL,
2472 C 1   NUMS, NUMW
2473 C   COMMON / IO / LU, PL, GL, AL, JL, IL, TL
2474 C   COMMON / CHEM / D, F, P, SIGMA, POR, RHO, ISKP
2475 C   COMMON / AQF / THICK, AQ, FL, BND
2476 C   COMMON / LINE / NLINE, STM, DEC, MXPTS
2477 C   COMMON / ZON / LOCZ
2478 C
2479 C
2480 C   DIMENSION BND (4), CHEM (500,17), CNST (300), COEF (300, 300),
2481 C 1   NLINE (100), NUMS (100, 2), NUMW (30), Q (30), STRT (100), WRAD
2482 C 2   (30), ZWL (30), POR (4), P (4), RHO (4)
2483 C
2484 C   COMPLEX   BND, DODZ, DOD2, DVEL, D2ODZ, FLXVC, I, OMEGA, STRT,
2485 C 1   ZWL, Z
2486 C   INTEGER   AL, GL, PL, STM, TL
2487 C   REAL      KL, LASTL, MPERM
2488 C
2489 C   DATA     POND, ZERO, UNCF, CONF / 4HPOND, 4HZERO, 4HUNCF, 4HCONF /
2490 C
2491 C   INITIALIZATION.
2492 C
2493 C   MASS TRANSPORT INTERFACE FILE ON LU=14
2494 C
2495 C   MINI = - 1
2496 C   IF (MINUS .EQ. - 2) GO TO 1030
2497 C
2498 C   THE SECOND PARTIAL OF PHI WITH X AND Y IS GIVEN ANALYTICALLY.
2499 C   NOTE THAT RE(D2ODZ)=D2(PHI)/D2(X) AND IM(D2ODZ)=D2(PHI)/D(X)D(Y),
2500 C   D2(PHI)/D2(Y) IS FOUND FROM CAUCHY REIMANN CONDITIONS SINCE:
2501 C       D2(PHI)/D2(X) = -D2(PHI)/D2(Y) AND
2502 C       D2(PHI)/D(X)D(Y) = -D2(PHI)/D(Y)D(X),
2503 C   OR FROM THE CONSERVATION EQUATION SINCE:
2504 C       D2(PHI)/D2(X) + D2(PHI)/D2(Y) = 0.0
2505 C
2506 C   IF (FL .EQ. CONF) SATT = THICK
2507 C   IF (FL .EQ. UNCF) SATT = HEAD
2508 C   IF (FL .EQ. ZERO .OR. FL .EQ. POND) RETURN
2509 C
2510 C   PERMEABILITY CONVERTED FROM FT./HR. TO CM./SEC.
2511 C
2512 C   MPERM = PERM * 30.48 / 3600.
2513 C
2514 C   SPECIFIC DISCHARGE AT A POINT IS OBTAINED BY DIVIDING D2ODZ BY
2515 C   THE SATURATED THICKNESS, (THICK) IN THE CONFINED CASE
2516 C   AND (HEAD) IN THE UNCONFINED CASE. (HEAD) IS ALWAYS MEASURED IN
2517 C   FEET FROM THE BOTTOM CONFINING LAYER.
2518 C

```

```

2519 C      ALL CHEM ARRAY ENTRIES CONVERTED TO C.G.S. FOR USE IN
2520 C      KINETIC MODEL.
2521 C
2522 C      CHEM( ICT, 1) = REAL(Z)
2523 C      CHEM( ICT, 2) = IMAGINARY(Z)
2524 C      CHEM( ICT, 3) = REAL FLUX VECTOR.
2525 C      CHEM( ICT, 4) = IMAGINARY FLUX VECTOR.
2526 C      FLXVC = (X,Y) FLUX VECTOR.
2527 C      CHEM( ICT, 5) = RESULTANT FLUX VECTOR.
2528 C      CHEM( ICT, 6) = HEAD AT EQUAL INTERVALS.
2529 C      VLXX = DERIVATIVE OF X VELOCITY VECTOR WITH X.
2530 C      VLYY = DERIVATIVE OF Y VELOCITY VECTOR WITH Y.
2531 C      VLXY = DERIVATIVE OF X VELOCITY VECTOR WITH Y.
2532 C      CHEM( ICT, 7) = DERIVATIVE OF X FLUX WITH X.
2533 C      CHEM( ICT, 8) = DERIVATIVE OF Y FLUX WITH Y.
2534 C      CHEM( ICT, 9) = DERIVATIVE OF X FLUX WITH Y.
2535 C      CHEM( ICT, 10) = REAL(OMEGA) (EQUAL INTERVAL HEAD).
2536 C      CHEM( ICT, 11) = IMAGINARY (OMEGA).
2537 C      KL = DISPERSION COEFFICIENT (FT**2/SEC.)
2538 C      CHEM( ICT, 12) = RHO (ROCK DENSITY)
2539 C      CHEM( ICT, 13) = CONVECTION COEFFICIENT (ALPHA)
2540 C      CHEM( ICT, 14) = DISPERSION COEFFICIENT (BETA)
2541 C      CHEM( ICT, 16) = NORMALIZED DELTA HEAD.
2542 C      CHEM( ICT, 17) = POROSITY
2543 C      VL = VELOCITY(RESULTANT VECTOR).
2544 C
2545 C
2546 C      CHEM ( ICT, 1) = REAL (Z) * 30.48
2547 C      CHEM ( ICT, 2) = AIMAG (Z) * 30.48
2548 C      FLXVC = CMPLX (REAL (DODZ), - AIMAG (DODZ)) * 30.48 / SATT /
2549 C      3600.
2550 C      VL = CABS (FLXVC) / POR (LOCZ)
2551 C      KL = D / (F * POR (LOCZ)) + 0.5 * VL * SIGMA * P (LOCZ)
2552 C      CHEM ( ICT, 3) = REAL (FLXVC)
2553 C      CHEM ( ICT, 4) = AIMAG (FLXVC)
2554 C      CHEM ( ICT, 5) = CABS (FLXVC)
2555 C      CHEM ( ICT, 6) = HEAD * 30.48
2556 C      CHEM ( ICT, 7) = REAL (D2DDZ) / SATT / 3600.
2557 C      VLXX = CHEM ( ICT, 7) / POR (LOCZ)
2558 C      CHEM ( ICT, 8) = - CHEM ( ICT, 7)
2559 C      VLYY = - VLXX
2560 C      CHEM ( ICT, 9) = - AIMAG (D2DDZ) / SATT / 3600.
2561 C      VLXY = CHEM ( ICT, 9) / POR (LOCZ)
2562 C      CHEM ( ICT, 10) = REAL (OMEGA) * 30.48 ** 3 / 3600.
2563 C      CHEM ( ICT, 11) = AIMAG (OMEGA) * 30.48 ** 3 / 3600.
2564 C      CHEM ( ICT, 15) = CHEM ( ICT, 10)
2565 C      CHEM ( ICT, 17) = POR (LOCZ)
2566 C      CHEM ( ICT, 12) = RHO (LOCZ)
2567 C
2568 C      CALCULATE STREAMLINE CONVECTION AND DISPERSION TERM COEFFICIENTS
2569 C      FOR INPUT TO MASS TRANSPORT MODEL.
2570 C
2571 C      TERM1 = CHEM ( ICT, 5) ** 2
2572 C      TERM2 = (2.0 * CHEM ( ICT, 3) * CHEM ( ICT, 4) / CHEM ( ICT, 5) **
2573 C      2) * KL * CHEM ( ICT, 9)
2574 C      TERM3 = KL * (CHEM ( ICT, 3) ** 2 / CHEM ( ICT, 5) ** 2 + 1.0) *
2575 C      CHEM ( ICT, 7)
2576 C      TERM4 = KL * (CHEM ( ICT, 4) ** 2 / CHEM ( ICT, 5) ** 2 + 1.0) *
2577 C      CHEM ( ICT, 8)
2578 C

```

```

2579 C      ALPHA
2580 C
2581 C      CHEM (ICT, 13) = (1 / MPERM) * (TERM1 - TERM2 - TERM3 - TERM4)
2582 C
2583 C      BETA
2584 C
2585 C      CHEM (ICT, 14) = KL * ((CHEM (ICT, 5) ** 2) * (1 / MPERM) ** 2)
2586 C
2587 C      CREATE OUTPUT FILE FOR INPUT TO MASS TRANSPORT PROGRAM.
2588 C
2589 C      IF (ICT .NE. 1) GO TO 1020
2590 C      WRITE (TL, 10) NWL
2591 C
2592 C          DO 1010 KWL = 1, NWL
2593 C              WRITE (TL, 20) NUMW (KWL), ZWL (KWL)
2594 C          1010 CONTINUE
2595 C
2596 C      WRITE (TL, 10) MINUS
2597 C      WRITE (TL, 20) NPT
2598 C      1020 CONTINUE
2599 C      IF (IHD .GT. 1) GO TO 1080
2600 C      1030 PH11 = CHEM (ICT, 6)
2601 C      IF (ICT .EQ. 1) GO TO 1080
2602 C      LST = ICT - LASTH + 1
2603 C      KCT = ICT - 2
2604 C
2605 C      WRITE (LU, 30) PH1D
2606 C
2607 C      CALCULATE DISTANCE OF LAST POINT FROM PROD. WELL.
2608 C
2609 C      LSTPT = IPT - 1
2610 C      IF (NUMS (LSTPT, 2) .GT. 0) GO TO 1040
2611 C      QLINE = - 10.0
2612 C      VN = - 10.0
2613 C      GO TO 1060
2614 C
2615 C      FOR EACH STREAMLINE CALCULATE INJECTION VOLUME, DISTANCE FROM
2616 C      RECOVERY WELL, AND THE STREAMTUBE CROSECTIONAL AREA AT THE
2617 C      RECOVERY WELL.
2618 C
2619 C      1040 DO 1050 KWL = 1, NWL
2620 C          QW = Q (KWL) / 3600.
2621 C          IF (NUMS (LSTPT, 1) .EQ. NUMW (KWL)) QLINE = ABS (QW / NLINE-
2622 C      1 (LSTPT)) * 30.48 ** 3
2623 C
2624 C          IF (NUMS (LSTPT, 2) .NE. NUMW (KWL)) GO TO 1050
2625 C          QPROD = QW * 30.48 ** 3
2626 C          DIST = CABS (ZWL (KWL) - CMPLX (CHEM (KCT, 1), CHEM (KCT, 2)) /
2627 C      1 30.48)
2628 C      1050 CONTINUE
2629 C
2630 C      VN = (QLINE / QPROD) * PI * SATT * DIST ** 2 * 30.48 ** 3
2631 C      1060 CONTINUE
2632 C
2633 C      RESCALE ALPHA AND BETA ACCORDING TO STREAMLINE LENGTH OF ONE.
2634 C
2635 C      LAST1 = LASTH - 2
2636 C      CH16 = -1.0 - (CHEM (KCT, 6) - CHEM (LST-1, 6)) / PH1D
2637 C      WRITE (TL, 50) LSTPT, LAST1, CHEM (KCT, 11), NUMS (LSTPT, 1),
2638 C      1 NUMS (LSTPT, 2), QLINE, VN, STM, CH16

```

```

2639 C
2640      DO 1070 KPT = LST, KCT
2641      CHEM (KPT, 13) = CHEM (KPT, 13) / PHID
2642      CHEM (KPT, 14) = CHEM (KPT, 14) / (PHID ** 2)
2643      CHEM (KPT, 16) = (CHEM (KPT, 6) - CHEM (KPT - 1, 6)) / PHID
2644 C
2645      WRITE (LU, 60) CHEM (KPT, 13), CHEM (KPT, 14), CHEM (KPT, 16),
2646      1      KPT
2647      WRITE (TL, 20) LSTPT, CHEM (KPT, 1), CHEM (KPT, 2), CHEM (KPT,
2648      1      10), CHEM (KPT, 13), CHEM (KPT, 14), CHEM (KPT, 16), CHEM (KPT,
2649      2      12), CHEM (KPT, 17)
2650      1070      CONTINUE
2651 C
2652      WRITE (TL, 10) MINI
2653      IF (MINUS .EQ. - 2) WRITE (TL, 10) MINUS
2654      1080      PHID = PHID - CHEM (ICT, 6)
2655      LASTH = IHD
2656 C
2657      RETURN
2658 C
2659 C
2660      10      FORMAT ( I4 )
2661      20      FORMAT ( I4, 8E15.5 )
2662      30      FORMAT ( // 1X, 21HSTREAMLINE POT. DIFF., E8.3, 11HCM.**3/SEC.,
2663      1      / 10X, 5HALPHA, 9X, 5HBETA , 9X, 14HHEAD DECREMENT, 5X,
2664      2      7HPT. NO.)
2665      50      FORMAT ( 2I4, E15.5, 2I4, 2E15.5, I4, E15.5)
2666      60      FORMAT ( 3X, E12.5, 5X, E12.5, 5X, E12.5, 5X, 15 )
2667 C
2668      END
2669      END$

```



17

11